PHOTOGRAPH THIS SHEET

AD-A156 065

DTIC ACCESSION NUMBER

III

LEVEL

1

INVENTORY

DNA-TR-83-53

DOCUMENT IDENTIFICATION

1 JAN 1984

This document has been approved for public release and sale; its distribution is unlimited.

DISTRIBUTION STATEMENT

ACCESSION FOR		
NTIS	GRA&I	☒
DTIC	TAB	☐
UNANNOUNCED		☐
JUSTIFICATION		
BY		
DISTRIBUTION /		
AVAILABILITY CODES		
DIST	AVAIL AND/OR SPECIAL	
A-1		

DISTRIBUTION STAMP

DTIC ELECTE JUN 20 1985 S D

DATE ACCESSIONED

DATE RETURNED

85 6 20 078

DATE RECEIVED IN DTIC

REGISTERED OR CERTIFIED NO.

PHOTOGRAPH THIS SHEET AND RETURN TO DTIC-DDAC

DTIC FORM 70A DEC 83

DOCUMENT PROCESSING SHEET

PREVIOUS EDITION MAY BE USED UNTIL STOCK IS EXHAUSTED.

DISCLAIMER NOTICE

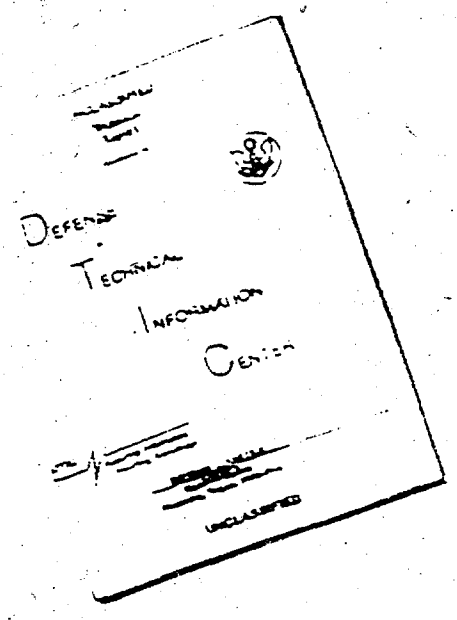

THIS DOCUMENT IS BEST QUALITY AVAILABLE. THE COPY FURNISHED TO DTIC CONTAINED A SIGNIFICANT NUMBER OF PAGES WHICH DO NOT REPRODUCE LEGIBLY.

DNA-TR-83-52

STUDIES IN URBAN-SCALE-FIRE THERMOHYDRODYNAMICS

G. Carrier
F. Fendell
P. Feldman
TRW Electronics & Defense Sector
One Space Park
Redondo Beach, CA 90278

1 January 1984

Technical Report

CONTRACT No. DNA 001-83-C-0104

APPROVED FOR PUBLIC RELEASE;
DISTRIBUTION UNLIMITED.

THIS WORK WAS SPONSORED BY THE DEFENSE NUCLEAR AGENCY
UNDER RDT&E RMSS CODE B345083466 G54CMXGR00011 H2590D.

Prepared for
Director
DEFENSE NUCLEAR AGENCY
Washington, DC 20305

Destroy this report when it is no longer needed. Do not return to sender.

PLEASE NOTIFY THE DEFENSE NUCLEAR AGENCY, ATTN: STTI, WASHINGTON, D.C. 20305, IF YOUR ADDRESS IS INCORRECT, IF YOU WISH TO BE DELETED FROM THE DISTRIBUTION LIST, OR IF THE ADDRESSEE IS NO LONGER EMPLOYED BY YOUR ORGANIZATION.

UNCLASSIFIED

SECURITY CLASSIFICATION OF THIS PAGE

REPORT DOCUMENTATION PAGE

1a. REPORT SECURITY CLASSIFICATION UNCLASSIFIED	1b. RESTRICTIVE MARKINGS
2a. SECURITY CLASSIFICATION AUTHORITY	3 DISTRIBUTION/AVAILABILITY OF REPORT Approved for public release; distribution unlimited.
2b. DECLASSIFICATION/DOWNGRADING SCHEDULE N/A since UNCLASSIFIED	
4. PERFORMING ORGANIZATION REPORT NUMBER(S) 42132-6001-UT-00	5. MONITORING ORGANIZATION REPORT NUMBER(S) DNA-TR-83-52
6a. NAME OF PERFORMING ORGANIZATION TRW Electronics & Defense Sector 6b. OFFICE SYMBOL (If applicable)	7a. NAME OF MONITORING ORGANIZATION Director, Defense Nuclear Agency
6c. ADDRESS (City, State, and ZIP Code) One Space Park Redondo Beach, California 90278	7b. ADDRESS (City, State, and ZIP Code) Washington, DC 20305
8a. NAME OF FUNDING/SPONSORING ORGANIZATION 8b. OFFICE SYMBOL (If applicable)	9 PROCUREMENT INSTRUMENT IDENTIFICATION NUMBER DNA 001-83-C-0104
8c. ADDRESS (City, State, and ZIP Code)	10. SOURCE OF FUNDING NUMBERS

PROGRAM ELEMENT NO	PROJECT NO	TASK NO	WORK UNIT ACCESSION NO
62715H	G54CMXG	R	006694

11 TITLE (Include Security Classification)
STUDIES IN URBAN-SCALE-FIRE THERMOHYDRODYNAMICS

12. PERSONAL AUTHOR(S) G. Carrier P. Feldman
F. Fendell

13a. TYPE OF REPORT	13b. TIME COVERED	14. DATE OF REPORT (Year, Month, Day)	15. PAGE COUNT
Technical	FROM 83/22/2 TO 84/22/2	84/1/1	110

16. SUPPLEMENTARY NOTATION
This work was sponsored by the Defense Nuclear Agency under RDT&E RMSS Code B345083466 G54CMXGR00011 H2590D.

17 COSATI CODES			18. SUBJECT TERMS (Continue on reverse if necessary and identify by block number)
FIELD	GROUP	SUB-GROUP	Buoyant Plume, Firestrom, Nuclear Weapon Effects, Fire, Flame Spread, Turbulent Entrainment
18	3		
13	12		

19. ABSTRACT (Continue on reverse if necessary and identify by block number)

Incendiary effects of thermonuclear weapons on urban and wildland environments can involve multiple simultaneous ignitions in the presence of heavy loading of combustibles, blasted into strewn debris. Subsequent merger of fires from initially separated ignitions results in large-area fire. Generalization of conventional integral-type modeling of buoyant plumes (to encompass strongly buoyant convection through a significant depth of the troposphere) permits three items to be addressed: (1) the limit on, and mechanism for, enhancement of entrainment into the lower, flaming portion of the plume; (2) the plausible degree of necking in of the plume in the lower troposphere; and (3) the height to which the plume rises (found to be below the tropopause unless quite exceptional ambient conditions and/or fire size hold). However, two special preexisting atmospheric conditions could alter the nature of the large-area fire significantly, and these are also examined by simple approximate analyses. First, preexistence of a well-developed atmospheric cyclone over the fire area could bring conservation-of-angular-momentum considerations to paramount

20. DISTRIBUTION/AVAILABILITY OF ABSTRACT ☐ UNCLASSIFIED/UNLIMITED ☒ SAME AS RPT. ☐ DTIC USERS	21. ABSTRACT SECURITY CLASSIFICATION UNCLASSIFIED
22a. NAME OF RESPONSIBLE INDIVIDUAL Betty L. Fox	22b. TELEPHONE (Include Area Code) (202) 325-7042 22c. OFFICE SYMBOL DNA/STTI

DD FORM 1473, 84 MAR 83 APR edition may be used until exhausted. All other editions are obsolete.

SECURITY CLASSIFICATION OF THIS PAGE

UNCLASSIFIED

19. ABSTRACT (Continued)

importance; criteria for onset of a combustion-heat-intensified cyclone (firestorm) are proposed. Second, preexistence of a strong sustained wind of fairly well-defined direction could permit the fire to propagate rapidly beyond the area encompassing the initial ignitions, with only an exhaustion of fuel, noteworthy change of weather conditions, and/or significant topograpic fire break terminating the flame sperad.

PREFACE

The authors wish to thank Michael Frankel, the technical monitor, for the opportunity to pursue this investigation; they are also grateful for encouragement and assistance from Robert Flory and Tom Kennedy. The authors are grateful for several discussions with Stephen Pyne of the University of Iowa, who furnished useful summaries of large wildland fires in North America during the last two centuries. The authors also are indebted to Frank Albini and Donald Haines of the U.S. Forest Service, and to Brian Stocks of the Canadian Forest Service, for photography and descriptions of wildland fire in the presence of a crosswind. The authors acknowledge the helpful assistance of Ann McCollum in preparation of the manuscript and to Asenatha McCauley in preparation of the figures.

TABLE OF CONTENTS

		Page
	PREFACE	1
1.	INTRODUCTION	3
2.	CATEGORIZING URBAN-SCALE FIRES	5
3.	WIND-AIDED FLAME SPREAD ACROSS STREWN-DEBRIS-TYPE FUEL	7
	3.1 Preliminary Comments	7
	3.2 A Conjecture About Wind-Aided Flame Spread	10
4.	SUGGESTED DIRECTIONS FOR FURTHER RESEARCH	15
	4.1 Introductory Comments	15
	4.2 Brief Description of Useful Experiments	16
	REFERENCES	19
	APPENDIX A	21
	APPENDIX B	67

STUDIES IN URBAN-SCALE-FIRE THERMOHYDRODYNAMICS

by

G. F. Carrier, F. E. Fendell, P. S. Feldman
Engineering Sciences Laboratory, Space and Technology Group
TRW Electronics and Defense Sector
One Space Park
Redondo Beach, CA 90278

1. INTRODUCTION

The primary consequences of thermonuclear weapons outside the area of 150-mb peak overpressure are likely to be of an incendiary nature. Yet examination of basic references (e.g., Glasstone and Dolan 1977) readily reveals the relatively miniscule effort devoted to, and rather debatable statements about, fire effects; blast, radiative, and fallout effects have been examined more extensively and are far better quantified.

It is now recognized that a much better understanding of urban-scale fires is needed if one is to anticipate the effects on the atmosphere of such events (Crutzen and Birks 1982; Pyne 1982; Tilling 1982; Holden 1983; Raloff 1983; Wooley and Bishop 1983). In particular, information on plume height, smoke content and early scavenging [particularly fires burning in a humid environment (Morton 1957)] deserves attention.

In this report we present some preliminary studies of urban-scale uncontrolled fires. In these broad-brush preliminary examinations, the aim is to include, in the simplest reasonable manner, only the most important

physical processes; more refined treatment may entail need for normally unavailable input or may sacrifice the generality of results sought.

2. CATEGORIZING URBAN-SCALE FIRES

Incendiary effects of thermonuclear weapons on urban and wildland environments can involve multiple simultaneous ignitions in the presence of heavy locating of combustibles, blasted into strewn debris.* It seems plausible that the urban environment after blast is likely to have a far more continuous (even if still discrete) distribution of combustibles, such that the ground-level/canopy-level fuel distribution of forests is more closely approached in the blasted city. However, whereas ladder (intermediate-height) fuels are limited in forests to down branches, young trees, mixed species, lichen, etc., ladder fuels should be plentiful in a multistory urban environment even after blast (in those outer areas where the incendiary aftermath constitutes the principal nuclear effects). Subsequent merger of initially separated ignitions across normally-effective firebreaks may be abetted in the blasted environment, especially since the disruption of transportation, communication, and water-distribution, casualties in trained personnel and in firefighting apparati, etc., probably curtail effective countermeasures.

Attempts to anticipate the precise number and nature of ignitions in a specific locale seems difficult in view of the accidental character of firestarts after earthquakes. Rather, the occurrence of ignitions and early spread is accepted here. It seems more productive to seek insight concerning (1) the rate and areal extent of the spread of the fire front through thinner (and more rapidly burned) fuels; (2) the completeness of consumption of thicker (and more slowly burned) fuels; (3) the magnitude and overall character of winds; (4) the properties

---

*Despite intense burning in the aftermath of the atomic bombings of Hiroshima and Nagasaki in August 1945, the suggestion arose in the late 1970's that blasted-gas arrival at the site of radiation-precursor-initiated diffusion flames would effect forced-convection extinction of the primary fires. However, blowing out of the diffusion flame supported by a sublimating or evaporating fuel results in rapid lowering of the temperature of liquid or solid fuel by convective cooling, such that, even after the wind decreases, burning is not restored because the fuel vapor pressure is too low; thus, even a rather brief positive phase suffices to extinguish burning permanently. However, wildland and urban combustibles are predominantly char-forming polymers that retain heat in a porous-carbonaceous-matrix layer that forms under thermal degradation to envelop the pristine core; the heat-retaining properties of the char sustains pyrolyzation of further fuel for a finite interval of convective cooling, such that autoreignition of hot outgassed fuel vapor may occur at the end of the positive phase. In fact, heterogeneous oxidation of the char by the wind during the positive phase helps counter convective cooling (Carrier et al. 1982).

of the buoyant convection (its height and width, its propensity to loft soot and firebrands, its tendency to initiate precipitation); and (5) the mechanisms and time scale for ultimate extinction of the fire.

If the primary (radiation-precursor-initiated) and secondary (blast-caused) fires tend to persist and merge, then one has what is termed henceforth a big (i.e., large-area) fire. In that many phenomena may be of significance, it seems particularly difficult to give generally valid results via simple analyses. That is, even if one postulates that (1) the ambient meteorological state (atmospheric stability and moisture content and cloudiness, and wind magnitude and direction, as a function of altitude) is known; (2) the spatial distribution of combustibles (the total mass, the size distribution, ignitability, outgassing characteristics, exothermicity, char-forming and soot-forming characteristics, and moisture content) is known; and (3) the topography is known, still it is quite challenging to describe the evolution of the fire from a given initial condition. However, work submitted for publication on the necking in and height of the buoyant plume, on the magnitude and mechanism for enhanced entrainment into the lower flaming portion of the plume, and on the treatment of situations involving appreciable buoyancy persisting high into the tropopause is presented as Appendix A.

Two special atmospheric circumstances result in a small number of phenomena being of particular importance in the mass, momentum, and heat balances, and thus would seem to offer simple analysis better prospects for yielding insight. First, in a relatively small number of cases, there may happen to exist a preexisting, relatively weak cyclone at the site of the large fire; as a result, spin-up under convectively-induced advection may already be under way, and the fire may lead to a so-called firestorm. Criteria for the onset of a nonpropagating but exceptionally intense fire (in which conservation of angular momentum furnishes key constraints) have been developed in other work also submitted for publication, and are presented here as Appendix B. Second, in a larger number of cases, there may exist a significant preexisting low-altitude wind, persisting in direction and sustained in magnitude. The result is a wind-aided flame spread across strewn debris. Notes on this subject have not been submitted for publication by the authors and constitute the remainder of the main body of this final report.

3. WIND-AIDED FLAME SPREAD ACROSS STREWN-DEBRIS-TYPE FUEL

3.1 Preliminary Comments

The spectacular urban fires of modern times have usually been associated with strong sustained winds (London, 1666; Lisbon, 1775; Moscow, 1812; Chicago, 1871; Boston, 1872; Baltimore, 1904; Tokyo/Yokohama, 1923; Bandon, Oregon, 1936; Tokyo, 1945). Many of the memorable wildland fires (Pyne 1982) were consequences of wind-aided flame spread (Miramichi River Valley, New Brunswick, Canada, 1825; Peshtigo, Wisconsin, 1871; Hinkley, Minnesota, 1894; northern Rockies, 1910; Cloquet, Minnesota, 1918; Matilija, southern California, 1932; Tillamook County, Oregon, 1933; Shoshone National Forest, Wyoming, 1937; Victoria, Australia, 1939; southern Maine, 1947; Inja and Santa Monica Mountains, southern California, 1956; Sundance Mountain, Idaho, 1967; Mack Lake, Michigan, 1980; Victoria, Australia, 1983). This list is hardly exhaustive. What it suggests is that ignition often occurs in heavily fuel-laden areas in times of drought, but it is the coincidence of persistent winds of appreciable speed that causes a "blow-up." The arising of strong winds initiates a startling run that ends only when the wind subsides, combustible matter is exhausted, or precipitation arrives. Normal firebreaks, such as lakes, rivers, or strips of land nearly barren of combustibles may not terminate spread owing to branding. Clearly it is the wind-aiding, not the mode of ignition, that is the key common factor in most fire catastrophes.

What is desired in analysis of fire spread (whether in a single structure or on an urban scale) is the capacity to predict with confidence the rate of flame spread, i.e., the expected position of the fire front at future time, given its position at the current time. What is limiting to meaningful prediction is quantitative formulation (and then solution) of the principal physical processes controlling spread. With such insight, and with appropriate meteorological, topographical, and fuel-loading data, current computer storage and speed of processing seem adequate to display fire-front positions at future time in the absence of countermeasures; in concept, this Lagrangian-type calculation is quite simplistic.

The fastest spread rates are almost invaviably associated with wind-aiding: upslope spread usually exceeds downslope spread; spread under a sustained breeze

usually exceeds spread in a calm. The more rapid spread may be ascribed to several factors: hot product gas blown downwind preheats previously uninvolved fuel in the fire path; more-distant transport of lofted firebrands is likely; and bent-over plumes may ignite downwind fuel by contact or by enhanced radiative transfer (larger view factor).

While interest may center on an urban environment blasted into disarray, it has already been noted that (1) the debris-strewn setting in the thermonuclear aftermath has a far more continuous distribution of combustible material than the fire-code-satisfying preblast city, and (2) the interiors of (possibly partially toppled) structures are likely to be opened. Thus, the closer proximity to a wildlands setting makes it perhaps worthwhile to note that in a forest setting, flame spread is usually through the large-pore matrix of the understory (slash, brush, grass, litter, down woody matter), with an occasional crown taken. However, in severe, high-wind conditions, a "wall" of flame consumes all the readily combustible fuel from understory to overstory (canopy) in one tall front. Only very rarely does flame race from crown to crown, either in the absence of an understory fire or far in advance of the surface-level fire (Van Wagner 1977). Though the taking of a crown is spectacular, aside from radiative transfer the event may not be that much more significant than the exothermicity contributed by reaction of a comparable mass of understory fuel. However, the particular point perhaps most worth noting from forest fires is that the small diameter, thin, leafy matter (which is relatively quickly dried out) is consumed as the fire front passes; it is the loading of thin fuels that is pertinent to the rate of front progression. The thicker fuels are dried out and consumed (if ever consumed at all) on a time span longer than that associated with passage of the fire front. There may be a flare up behind the front as a certain thickness of fuel finally is consumed, but such flaming usually is isolated from the fire-front energetics.

Hence, it may be useful conceptually to subdivide the structure of a wind-aided fire spread into (1) a broad preheat zone in which previously uninvolved fuels are desiccated and brought up to temperatures at which there is significant outgassing of (at least partly combustible) vapor via heat from the flaming

zone; (2) the relatively narrow vigorous burning front itself, a region of strong convection in which the thermally thin fuels are consumed rapidly; and (3) the burn-up zone, in which thicker fuels are dried and burned, often by heterogeneous as well as homogeneous combustion. Wind-aided flame spread through a porous, vertically extensive fuel bed entails (at least) two-dimensional spread, with reactants initially in different phases; furthermore, energetics cannot be treated too cavalierly because heat that dries and gasifies fuel is not recovered to sustain the spread.

The strongly buoyant updraft may form a "barrier" to the oncoming flow in the two-dimensional, line-fire case to be examined here; even in the three-dimensional case, the low-level oncoming flow may be largely diverted around a strongly buoyant column. Of course, if the oncoming wind* is strong enough, it should be able to blow over the convective column (so fire at the front is confined to surface fuels only); in contrast for a weak enough oncoming flow, the aspect of wind-aiding would not be of consequence (and unless radiation to downwind fuel brings that fuel to pyrolysis temperature despite radiative, conductive, and convective heat loss from the fresh fuel to the air, there may be a minimum wind below which there is no spread). For an intermediate-strength oncoming flow, the convective updraft should remain fairly vertical, and tilted only modestly downwind. But there may be a tendency for the configuration to be in the intermediate, nearly vertical configuration for a range of oncoming flow speeds, because if the plume is blown over, the ignition by contact of the surface fuels may adjust (i.e., enhance) the convective-flow strength to meet the oncoming-flow strength (Taylor 1962).

---

*The wind is constant neither in magnitude nor in direction. Hence, utilization of fire-front-propagation insight will probably entail adopting a (well-justified) quasisteady approximation: the propagation of flame normal to the front depends only on the component of wind instantaneously normal to the front, even though that wind be varying in magnitude and direction. During calms the fire may diminish in intensity so flames do not reach as high at the front. In fact, an elliptical, preferred-axis fire-front configuration is likely to arise from a localized ignition in a crosswind: the fire at the flanks tends to have a weak aiding wind (normal to the front). Thus, it is hoped that results from the line-fire configuration being examined are applicable locally to each of several elliptically shaped heads that typically evolve in a wind-aided fire, especially for multiple sites of ignition.

3.2 A Conjecture about Wind-Aided Flame Spread

The preceding discussion suggests that the multizone, multiparameter model necessary to describe in detail the structure of a wind-aided fire front may be bypassed for some purposes, because perhaps one parameter is of foremost importance.

Verbally, the argument may be stated thus: the speed of the crosswind implies a rate of entrainment into a two-dimensional plume, if that oncoming wind cannot penetrate the plume. But the entrainment requirement of a maintained buoyant column over a line-type source is dependent on the strength of the buoyant updraft, according to now-classical concepts for maintained plumes. In turn, the strength of the updraft is dependent on the intensity of the line source, i.e., the heat per length per time released (here, by exothermic combustion). And this intensity by definition is simply the product of the mass of thin-fuel loading per unit area, the exothermic heat derived per mass of fuel (after adjustment for drying and gasification), and the speed of fire propagation. Thus, through intermediate mechanisms, the flame speed is a function of the crosswind speed.

There are several refinements to the above discussion, some of which are now addressed. For plume-fixed coordinates, the oncoming wind is reduced by the fire-propagation speed. Furthermore, there is inflow into the plume from the downwind side equal to the fire-propagation speed; that is, there is a counterflow on the downwind side of the plume for a plume-fixed observor. Whether entrainment into the plume is quite so predominantly from the upwind side (since the oncoming wind often would far exceed the fire-propagation speed) need not be resolved for present purposes.* Also, the classical entrainment concept relating plume-axis updraft to plume-edge inflow pertains to small density discrepancy between in-column air and surrounding air. For large density discrepancy between in-plume and ambient air, perhaps the relation is more accurately stated in terms of mass flux than volumetric flux. Furthermore, at low altitudes (i.e., in the flaming domain), the entrainment is augmented significantly beyond the classical value, and perhaps another formulation is required. However, no simple refinement of the classical relation has gained widespread acceptance; initially the classical relation is used here.

*The plume probably is cellular and effectively three-dimensional at low levels, so there is likely to be entrainment from all sides; the cells merge to form a two-dimensional plume at some height above the surface.

If the classical entrainment relation is adopted tentatively, it is self-consistent to adopt the Boussinesq approximation in the statement of the conservation relations. If x is the horizontal coordinate, y is the vertical coordinate, u is the horizontal velocity component, w is the vertical velocity component, p is pressure, ρ is density, T is temperature, and subscript infinity denotes the ambient state (for which the density is invariant over the height of interest), then the conservation equations for mass, momentum, and energy for the two-dimensional plume over a line source may be taken in the following form (Lee and Emmons 1963):

$$u_x + w_y = 0 \; ; \tag{1}$$

$$p_x = 0 \Longrightarrow \frac{dp_\infty}{dy} = - \rho_\infty g \; ; \tag{2}$$

$$\rho_\infty (u w_x + w w_y) = - \frac{dp_\infty}{dy} - \rho g \; ; \tag{3}$$

$$\left[u \left(T - T_\infty \right)_x + w \left(T - T_\infty \right)_y \right] = - w \left(\frac{dT_\infty}{dy} + \frac{g}{c_p} \right) \; ; \tag{4}$$

here, subscripts x and y denote partial differentiation. For the Boussinesq approximation,

$$\rho \doteq \rho_\infty + \left(\frac{\partial \rho}{\partial T} \right)_p \left(T - T_\infty \right) \; , \tag{5}$$

or for a perfect gas,

$$\frac{\rho_\infty - \rho}{\rho_\infty} = \frac{T - T_\infty}{T_\infty} \; . \tag{6}$$

For Gaussian profiles for the dependent variables, the axial values [W(y) and R(y)] and the e-folding distance, or plume width, b(y) appear as follows:

$$w(x,y) = W(y) \exp\left[-x^2 / b^2(y) \right] \; , \tag{7}$$

$$g \frac{\rho_\infty - \rho(x,y)}{\rho_\infty} = R(y) \exp\left[-x^2 / b^2(y) \right] \; . \tag{8}$$

Application of the integral method to (1), (3), and (4), under (2) and (5)-(8), gives three ordinary differential equations for the three dependent variables b(y), R(y), W(y). That is,

$$\frac{d}{dy}\int_0^\infty w(x,y)dy = -u(\infty,y) \Rightarrow \frac{d}{dy}(bW) = \frac{2}{\pi^{\frac{1}{2}}}\alpha W \ , \tag{9}$$

under the Taylor entrainment hypothesis

$$-u(\infty,y) = \alpha w(0,y) = \alpha W(y) \ , \tag{10}$$

where $\alpha \doteq 0.16$ (Lee and Emmons 1963). Similarly

$$\frac{d}{dy}\int_0^\infty w^2(x,y)dx + u(x,y)\, w(x,y)\Big|_{x=0}^{x\to\infty} = g\int_0^\infty \frac{\rho_\infty - \rho(x,y)}{\rho_\infty}\,dy \Rightarrow \frac{d}{dy}(bW^2) = 2^{\frac{1}{2}} R\, b \ . \tag{11}$$

For a dry-adiabatic lapse rate (neutrally stable atmosphere), the right-hand side of (4) vanishes, and

$$\rho_\infty c_p T_\infty \int_0^\infty w(x,y)\left[\frac{\rho_\infty - \rho(x,y)}{\rho_\infty}\right] dx = \frac{\dot{Q}}{2} \ , \tag{12}$$

where the constant of integration $\dot{Q}$ is the full-infinite intensity of the line source; hence, by (7) and (8),

$$bWR = \left(\frac{2}{\pi}\right)^{\frac{1}{2}} \frac{g\dot{Q}}{\rho_\infty c_p T_\infty} \ . \tag{13}$$

Equations (9), (11), and (13) admit solution in the form

$$b = \beta z \ , \quad W = \gamma \ , \quad R = T z^{-1} \tag{14}$$

where the constants β, γ, T are identified by

$$\beta = \frac{2}{\pi^{\frac{1}{2}}}\alpha \ , \quad \gamma = \left(\frac{g\dot{Q}}{\alpha\rho_\infty c_p T_\infty}\right)^{1/3} \ , \quad T = \frac{1}{2^{\frac{1}{2}}}\left(\frac{g\dot{Q}}{\alpha\rho_\infty c_p T_\infty}\right)^{2/3} \ . \tag{15}$$

Thus, the updraft on the axis of the linearly growing plume is invariant with height, but the density discrepancy does decrease inversely with altitude, the model clearly being singular at the source z = 0.

Under the Taylor hypothesis that the crosswind is compatible with the entrainment requirements, in view of (10) and of the expectation that the entrainment is predominantly from the upwind side of the two-dimensional plume, if U is the crosswind,

$$U \doteq 2\alpha \left(\frac{\dot{Q} g}{\alpha \rho_\infty c_p T_\infty} \right)^{1/3} . \tag{16}$$

But the fire intensity $\dot{Q}$ is given by

$$\dot{Q} = Q \sigma v_f , \tag{17}$$

where Q is the effective chemical heat per mass of thin fuel, σ is the mass of thin fuel per area, and v_f is the fire-propagation speed. Hence,

$$\frac{v_f}{U} = \frac{1}{8\alpha^2} \frac{\rho_\infty c_p T_\infty U^2}{g Q \sigma} , \tag{18}$$

or $v_f \propto (U^3/\sigma)$, since Q is relatively invariant for most fuels of interest. The very often-cited general relation that buoyant strength $\dot{Q}$ goes as the cube of the crosswind speed U in the near-critical (i.e., almost blow-over) condition, as displayed in (16), may be traced to Rouse (1947). Taylor's interpretation permits relating the proportionality factor to a well-known and already-measured empirical constant, the entrainment constant α.

According to (18) the flame-propagation speed v_f increases as the exothermicity Q and thin-fuel loading σ decrease, but increases as the ambient temperature T_∞ increases. These proportionalities reflect the requirement to generate sufficient exothermicity per length per time $\dot{Q}$ to "match" the crosswind U. The assumption of reaction rate sufficient for the flow rate is implicity adopted; if the so-called first Damköhler number is not large enough (and forced-convective extinction occurs), one of the bases of (18) is violated and the relation does not hold. Also, if a strong gust of wind arises, the flame-propagation

rate cannot adjust instantaneously, the quasisteady relation (18) is inapplicable, and the plume is blown over; in time, the propagation speed v_f may increase to restore a fairly vertical plume and (18) holds again. Since by measurement $(2\alpha) < 1$, from (16) one expects $W > U$. Further, <u>if</u> one anticipates $(v_f/U) < 1$, then

$$U < 2\alpha \left(\frac{2gQ}{\rho_\infty c_p T_\infty} \right)^{\frac{1}{2}} ; \tag{19}$$

that is, for too strong a crosswind, even if the burning rates can keep pace, the exothermicity capacity of the fuel loading cannot, and the plume is blown over.

For wind-aided spread through a coniferous stand, the following parametric values hold (Brian Stocks, private communication):

$$U \doteq 670 \text{ cm/s}, \ \sigma \doteq 0.3 \text{ g/cm}^2, \ Q \doteq 1.9 \times 10^{11} \text{ ergs/g}. \tag{20}$$

Hence, (18) gives $v_f \doteq 166$ cm/s, whereas the observed value is 110 cm/s. In view of the approximations (Boussinesq approximation, neutrally stable ambient, line source of heat, etc.), perhaps a factor-of-two error is to be expected. However, the point may be worth making that if the entrainment parameter were ascribed the enhanced value 0.2, theory and experiment would be in close accord; in appendix A, it is argued that an enhanced value of the entrainment parameter may be appropriate for the burning zone of a fire.

4. SUGGESTED DIRECTIONS FOR FURTHER RESEARCH

4.1 Introductory Comments

Whereas earlier sections have presented theoretical models of types of urban-scale fire, this concluding section comments on experimental testing of models to give them credibility. Since urban-scale fire experiments are implausible, full validation of the models is not to be expected, and there will remain a large role for engineering judgment in the acceptance/rejection of predictions.

More explicitly, relatively few of the dimensionless parameters pertinent to urban-scale free burning are likely to take on the same value in feasible laboratory (and somewhat larger-scale) experiment; thus, execution of laboratory-scale and moderately larger-scale experiments does not permit one to predict definitively by dimensional analysis what would occur on the urban scale. However, if one could demonstrate, by comparison against a wide range of experimental data, that a theoretical model could predict (as accurately as required for the user's purposes) physical events from boundary and initial conditions, the model is given credibility. The wider the range with successful comparison, the greater the credibility. In complicated, interdisciplinary, urban-scale phenomena, the range of experimental data normally is not great enough to encompass the actual situation of ultimate interest, so corroboration of the model remains incomplete.

Of course, even if full-scale experimentation were possible, laboratory-scale experimentation usually should precede. If nothing else, prior laboratory testing makes proper instrumentation (with respect to resolution, dynamic range, etc.) of the large-scale test more likely. But laboratory-scale experimentation permits attaining much data relatively quickly and relatively inexpensively, so appreciable parametric variation and considerable repetition (to check for error) is possible. There is likely to be better environmental definition, more extensive and sophisticated diagnostic instrumentation, and better isolation of constituent components, in the laboratory than in some possibly remote, possibly hostile large-scale environment. Conversely, in large-scale tests, relatively few data points are obtained (with redundancy perhaps being impractical because of limited environmental control), and even these few points

are obtained sometimes at large intervals of time. There is often a temptation to change too many parameters from one test to the next, so field tests may degenerate into anecdotes (isolated, incompletely monitored events of uncertain reproducibility).

4.2 Brief Description of Useful Experiments

Some specific experimental tasks that seem to merit undertaking are now very briefly sketched. The ordering is suggestive of priority.

First, it has already been noted that an item of particular uncertainty in the "nuclear-winter" scenario is whether or not saturation and precipitation owing to intense-fire-induced convection in a moist ambient would lead to early rainout of significant amounts of combustion-generated soot, such that the upper-tropospheric carbon-particulate layer would contain less mass. Whether soot is wetted by the condensed moisture, whether soot tends to coagulate within droplets, whether significant contributions to the energetics are connected with such phenomena, etc., ought to be clarified experimentally; while existing cloud-chamber facilities may be modified to undertake the simulation of the "black-rain" phenomenon, perhaps specially designed facilities are called for.

Second, over the last decade or so experimental burns in sections of the Canadian National Forest have been carried out in connection with suppression of spread of tree diseases; Brian Stocks of the Great Lakes Forest Research Station of the Canadian Department of the Environment has participated in the planning and execution of these tests, which are often conducted in heavily fuel-laden coniferous stands (with total thin-fuel loading of about 0.3 g/cm^2). One type of test typically has concerned wind-aided spread across a firebreak-isolated 170 m x 170 m pine-type stand, with the entire upwind edge ignited effectively simultaneously; cinematography affords not only the rate of spread across a stand of known loading and fuel type under known wind, temperature, and humidity, but also provides insight into smoke formation, stability of a planar fire front, and fire-front structure. Not only would the results of already-executed tests furnish useful data with which to test theoretical models, but execution of further tests would be worthwhile [for example, a test is here advocated in which only the (say) left-half of the leading edge would be ignited, to

examine edge effects, i.e., flank effects in wind-aided spread]. A totally distinct type of "test" involves a large-area burn executed in the absence of high wind; while such a burn typically is "forced" artificially (by continual dispersal of torches) for rapidity of execution, it seems worthwhile to ignite just a central area (and to intervene thenceforth only sparingly to maintain circular symmetry); the rate of fire-spread outward against the induced inflowing wind, the plume shape and height and soot content, the nature of branding, etc., would be of interest in large-area fire modeling. While large experimental burns are occasionally carried out in remote sections of Australia, the relatively close proximity of the Canadian tests makes them particularly noteworthy.

Third, laboratory-scale experiments on wind-aided flame spread through a well-defined matrix of discrete fuel elements (in a combustion tunnel with provision for unconstrained plume dynamics) seem a useful complement to the Canadian tests just noted. These tests afford opportunity to examine spread with or against a wind of specified magnitude, to ascertain structure, spread rate, firebreak dimensions, etc. Of course, without special provision, radiative transfer cannot assume the role in laboratory-scale flame that it can in field tests. Since a soon-forthcoming report by the authors is to be devoted to the design, construction, instrumentation, and test execution of such a free-burning-fire facility, only a few additional comments are appended here. The walls of such a tunnel should be removable so that one may also seek elucidation of some aspects of large-area fires in the absence of a strong crosswind. In particular, one can check on the physical mechanism for augmentation of entrainment (over classical levels pertinent to higher, weakly buoyant portions of the plume) into the flaming, low-level portion of a plume sustained by burning of synthetic and/or natural polymers. The conjecture here is that the inevitably cellular nature of the low-level burning affords greater fire perimeter and hence increased entrainment, up to the altitude at which the cells merge into one column (above the completion-of-burning height). This cellular nature may be investigated by comparing the upflux over several cellular-plastic-"pool" configurations of equivalent total burning area. It is anticipated that one "plastic pool" does not entrain as much ambient air as an equivalent-area configuration with multiple pools. [Presumably the constraints of inviscid dynamics (i.e., the Bernoulli

equation) preclude indefinitely large augmentation of entrainment over classical levels.] The unconstrained plume above such a laboratory fire also permits one to measure the time-averaged total mass upflux, lateral temperature profile, and lateral updraft profile at each of several heights above the completion-of-burning altitude. These data can be used to ascertain whether entrainment is better described by relating plume-to-edge quantities associated with volumetric flux or with mass flux; the distinction is negligible for the classical context in which in-plume and ambient densities are of comparable value, but for highly exothermic combustion the distinction is likely to be of quantitative consequence. While the more appropriate formulation of entrainment may not [illegible] of indispensable value, it seems of enough quantitative significance to be well worth clarification.

Fourth, while execution of an urban-scale burn in a postblast environment is impractical, there have been over thirteen million-acre burns in North American wildlands since 1825 (Pyne 1982). There also have been many smaller-scale, but highly intense, forest and rural-area fires since World War II; these more recent events are often characterized by sophisticated aerial and ground-level monitoring of the environment, the topography, the fuel properties, the low-altitude-flow and plume behavior, the spread rate, and the residual unburned matter. While the earlier of these huge uncontrolled events entail less-than-ideal, often incomplete, eyewitness-type accounts, it seems a worthwhile investment to collect, evaluate, and summarize this unique source of data on urban-scale fire in heavily loaded dispersals of fuel.

Fifth, a key tenet of the proposed interpretation of the firestorm event is the appreciable reduction of entrainment whenever a buoyant column rises in a rotating surroundings (such that the lateral variation of angular momentum is nondecreasing). This reduction of entrainment permits the relatively undiluted updraft of strongly buoyant air to persist to exceptional altitude. The qualitative validity of the concept (specifically, that cyclostrophic balance tends to suppress radial influx into a buoyant column) seems established, but adequate quantitative work has yet to appear. The quantification would be of value in a variety of meteorological contexts, but since the firestorm is such an exceptional event in free burning, very high priority cannot be given to the instrumentation of a laboratory firewhirl-type apparatus (rotating screen surrounding a pool fire).

REFERENCES

Carrier, G., Fendell, F., Feldman, P., and Fink, S. (1982). Forced-convection extinction of a diffusion flame sustained by a charring body. Combustion Sci. & Tech. 28, 271-304.

Crutzen, P. J., and Birks, J. S. (1982). The atmosphere after a nuclear war: twilight at noon. Ambio 11 (No. 2-3), 114-125.

Holden, C. (1983). Scientists describe "nuclear winter." Science 222, 822-823.

Lee. S.-L., and Emmons, H. W. (1963). A study of natural convection above a line fire. J. Fluid Mech. 11, 353-368.

Morton, B. R. (1957). Buoyant plumes in a moist environment. J. Fluid Mech. 2, 127-144.

Morton, B. R. (1965). Modeling fire plumes. Tenth Symposium (International) on Combustion, 973-982. Pittsburgh, PA: Combustion Institute,

Pyne, S. J. (1982). Fire in America. Princeton, NJ: Princeton University.

Raloff, J. (1983). Beyond Armageddon. Science News 124, 314-317.

Rouse, H. (1947). Gravitational diffusion from a line source in two-dimensional flow. J. Appl. Mech. 14, A225-A228.

Simkin, T., and Fiske, R. S. (1983). Krakatau 1883--a centennial retrospective on the eruption and its atmospheric effects. Weatherwise 36, 244-254.

Taylor, G. I. (1961). Fire under the influence of natural convection. International Symposium on the Use of Models in Fire Research, 10-28. Washington DC: National Academy of Sciences - National Research Council (Publication 786).

Tilling, R. I. (1982). Volcanic cloud may alter earth's climate. National Geographic 162, 672-675.

Van Wagner, C. E. (1977). Conditions for the start and spread of crown fire. Canadian J. Forestry Res. 7, 23-34.

Woolley, A., and Bishop, C. (1983). Krakatoa! The decapitation of a volcano. New Scientist 99, 561-567.

Appendix A. Big Fires.*

BIG FIRES

by

George Carrier
Pierce Hall, Harvard University, Cambridge, MA 02138

and

Francis Fendell and Phillip Feldman
TRW Space and Technology Group, Redondo Beach, CA 90278

*Text of a technical paper to appear in the journal
Combustion Science and Technology 39 (1984), 135.

Abstract

We present here the results of a study of the buoyant column of air which accompanies a very large fire. In contrast to earlier studies (of smaller fires), we find it necessary to compute the pressure deficit in the plume for use in the significant modification of the classical entrainment rule appropriate for the burning region. Results are given for various levels of the heat release, atmospheric stability, and lateral size.

1. INTRODUCTION

Recent interest in atmospheric soot deposition from large fires has led to new, hydrocode estimates (Brode et al. 1983; Hassig & Rosenblatt 1983; Small et al. 1983) of plume heights which are significantly higher than those obtained using traditional plume theory (Morton et al. 1956). In view of this discrepancy, an attempt is made to incorporate into plume theory the hypothesized hydrodynamic effects of the pressure deficit inherent in a tall buoyant plume of large diameter.

We consider here a fully developed free-burning fire over a large area where there is neither a signficant cross wind nor enough ambient circulation to imply the development of a fire whirl. We shall construct a description of the axisymmetric convective column over this quasisteady fire by using a modification of the well-known integral-type treatment of weakly buoyant plumes (Morton et al 1956; Lee & Emmons 1961). Other extensions of the traditional transversely averaged treatment of weakly buoyant plumes have been considered (Morton 1965; Smith 1967); here, however, a fire of urban scale is of interest; the radius of the plume at low altitudes might be as large as 2 km, and its height could reach 10 km; for these proportions, the earlier theories may not suffice.

In a completely self-contained theory the burning rate, and hence the vertical heat flux, would be an output of the analysis. In this study, however, we postulate the burning rate and, on the hypothesis that the combustion has been completed at an altitude ($z = 0$) at which the entrained air is a few times that needed for stoichiometric burning, we have an a priori inference of the mass flux at that altitude. In such an analysis, of course, the domain lies in $-z_1 < z < z_2$ where $-z_1$ is the level at which the vertical mass flux is that corresponding to the pyrolization rate consistent with the adopted burning rate; z_2 is the altitude at which the vertical velocity becomes zero.

For an intense urban-scale fire, treatment of the plume from near-ground level to the height of stagnation of the updraft requires provision for (1) large lateral density variation, with its implication that the conventional Boussinesq approximation is <u>not</u> uniformly adequate; (2) large vertical rise

through much of the troposphere (variation of ambient density with altitude must be included); (3) a modification of the classical entrainment relation (the large inflow velocities associated with the burning zone of large fires are not consistent with the conventional entrainment law); and (4) a retention of the pressure gradient in the momentum balance for the burning zone. These last two provisions seem not to have been considered previously in non-rotating contexts, but it does seem apparent that the large radial velocities ($O[10^2$ ft/sec]) which are present in large fires could only be supported by pressure deficits of the order of several millibars. On an a priori basis, it seemed that this pressure deficit might also alleviate somewhat the strong buoyancy effects, but that alleviation seems to be of negligible size over most of the plume length.

In the real fire, the chemical heat release occurs over a limited axial distance, which, in our analysis, is taken to occur in $-z_1 < z < 0$. The distance (z_1) is that required for the entrainment of an amount of air which ensures the almost complete combustion of the pyrolizate. In experiments in which the fuel is inserted in momentum-dominated jets, it is known that the required entrainment is three times that required for stoichiometric proportions (J. E. Broadwell, private communication) but, as we argue in a later section, a somewhat larger amount of oxidant may be needed in buoyancy-dominated configurations.

There has been a thorough observational verification of the Morton-Taylor-Turner hypothesis that air is entrained in a weakly buoyant plume according to a simple rule wherein the far-field radial mass flux at a given level is an invariant multiple, α, of a characteristic feature of the vertical velocity at the same altitude. In the burning zone where the flow is very intense, it is highly probably (but only anecdotal accounts are available) that the radial inflow is more nearly in keeping with inviscid (infinite Reynolds number) hydrodynamics. Accordingly, we will explore here the implications of a burning-zone entrainment which is more consistent with observed fire plumes.

A convenient one-parameter characterization of the stability of a dry (fire-prone) atmosphere is furnished by the polytropic relation. The polytropic constant is related to the (constant) rate of thermal decrease with increase of

altitude. It turns out that a simple power law describes density decrease with altitude through the troposphere to an accuracy quite satisfactory for present purposes.

While no radiative transport is included in our analysis, we anticipate that, with minor modifications in the formulation, it could be incorporated; we also intend to extend this study to take account of (a) the evaporation and possible re-condensation of moisture initially contained in the fuel, and (b) the condensation of the water vapor initially contained in the ambient air.

2. ENTRAINMENT

When a solid fuel is distributed over a more-or-less horizontal surface in a very nonuniform way, the availability of pyrolizate also has a very nonuniform distribution, not only because of the variations in fuel per unit area but also because of the nonuniformity in the distribution of the radiative flux (from the fire above) on that fuel. Consistent with the foregoing variability is an intense nonhomogeneity in the density of the gas just above the surface which is fomented by the rather coarse-grained interpenetration of the cooler entrained air with the pyrolizate. That variability in the density distribution is further enhanced by the fact that the chemical heat release occurs at the boundary surfaces (interfaces) between blobs of air and blobs of pyrolizate. These enhanced density contrasts imply a vigorous autoconvection throughout the layer $-z_1 < z < 0$ ($z = 0$ lies at the loosely defined altitude at which the combustion of the rising gas has been completed). There is one important aspect of this particular autoconvective layer which differs markedly from others with which the authors are acquainted. In the convective layer of our sun, for example, the heat is supplied (radiatively) from below and the convection is necessitated by the instability of the configuration which would prevail in the absence of such convection. In the solar case, the governing parameters are so extreme that it is appropriate to assert that the horizontally averaged temperature through that layer has a distribution with altitude which is very close to adiabatic. Despite the fact that, in our configuration, the heat is released <u>within</u> the convecting layer, the large lateral scales and the intense density contrasts also imply a very vigorous convection with a horizontally averaged thermodynamic state whose vertical distribution could not be appreciably more stable than the (neutral) adiabatic one* but which <u>might</u> be somewhat less stable. Since the layer of interest has only (at most) a thickness of a few hundred feet, the neutral state is virtually one of constant (horizontally averaged) temperature. It is known that, in the burning region of the larger laboratory "floor fires", the entrainment of air into the rising column of gas greatly exceeds that which is postulated by Morton et al. (1956)

*Any greater degree of stability would act to depress the convection.

and which is verified experimentally for a weakly buoyant nonreacting plume. It is our hypothesis that this augmented entrainment is a consequence of the convective process described in the foregoing. The quantification of that argument follows.

Suppose that the typical radius of the rising column of gas in one of the cells is $\tilde{b}(z)$ and that its vertical velocity is $\tilde{w}$. If it were not hemmed in by other cells, the entrainment $\tilde{b}\tilde{u}$ into that column (where u is radial velocity) would be $\alpha\tilde{b}\tilde{w}$ under the Morton et al. rule. In this recipe, $\tilde{w}$ is several times W, the average upward velocity, but, in the cellular configuration, α might be somewhat depressed. Suppose that the cross-sectional area of the fire is $A = Nm\pi\tilde{b}^2 = \pi b^2$ where N is the number of cells and $m^{-1}(z)$ is some mean of the ratio of the updraft area in one cell to the total cell area. The gross upflow enhancement (i.e., the gross entrainment bu_e) at a level where the upflow in one cell has speed $\tilde{w}$ is $bu_e = N\alpha\tilde{b}\tilde{w} = (N/m)^{\frac{1}{2}}\alpha b\tilde{w}$, where subscript e denotes edge. However, $\tilde{w}$ must be at least of the order of mW and it follows that $bu_e > N^{\frac{1}{2}}\alpha bW$.

There is an important caveat to this argument! The foregoing microentrainment can occur at something close to the Morton rate only if the pressure deficit at $r = b$ can support the external inflow field. At the enormous Reynolds numbers of interest here, the Bernoulli estimate (subscript a denotes ambient)

$$u_e(z) = \left\{2\left[p_a(z) - p_e(z)\right]/\rho_e(z)\right\}^{\frac{1}{2}},$$

would limit that inflow and, avoiding niceties of detail, we suggest

$$u_e(z) = TS\left\{N^{\frac{1}{2}}\alpha W(z), \left[2(p_a(z) - p_e(z))/\rho_a(z)\right]^{\frac{1}{2}}\right\}, \tag{2.1}$$

where TS means "the smaller of".

We do not know N, of course, but for urban-scale fires, one can anticipate confidently that

$$u_e(z) = TS\left\{N^{\frac{1}{2}}\alpha W(z), \left[2(p_a(z) - p_e(z))/\rho_a(z)\right]^{\frac{1}{2}}\right\} \equiv \left[2(p_a(z) - p_e(z))/\rho_a(z)\right]^{\frac{1}{2}}. \tag{2.2}$$

Since the suggestion is somewhat gratuitous, we shall explore the consequences of (2.1) for several "evaluations" of $u_e(z)$, the largest of which will be (2.2).

When a jet of fuel entrains oxidant, it is known that for cases in which kinetic rates are not at issue, the oxidation is completed at that downstream position at which the entrained air is thrice that needed to provide stoichiometric proportions. For a fuel whose adiabatic stoichiometric flame temperature would be about 2100 K and whose pyrolization temperature is about 600 K, the requirement that the temperature change from the fuel bed surface to the end of the combustion zone be small would imply that the entrained air be six times the stoichiometric value*. With (1.1) and with this hypothesis concerning the amount of entrained air in hand, only an elementary calculation will be required to get a description of the macroscopic features of the lower part of the plume.

Above the fire, the autoconvection will decay rather quickly with height and the traditional entrainment rule should be applicable. Actually, of course, the autoconvection will begin to decay somewhat below the "fire-completion altitude" and the entrainment will have a smooth transitional character which is approximated only crudely by the discontinuous picture outlined in the foregoing account. It is unlikely that the prediction of plume height or of the macroscopic feature of the variation of the vertical velocity with altitude would be sensitive to this approximation.

---

*This value is arrived at by noting that the burning of a simple hydrocarbon with about fifteen times as much air by mass (a typical stoichiometric proportion) yields an increase in temperature of the fuel-air mixture of roughly 1800 K. If one then admixes five times more air, the increase in temperature distributed over the total mixture is reduced to 300 K. But an increase of 300 K over ground-level ambient characterizes pyrolysis temperatures for polymeric fuels of interest. Thus combustion with six times stoichiometric air implies a horizontally averaged burning-zone temperature which remains close to the pyrolysis temperature.

3. FORMULATION

3.1 Conservation Equations

The following inviscid axisymmetric conservation relations are adopted for the analysis of the plume (with subscripts r and z denoting partial differentiation with regard to the cylindrical and axial coordinates):

$$(\rho r w)_z + (\rho r u)_r = 0 \; ; \tag{3.1}$$

$$(\rho r u w)_z + r p_r + (\rho r u^2)_r = 0 \; ; \tag{3.2}$$

$$(\rho r w^2)_z + (\rho r u w)_r + (r p)_z + \rho r g = 0 \; ; \tag{3.3}$$

$$\left[\rho w r\, c_p (T - T_a)\right]_z + \left[\rho u r\, c_p (T - T_a)\right]_r + \rho w r \left[c_p T_{a,z} + g\right] = 0 \; . \tag{3.4}$$

The notation to be used is conventional: u and w are the radial and axial components of velocity; ρ, p, and T are the gas density, pressure, and temperature; g is the magnitude of the gravitational acceleration; c_p, c_v, R, and γ are, respectively, the heat capacity (taken as constant) at constant pressure, the heat capacity at constant volume, $(c_p - c_v)$, and (c_p/c_v). The subscript a denotes evaluation as $r \to \infty$, i.e., in the ambient, where quantities are a function of z only.

Since fire-prone ambients are usually quite low on moisture, the dry-adiabatic lapse rate,

$$T_{a,z} = - \frac{g}{c_p} \; , \tag{3.5}$$

is the limiting case of interest; exceptional, autoconvectively unstable lapse rates $[T_{a,z} < (-g/c_p)]$ are outside the scope of interest, which is concentrated on the cases $T_{a,z} > (-g/c_p)$. The neutrally stable case is referred to often as the adiabatic atmosphere, a name whose significance is made more apparent when (3.4) is manipulated into the equivalent form:

$$\left[\rho w r\, c_p (T - T_a)\right]_z + \left[\rho u r\, c_p (T - T_a)\right]_r + \frac{\rho w r}{\rho_a (\gamma - 1)} p_a \left[\ell n \left(\frac{p_a}{\rho_a^{\gamma}}\right)\right]_z = 0 \; . \tag{3.6}$$

In establishing the equivalence of (3.4) and (3.6), use was made of the hydrostatic relation in the ambient,

$$p_{a,z} = -\rho_a g \ , \tag{3.7}$$

and of the equation of state,

$$p = \rho R T \leftrightarrow p_a = \rho_a R T_a \ . \tag{3.8}$$

Our analysis will make use of the standard integral method, and ordinary differential equations in z will emerge from (3.1)-(3.3) and (3.6). Accordingly, we define $W(z)$, $\Psi(z)$, $b(z)$, $f(z)$, and $\sigma(z)$ as follows. For $r < b(z)$,

$$w(r,z) = W(z), \ p(r,z) = p_a(z)\,[1 - \sigma(z)] \ ,$$

$$\rho(r,z) = \rho_a(z)\,[1 - f(z)] \ , \ -\rho(r,z)\, r\, u(r,z) = \Psi(z)\, r^2/b^2(z) \ .$$

But for $r > b(z)$,

$$w(r,z) = 0 \ , \ p(r,z) = p_a \ , \ \rho(r,z) = \rho_a(z) \ , \ -\rho(r,z)\, r\, u(r,z) = \Psi(z).$$

Thus, aside from $\rho(r,z)\, r\, u(r,z)$, top-hat profiles are adopted.

When these profiles are substituted into (3.1)-(3.4), and when these equations are integrated over r from $r = 0$ to $r \to \infty$, we obtain, with the use of (3.7) and (3.8),

$$\left[\rho_a W b^2 (1 - f)\right]_z = 2\alpha\, \rho_a W b \ , \tag{3.9}$$

$$p_a b \sigma = \left(\frac{\alpha b^2 W^2 \rho_a}{3}\right)_z \tag{3.10}$$

$$\left[\rho_a (1 - f) W^2 b^2\right]_z - (p_a b^2 \sigma)_z - \rho_a g f b^2 = 0 \ , \ . \tag{3.11}$$

$$\left[p_a \, (f - \sigma) \, W b^2 \right]_z = - \, p_a \, (1 - f) \, W b^2 \left(\frac{2}{\gamma} \right) \left[\ell n \left(p_a / \rho_a^{\gamma} \right) \right]_z \, . \qquad (3.12)$$

In (3.9) and (3.10), the already-discussed classical entrainment relation,

$$\mathcal{V}(z) = \alpha \, \rho_a(z) \, b(z) \, W(z) \, ,$$

is used, where $\alpha = O(0.1)$.

Equations (3.9), (3.11), and (3.12), with $\sigma = 0$, are minor modifications of the classical plume equations, and they have the same peculiar structure near the top of the plume. More explicitly, near $z = z_2$ (where $W = 0$), $b \sim (z_2 - z)^{-\frac{1}{4}}$, $W \sim (z_2 - z)^{\frac{1}{2}}$, and f remains finite (and nonzero) as $(z_2 - z) \to 0$. Despite this unphysical local behavior, the suitability of the predictions of that plume theory is well established.

When (3.9)-(3.12) are used, the locally commensurate behaviors are $b \sim (z_2 - z)^{-\frac{1}{2}}$, $W \sim (z_2 - z)$, $f \sim (z_2 - z)$, and $\sigma \sim (z_2 - z)$. As in the classical theory, the mass flux through z_2 is not zero, but that artifact of the entrainment law is no more reprehensible in this model than in the earlier one. Furthermore, as we shall see, the contribution of σ to (3.10) and (3.11) is negligibly small except in the immediate neighborhood of z_2, and, without the loss of any meaningful accuracy, we neglect the contribution containing σ in (3.11) and (3.12). Equation (3.10) remains a recipe for σ from which we can obtain the pressure deficit at $z = 0$, and thereby estimate the entrainment in the fire zone, $z < 0$.

4. ORDERS OF MAGNITUDE

It is useful to estimate the orders of magnitude of the state variables and of the length scales on which they vary, both to justify the foregoing statements about the role (or lack thereof) of the pressure deficit and also to get an a priori estimate of the plume height. We start with values at $z = 0$ of dependent variables b and f, and note that the ranges of interest are $0 < b_0 \ll 2$ km and $0 < f_0 \leq \frac{1}{2}$, but the values of great interest here are $b_0 = 2$ km and $f_0 = \frac{1}{2}$. The notation is $f(0) = f_0$, $b(0) = b_0$.

According to (3.9), the fractional increase in $\rho W b^2$ over the height of the phenomenon is

$$\frac{\Delta(\rho W b^2)}{\rho W b^2} \doteq \frac{\alpha z_2}{b} \quad . \tag{4.1}$$

When b is of order z_2, this fractional change is small and (3.12) then implies

$$\frac{f_z}{1 - f} \doteq - \frac{2}{\gamma} \left[\ell n \left(\frac{p_a}{\rho_a^{\gamma}} \right) \right]_z = - O\left(\frac{1}{5 \text{ km}} \right) \quad . \tag{4.2}$$

This relation, in turn, suggests, if z is in km,

$$\frac{1 - f}{1 - f_0} = O[\exp(z/5)] \quad . \tag{4.3}$$

For small f_0, f vanishes at about $z \doteq 5f_0$; in particular, for $f_0 = \frac{1}{2}$, f becomes zero at $z \doteq 3.5$ km. Thus, $z_2 = O(5f_0 \text{ km})$.

The vertical velocity is driven by the buoyancy term in (3.11), possibly with alleviation through the pressure-gradient term, so W^2 can be estimated, with the aid of (4.1), by

$$W^2 = O\left(\frac{f_0}{1 - f_0} g z_2 \right) \quad . \tag{4.4}$$

The reader may wish to recall that there is no implication that the updraft W actually reaches the value $[g f_0 z_2/(1 - f_0)]^{\frac{1}{2}} \doteq 160$ m/sec, but it does suggest that some moderate fraction of that value can be expected. The largest fuel loading which can be attributed to an urban area is 15 g/cm^2. Pyrolization of that fuel will occur at about 600 K. If the horizontally averaged temperature is to change very little with height, then (from Section 2) the entrained air at the fire-completion level will be six times stoichiometric. The time scale on which the preponderance of fuel was consumed during the most intense phase of the Hamburg, Germany fire of July 28, 1943 was about two hours. Use of these numbers gives a value for the updraft W as follows:

$$W \sim \frac{[15(g_{fuel}/cm^2)][90\ g_{gas}/g_{fuel}]}{[7200\ sec][0.5x10^{-3}\ g_{gas}/cm^3]} \sim 3.5\ m/s\ , \tag{4.5}$$

a value which is a very small fraction of the 160 m/s mentioned above. We shall return to this difficulty.

The general size of the pressure deficit can now be estimated using (3.10) and (4.4); if $b(0) \approx b_0$, $\gamma p_a(0)/\rho_a(0) = a_0^2$, then

$$\sigma = 0\left[\frac{\alpha \gamma^2 g\ b_0\ f_0}{3\ a_0^2\ (1 - f_0)}\right]\ , \tag{4.6}$$

which, for $b_0 \doteq 2$ km, gives approximately 10 millibars. This exceeds greatly the pressure deficit needed in $-z_1 < z < 0$ to permit inflow rates which have been observed [in, for example, the Hamburg fire (Carrier et al. 1983)], or which would be consistent with the observation that combustion is completed in a height, z_1, of about a hundred meters.

The discrepancies between the estimates given in (4.4) and (4.5), and the estimates inferred from experience, suggest one more characteristic feature to be expected in a large-area fire. It is known that the strongly wind-driven conflagrations known as crown fires (and other very energetic fires) have a structure

resembling that of Fig. 1. In the fire depicted in that figure, the heat which is released in A-B, and the still unburned pyrolizate which may accompany the burned gases, are carried almost horizontally into the almost vertically rising plume. In an approximately axially symmetric configuration with an intense radial inflow, we should expect that the outer reaches of the burning area would have the same convective aspects, and that the burning pyrolizate would be swept at low altitude (as in Fig. 2) into the base of a column of gas whose radius is smaller than that of the burning area and within which the processes described in Section 2 would take place. In order to formulate the problem in a way which, without completely arbitrary assignment of b_o, incorporates these considerations, we define two extreme cases. In the first, $b_o = R$, the radius of the fire. It is readily established that the exceptionally rapid necking shown in Fig. 3 would characterize the solution. Furthermore, the pressure deficit at $z = 0$ for that solution would permit the inflow needed to supply the (six times stoichiometric) mass flux through $z = 0$ to be incorporated in a distance z_1 of some 50 m. At the other end of the spectrum of remotely plausible values of b_o is that for which, as indicated in Fig. 4, $b_z(0)$ is zero. For that hypothesized value, b_o comes out to be 440 m and z_1 is 770 m.* Neither

---

*If the requirement $b_z(0) = 0$ is liberalized slightly to the requirement $[\rho_a(1-f)b^2]_z = 0$ at $z = 0$, then (3.9) gives for $f \doteq \frac{1}{2}$,

$$W_z(0) \doteq 4\alpha\, W(0)/b_o .$$

Also, (3.11) gives, without the pressure-gradient term,

$$2W(0)\, W_z(0) = g.$$

Combining these two rleations, one has

$$b_o = \frac{8\alpha W^2(0)}{g} = \frac{8\alpha W^2(0)\, b_o^4}{g\, b_o^4} .$$

But, from the estimate (4.5), if R is recalled to be the fire radius,

$$W^2(0)\, b_o^4 = (3.5\ \mathrm{m/sec})^2\, R^4;$$

hence,

$$b_o^5 = \frac{8\alpha}{g}\left(12\ \frac{\mathrm{m}^2}{\mathrm{sec}^2}\right) R^4 = R^5\left(\frac{1\ \mathrm{m}}{R}\right) .$$

(Continued next page)

of these values for b_0 gives a description commensurate with observation (e.g., Hamburg) and the range of possibilities lies well within 400 m < b_0 < 2000 m. If it turns out that the overall plume height and general geometry are insensitive to variations in b_0 over this range, a more definitive choice for b_0 is not needed.

Finally, before we carry out the analysis appropriate to the foregoing, we close the order-of-magnitude discussion by noting that, even if the estimates of (4.3) and (4.4) were not too large, the size of the pressure contributions to each of (3.11) and (3.12) could be, at most, of the order of 1% of the more important terms except near z_2, where, as noted in earlier discussion, the structure given by the model is unrealistic but harmless.

For R = 2 km, $b_0 \doteq 440$ m, and $W(0) \doteq 70$ m/s. Continuity considerations in $-z_1 < z < 0$ suggest, if $h \equiv -z_1$,

$$\pi b_0^{\,2}\, W(0) = 2\pi b_0 h \left[\left[\frac{2\sigma(0)}{\gamma} \right] \left[\frac{\gamma p_a(0)}{\rho_a(0)} \right] \right]^{\frac{1}{2}},$$

and, from (4.6),

$$\sigma \doteq \frac{\alpha b_0 g}{3 a_0^{\,2}} = 1.3 \times 10^{-3} .$$

Hence,

$$h \doteq \frac{b_0 W(0)}{2 (20)^{\frac{1}{2}}} \doteq 770 \text{ m.}$$

5. FINAL FORMULATION

The description of the state variables in $0 < z < z_2$ are those profiles given below (3.8). The differential equations which govern W, σ, f, and b are those approximations to (3.9)-(3.12) which emerge when the influence of the pressure deficit on the dynamics is ignored, viz.,

$$\left[\rho_a W b^2 (1 - f)\right]_z = 2\alpha\rho_a W b \ , \tag{5.1}$$

$$\left[\rho_a (1 - f) W^2 b^2\right]_z - \rho_a g f b^2 = 0 \ , \tag{5.2}$$

$$\left[p_a f W b^2\right]_z = - p_a (1 - f) W b^2 \left(\frac{2}{\gamma}\right) \left[\ell n \ (p_a/\rho_a{}^{\gamma})\right]_z \ , \tag{5.3}$$

$$p_a b\sigma = \left(\frac{\alpha b^2 W^2 \rho_a}{3}\right)_z \ . \tag{5.4}$$

The boundary conditions applicable to the first three of these are:

$$p_a(0) \ f(0) \ W(0) \ b^2(0) = \frac{\gamma - 1}{\pi\gamma} \ \dot{Q} \ , \tag{5.5}$$

where $\dot{Q}$, the total heat release rate, is given by

$$\dot{Q} = Q A m/\tau \ , \tag{5.6}$$

where Q is the heat of combustion per unit mass of fuel (typically 19 kJ/g), $A(=\pi R^2)$ is the burning area, m is the mass of fuel per unit area (as much as 15 g/cm^2 in major cities), and τ is the time scale on which the mass m is consumed (about 2 hours in the great Hambury fire);

$$\rho_a(0) \left[1 - f(0)\right] W(0) \ b^2(0) = \frac{\dot{Q}\nu}{\pi Q} \ , \tag{5.7}$$

where ν is the mass of air which must be mixed with a unit mass of fuel to produce a mixture six times as lean as stoichiometric.

The third boundary condition requires the specification of b(0), i.e.,

$$b(0) = b_o. \tag{5.8}$$

From Section 4, the range of b_o of interest is $R \geqslant b_o \geqslant b_{oo}$, where $b_o = b_{oo}$ implies $b_z(0)=0$. Actually, the smallest credible b_o is that for which the pressure discrepancy σ is adequate*, in accord with (2.2), to support the inflow into the fire which will supply the mass flux given by (5.7); that is, b_o must be such that

$$2\pi\rho_a(0)\left[2\,p_a(0)\,\sigma(0)/\rho_a(0)\right]^{\frac{1}{2}} b_o\, z_1 = \frac{\dot{Q}\nu}{Q} \quad . \tag{5.9}$$

Unfortunately, z_1 is not known in an a priori basis and the criterion becomes a recipe for z_1.

In any case, we may adopt an inverse method of solution and integrate (5.1)-(5.3), subject to the boundary conditions (5.5), (5.7), and (5.8), and to the ambient-defining relations (3.7), (3.8), and $p_a \sim \rho_a^{\kappa\gamma}$, where κ is a given constant (in general, $\gamma^{-1} < \kappa < 1$). The method of solution is inverse in that several trial values for the unknown b(0) are to be investigated for each case (fixed $\dot{Q}$, Q, ν, κ). From (5.4) the pressure deficit may be found a posteriori throughout the weakly buoyant domain $0 < z < z_2$. We reiterate that (from Section 4) the range of b(0) is restricted by the fact that too small values lead to $\sigma < 0$ and too large values lead to implausibly rapid necking in of the plume just above the completion-of-burning plane $z = 0$. Actually, it seems worth noting that results could be found at $z = 0$ for b, f, and W, and for their first derivatives, as well as for σ, without continuing the results to larger z.

---

*For b(0) slightly smaller than b_{oo}, W_z is large and negative, so that, from (3.10), the dimensionless pressure deficit $\sigma(0)$ becomes negative.

Equations (5.5) and (5.7) imply

$$f(0) = \frac{Q/[\nu c_p T_a(0)]}{1 + Q/[\nu c_p T_a(0)]} \quad . \tag{5.10}$$

From (5.10), (5.8), and either (5.5) or (5.7), we obtain $W(0)$; $f_z(0)$, $W_z(0)$, $b_z(0)$, $\sigma(0)$ follow from (5.1)-(5.4).

The inverse solution is completed by obtaining results for the burning zone $0 > z > -z_1$, where $z_1(>0)$ is to be found by the criterion that the mass flux at the ground plane is pure pyrolizate without any air dilution. Explicitly, since the thermodynamic variables p_a, ρ_a, f, σ are approximated adequately through the burning zone by their values at $z = 0$, the position z_1 is given by

$$b^2(-z_1)\, W(-z_1) = b^2(0)\, W(0)/\nu.$$

A procedure for finding $b(z)$, $W(z)$ in the burning zone is the topic of the next paragraph. Since $b(-z_1) \equiv R$, the radius of the burning zone, we find from (5.6) that ($A = \pi R^2$)

$$\frac{m}{\tau} = \frac{\dot{Q}}{QA} \quad . \tag{5.11}$$

That is, adoption of heat release rate $\dot{Q}$ and fuel exothermicity Q implies a plausible range of values for the radius $b(0)$ of the plume at the completion-of-burning plane; in turn, each radius $b(0)$ implies a fire area A and a value for the ratio of fuel loading m to duration of burning τ. Of course, tabulation of enough inverse cases furnishes solution of the directly posed problem by interpolation and/or extrapolation.

From (3.9) and (3.11), appropriately modified to reflect the approximate constant character of p_a, ρ_a, f, σ (assigned their $z = 0$ values) in the burning zone $0 > z > -z_1$, we obtain two equations for the two unknowns $b(z)$, $W(z)$:

$$\rho_a(1-f)(Wb^2)_z = 2\rho_a b\,(2\beta p_a \sigma/\rho_a)^{\frac{1}{2}} , \tag{5.12}$$

$$\rho_a(1-f)(W^2b^2)_z - p_a\,\sigma(b)_z = \rho_a g f b^2. \tag{5.13}$$

The entrainment speed used in (5.12) is taken in accord with (2.2), except that a constant factor β has been included to permit inclusion of losses from inviscid values ($1 \geq \beta > 0$, where β is assigned). It is convenient to introduce the ambient speed of sound a_o, where

$$a_o = [\gamma p_a(0)/\rho_a(0)]^{\frac{1}{2}} . \tag{5.14}$$

Hence,

$$(Wb^2)_z = \frac{2a_o}{1-f}\left(\frac{2\beta\sigma}{\gamma}\right)^{\frac{1}{2}} b , \tag{5.15}$$

$$(W^2b^2)_z - \frac{a_o^2\sigma}{(1-f)\gamma}(b^2)_z = \frac{fg}{1-f} b^2 . \tag{5.16}$$

We nondimensionalize by introducing

$$X = \left[\frac{1-f}{2^3\beta}\right]^{\frac{1}{2}} \frac{fg\gamma}{a_o^2\sigma} b , \quad U = \left[\frac{(1-f)\gamma}{\sigma a_o^2}\right]^{\frac{1}{2}} W , \quad s = \frac{f\gamma g}{\sigma a_o^2} z . \tag{5.17}$$

We obtain, upon solving for the derivatives,

$$(U^2 + 1)(X^2)_s = 2UX - X^2 , \tag{5.18}$$

$$X^2(U^2 + 1)\,U_s' = UX^2 - X(U^2 - 1) . \tag{5.19}$$

In the phase plane,

$$\frac{dX}{dU} = \frac{X(2U - X)}{2(XU - U^2 + 1)} , \tag{5.20}$$

$$\frac{ds}{dU} = \frac{X(U^2 + 1)}{XU - U^2 + 1} , \tag{5.21}$$

where s may be found sequentially. Since z = 0 corresponds to s = 0, and since X(0) may be found from b(0) [and U(0) from W(0)] by (5.17), (5.20) and (5.21) may be solved subject to the constraints

$$U = U_0 : X = X_0, \; s = 0 \; , \tag{5.22}$$

where U_0 denotes U(0) and X_0 denotes X(0). The stopping condition stated above (5.11) is rephrased

$$X^2(-s_1)\, U(-s_1) = \frac{X_0^{\,2} U_0}{\nu} \; . \tag{5.23}$$

Equation (5.20) is now examined to characterize solutions in the burning zone (Figure 5); the quadrant U > 0, X > 0 is of physical interest. There is a singular curve that behaves as

$$U \sim 1 + \frac{1}{3} X + \ldots . \quad \text{as } X \to 0 \; ; \tag{5.24}$$

$$U_X \sim \frac{3}{4} \qquad \text{as } X \to \infty \; . \tag{5.25}$$

This singular curve separates solutions of physical interest from other solutions. Solutions of physical interest have $U_X < 3/4$ at large X; these solutions permit U → 0 for some value of positive X. In particular, these solutions have dX/dU = 0 at U = X/2; thus, if $X_0 > U_0/2$, then X monotonically increases as U monotonically decreases and hence no necking occurs in the burning zone; otherwise, X initially decreases as U decreases for larger values of U, though X increases for small enough U. [Solutions with $U_X > 3/4$ are not of physical interest because U > 1 for all X; these mathematical solutions are probably more conveniently studied by examining U(X), i.e., by inverting (5.20), such that the locus $XU = U^2 - 1$ defines zero slope for solutions.]

6. RESULTS

Since very few fires of the scale of interest here have occurred, and fewer still have been reported, only limited parameter variation (of Q, m/τ, A, ν, κ) is undertaken. As already noted, the inverse procedure for solution adopted is to specify the quantities Q and the product $A(m/\tau)$, i.e., the quantities Q and $\dot{Q}$, and then to infer [by means of trials with b(0)] what value of (m/τ) is compatible with a particular value of A. In this way, for example, it is possible with systematic investigation to find the fire behavior, for fixed fire area A, as the fuel loading per burn time, m/τ, is increased.

For brevity of reference, the following set of parametric assignments is termed nominal (alternatively, the set is termed the Hamburg case, because it is the authors' best estimate of values pertinent to that severe fire):

$b_o = 500$ m, $c_p = 1.0 \cdot 10^3$ m^2/s^2/K , $g = 9.8$ m/s^2 , $p_o = 1.0 \cdot 10^5$ N/m^2,

$Q = 1.865 \cdot 10^7$ J/kg , $\dot{Q} = 1.0 \cdot 10^{12}$ W , $T_o = 300$ K,

$\alpha = 0.1$, $\beta = 1.0$, $\gamma = 1.4$, $\kappa = 0.95$, $\nu = 135$.

In accordance with the last paragraph, the quantities $\dot{Q}$ and b_o are specified, and the quantities A and (m/τ) derived, in the inverse approach adopted. For completeness, computation reveals $A = 12$ km^2, $(m/\tau) = 4.46 \cdot 10^{-3}$ kg/m^2/s; indeed, $\dot{Q}$ and b_o were chosen (by trial and error) to achieve these values. Unless explicitly stated otherwise, in all computations to be reported, parameters take their nominal values.

First, generic results are given for the initial-value problem for the burning zone. Figure 5 presents solutions to (5.20) and (5.22) for $U_o = 5$ for a series of values of X_o. The singular solution (dashed curve) emanating from $U = 1$, $X = 0$ distinguishes physically interesting solutions (solid curves) from physically irrelevant solutions (dotted curves). For large enough X_o, the dimensionless plume radius X increases monotonically as the dimensionless plume updraft U decreases. Figures 6 and 7 present the values of dimensionless distance s (below the completiong-of-burning plane) associated with the values of U,X of Figure 5; these results are obtained from (5.21) and (5.25).

Figures 8 - 10 present results for the initial-value problem for $z > 0$, i.e., above the completion-of-burning plane, from (5.1)-(5.8), for the nominal case. As modest necking in of the plume occurs with altitude, the updraft increases from about 10 m/s to about 50 m/s; then the updraft decreases with increasing altitude, such that the plume reaches a height of almost 10 km (cf. results cited at the beginning of Section 1). The fractional in-plume density discrepancy from ambient, f, vanishes several kilometers below the zero-updraft altitude, while the fractional in-plume pressure discrepancy from ambient, σ, vanishes just a few kilometers above the completion-of-burning plane (the large negative gradient of σ at the plume top is included purely for curiosity and is an artifact of a formulation that is incomplete near the plume top). The column radius and updraft in the flame zone are presented in Figure 11; the flame height is found to be about 90 m; over this altitude the updraft rises from nil (at the ground) to about 10 m/s, and the column radius decreases from about 2 km to 0.5 km.

Figures 12 and 13 present results for plume radius b and updraft W for the lowest 100 m of the buoyant plume above the completion-of-burning plane, $z = 0$; these results are for the nominal Hamburg data (except that b_o is varied). Since the results tend to merge above 100 m, it is seen that larger values of b_o imply implausibly large necking, whereas smaller values of b_o imply rather large updrafts just above the burning zone. Figures 14 and 15 present associated values for b and W in the burning zone, below $z = 0$ (solid lines); in addition to the solid-line results for $\beta = 1$ (inviscid dynamics), results for $\beta = 0.5$ (losses ascribed to friction) are given by dashed lines. The narrower plumes at the completion-of-burning plane are seen to be characterized by appreciably greater flame heights and greater sensitivity to frictional loss in the strongly buoyant region. If losses enter in the burning zone, then smaller fuel loadings over larger areas tend to give the same weakly buoyant-plume properties as would smaller burning areas with heavier loadings under purely inviscid dynamics, the total heat release rate $\dot{Q}$ being held fixed. This property of the model also may be noted from Table 1; Table 1 also indicates how other parametric variations from nominal alter the flame zone (see also Figures 16 and 17). Particular insensitivity of the flame-zone characteristics to atmospheric stability, reflected by κ,

and particular sensitivity to the dilution required for an isothermal burning zone, reflected by ν, are noteworthy. For the parametric variations collected at the top of Table 1 and displayed in Figures 16 and 17, it is reiterated that all parameters not called out have their nominal values; in particular, b_o = 500 m.

Virtually exclusive attention has been concentrated thus far on total heat release rate $\dot{Q} = 10^{12}$ W; this exceptionally large value is of especial interest because it characterized the Hamburg fire, and it seems rarely (if ever) to have been exceeded. Table 2 presents results for other heat fluxes; larger heat fluxes imply larger burning areas with heavier fuel loadings (or shorter burn-up time) for fixed fuel exothermicity--indeed, very large heat-release rate is incompatible with too narrow a plume, and rather moderate heat-release rate is incompatible with too wide a plume, according to the model.

While complete parametric investigation of the existing model, or refinement of the model (e.g., near the plume top), remains to be undertaken, perhaps the next step ought to be experimental investigation of the validity of the statements utilized to represent burning-zone entrainment. While larger-scale tests ultimately would seem required, laboratory-scale experiments may suffice to initiate validation of the key conjecture: enhanced fire perimeter in the inevitably multicellular burning zone of a fire results in enhanced low-level induction of ambient air [with the limit on enhancement (over Morton-Taylor-Turner values) expressed by inviscid dynamics, i.e., by the Bernoulli equation].

The study reported here was undertaken largely in the hope that one could estimate the heights to which the plumes of very large fires might extend. To generate these estimates it has been necessary to hypothesize that, even when the plume does not have a large aspect ratio, the ideas underlying the Morton-Taylor-Turner buoyant-column approach are still valid; the arguments never really did depend on the slenderness of the plume and there is little reason to doubt the validity of this approach for the extraction of the large-scale characteristics of large fires. It also was necessary to hypothesize that the entrainment limitation implied by the Bernoulli recipe could be used in a very simple

form for the altitudes within which the burning occurs, and to hypothesize that a strong convective mixing was implied therein by the heterogeneity of the fuel-consumption distribution. As it happens, such results as plume height and high-altitude diameter are not particularly sensitive to variations on these hypotheses, and the validity of our results is more nearly assured than is the detailed validity of the underlying conjectures. The results that emerge suggest strongly that, even for a fire whose fuel bed has the scale and "loading" of a major city, the plume is confined largely to the troposphere, except possibly in cases where very humid low level air would strongly augment the lifting process (a mechanism which has not been incorporated herein), and/or in cases where a strong, meteorological low-pressure feature was already centered near the city when the fire began (Carrier and Fendell 1983).

Acknowledgment

The authors are grateful to technical monitors Mike Frankel and Tom Kennedy for the opportunity to pursue this investigation. The authors also are grateful to Ann McCollum for preparation of the manuscript and to Asenatha McCauley for preparation of the figures. This work was supported under Defense Nuclear Agency Contract DNA-001-83-C-0104.

REFERENCES

Brode, H.L., Larson, D.A., & Small, R.D. (1983). Hydrocode studies of flows generated by large area fires. Proceedings 17th Asilomar Conference on Fire and Blast Effects of Nuclear Weapons, 48-53. Livermore, CA: Lawrence Livermore National Laboratory Report CONF-8305107.

Carrier, G.F., Fendell, F.E., and Feldman, P.S. (1983). Firestorms. Fire Dynamics and Heat Transfer, 55-64, New York, NY: American Society of Mechanical Engineers, Heat Transfer Division, Vol. 25.

Hassig, P.J. & Rosenblatt, M. (1983). Firestorm formation and environment characteristics after a large-yield nuclear burst. Proceedings 17th Asilomar Conference on Fire and Blast Effects of Nuclear Weapons, 54-59. Livermore, CA: Lawrence Livermore National Laboratory Report CONF-8305107.

Lee, S.-L. & Emmons, H.W. (1961). A study of natural convection above a line fire. J. Fluid Mech. 11, 353-368.

Morton, B.R. (1965). Modeling fire plumes. Tenth Symposium (International) on Combustion, 973-982. Pittsburgh, PA: Combustion Institute.

Morton, B.R., Taylor, G.I., & Turner, J.S. (1956). Turbulent gravitational convection from maintained and instantaneous sources. Proc. Roy. Soc. 234A, 1-23.

Small, R.D., Larson, D.A., and Brode, H.L. (1983). Fluid dynamics of large area fires. Fire Dynamics and Heat Transfer, 47-54. New York, NY: American Society of Mechanical Engineers, Heat Transfer Division, Vol. 25.

Smith, R.K. (1967). Radiation effects on large fire plumes. Eleventh Symposium (International) on Combustion, 507-515. Pittsburgh, PA: Combustion Institute.

Table 1. Parametric Variation at Heat Flux $\dot{Q} = 10^{12}$ W

Case	Q(J/s)	A(km^2)	m/τ ($kg/m^2/s$)
Hamburg	$1.865 \cdot 10^7$	12.0	$4.46 \cdot 10^{-3}$
$\dot{Q} = 1.2 \cdot 10^{12}$ W	$1.865 \cdot 10^7$	15.2	$4.22 \cdot 10^{-3}$
$Q = 1.492 \cdot 10^7$ J/s	$1.492 \cdot 10^7$	20.8	$3.22 \cdot 10^{-3}$
$\kappa = 0.85$	$1.865 \cdot 10^7$	12.0	$4.48 \cdot 10^{-3}$
$\nu = 90$	$1.865 \cdot 10^7$	4.4	$1.20 \cdot 10^{-3}$
For $\beta = 1$:			
b_o(km) = 2.0	$1.865 \cdot 10^7$	15.3	$3.50 \cdot 10^{-3}$
1.8		13.1	$4.09 \cdot 10^{-3}$
1.6		11.2	$4.80 \cdot 10^{-3}$
1.4		9.7	$5.54 \cdot 10^{-3}$
1.2		8.5	$6.29 \cdot 10^{-3}$
1.0		7.8	$6.92 \cdot 10^{-3}$
0.9		7.8	$6.88 \cdot 10^{-3}$
0.7		8.4	$6.37 \cdot 10^{-3}$
0.5		12.0	$4.46 \cdot 10^{-3}$
0.4		15.3	$3.51 \cdot 10^{-3}$
0.35		15.3	$3.51 \cdot 10^{-3}$
0.3		10.5	$5.11 \cdot 10^{-3}$
For $\beta = 0.5$:			
b_o(km) = 2.0	$1.865 \cdot 10^7$	16.6	$3.23 \cdot 10^{-3}$
0.9		11.0	$4.87 \cdot 10^{-3}$
0.7		13.3	$4.04 \cdot 10^{-3}$
0.5		21.7	$2.47 \cdot 10^{-3}$
0.4		31.3	$1.71 \cdot 10^{-3}$
0.35		40.1	$1.34 \cdot 10^{-3}$
0.30		47.0	$1.14 \cdot 10^{-3}$

Table 2. Parametric Variation for Various Heat Fluxes

Case	Q(J/kg)	A(km^2)	m/τ ($kg/m^2/s$)
For $\dot{Q} = 10^{10}$ W:			
b_o(km) = 2.0	$1.865 \cdot 10^7$	---	---
1.4		6.6 *	$8.18 \cdot 10^{-5}$
0.9		2.7 *	$1.98 \cdot 10^{-4}$
0.7		1.6	$3.28 \cdot 10^{-4}$
0.5		0.9	$6.04 \cdot 10^{-4}$
0.35		0.5	$1.17 \cdot 10^{-3}$
0.3		0.4	$1.51 \cdot 10^{-3}$
For $\dot{Q} = 10^{11}$ W:			
b_o(km) = 2.0	$1.865 \cdot 10^7$	13.4 *	$4.01 \cdot 10^{-4}$
1.4		6.5 *	$8.20 \cdot 10^{-4}$
0.9		3.0	$1.76 \cdot 10^{-3}$
0.7		2.0	$2.63 \cdot 10^{-3}$
0.5		1.4	$3.89 \cdot 10^{-3}$
0.35		1.2	$4.35 \cdot 10^{-3}$
0.3		1.3	$4.20 \cdot 10^{-3}$
For $\dot{Q} = 10^{12}$ W:			
b_o(km) = 2.0	$1.865 \cdot 10^7$	15.0	$3.50 \cdot 10^{-3}$
1.4		9.7	$5.54 \cdot 10^{-3}$
0.9		7.8	$6.88 \cdot 10^{-3}$
0.7		8.4	$6.37 \cdot 10^{-3}$
0.5		12.0	$4.46 \cdot 10^{-3}$
0.35		15.3	$3.51 \cdot 10^{-3}$
0.3		10.5	$5.11 \cdot 10^{-3}$
For $\dot{Q} = 10^{13}$ W:			
b_o(km) = 2.0	$1.865 \cdot 10^7$	50.0	$1.07 \cdot 10^{-2}$
1.4		64.7	$8.29 \cdot 10^{-3}$
0.9		98.8	$5.43 \cdot 10^{-3}$
0.7		13.8	$3.89 \cdot 10^{-2}$
0.5		---	---
0.35		---	---
0.3		---	---

Note: Asterisk (*) denotes cases for which $z_1 < 10$ meters such that $b_o \approx R$. A dashed line denotes cases for which no solution exists.

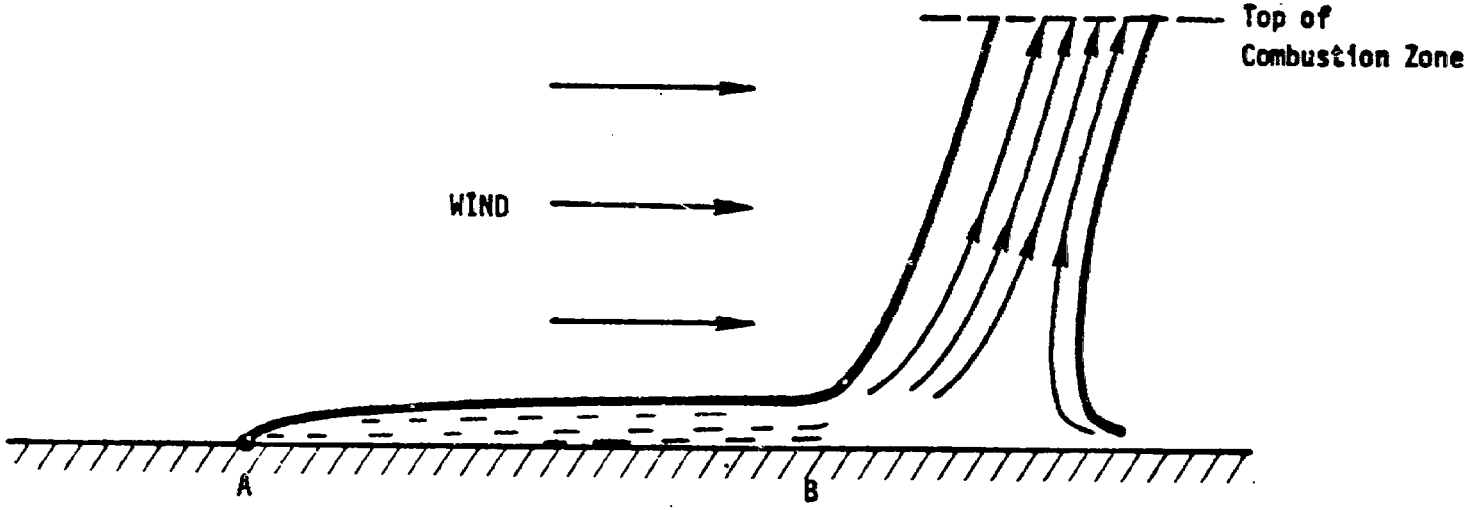

Figure 1. Schematic of the structure of a crown fire. Heat is released over the expanse A-B.

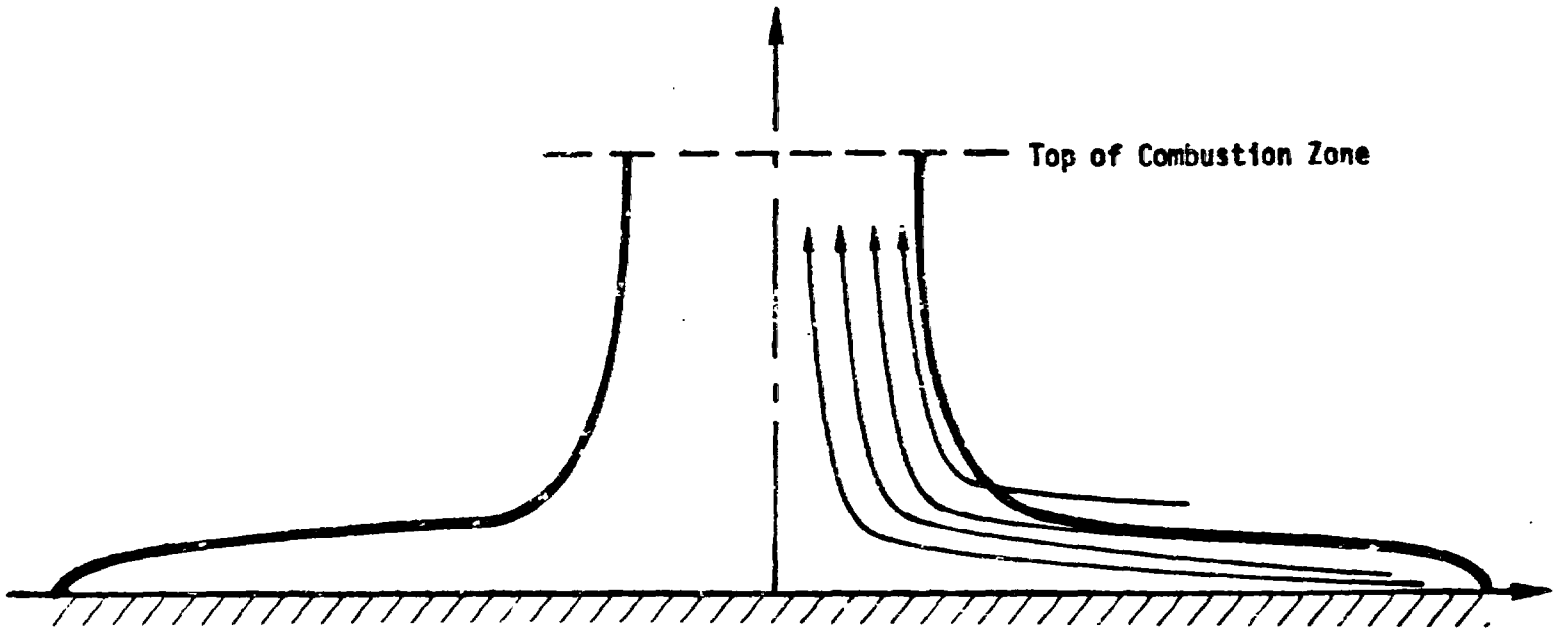

Figure 2. Schematic of the structure of a large-area fire in which the radius of the convective column at its base is smaller than the radius of the burning area.

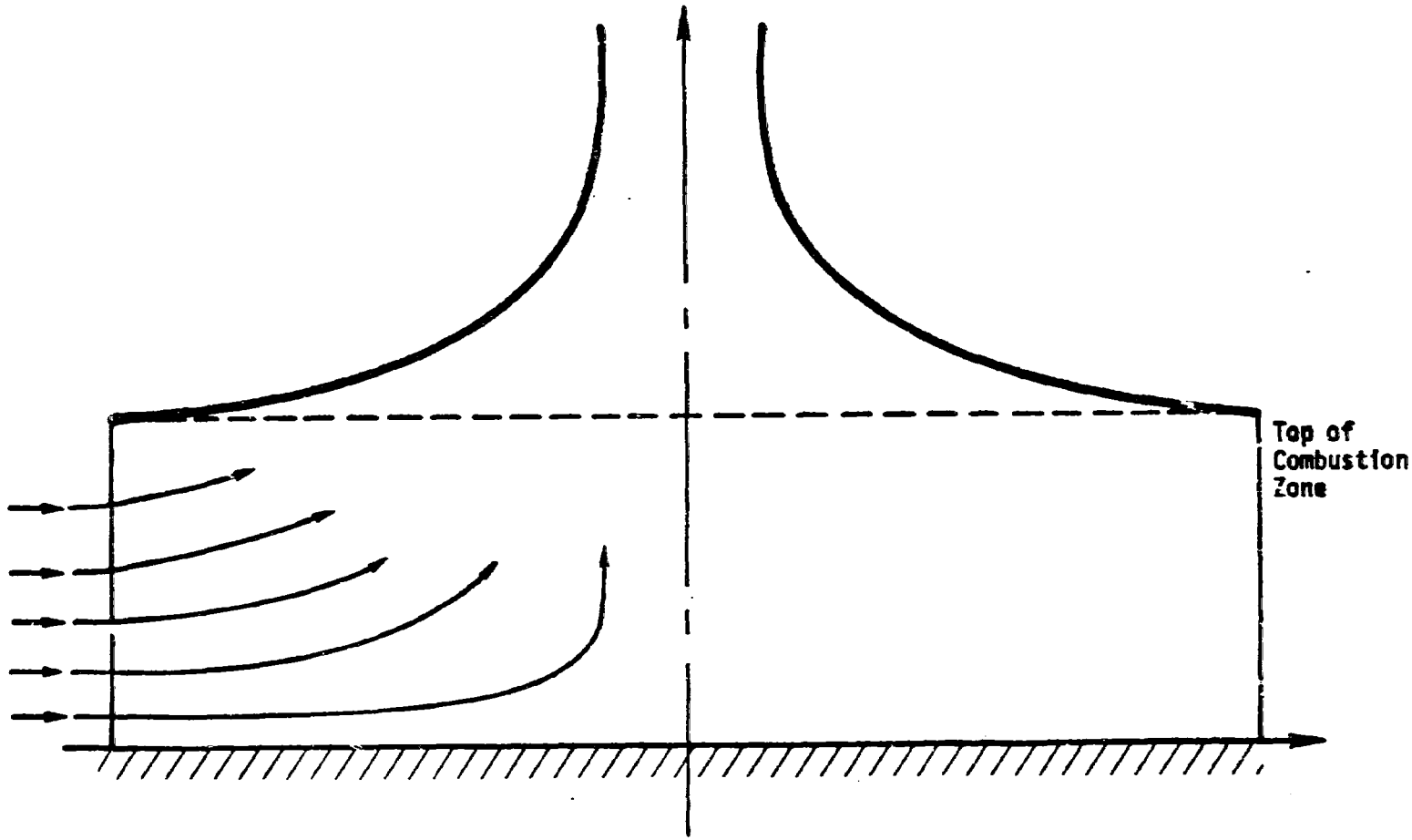

Figure 3. Schematic of the structure of a large-area fire in which there is exceptionally rapid necking of the plume above the completion-of-burning plane, because the plume remains of the order of the radius of the fire in the strongly buoyant burning zone.

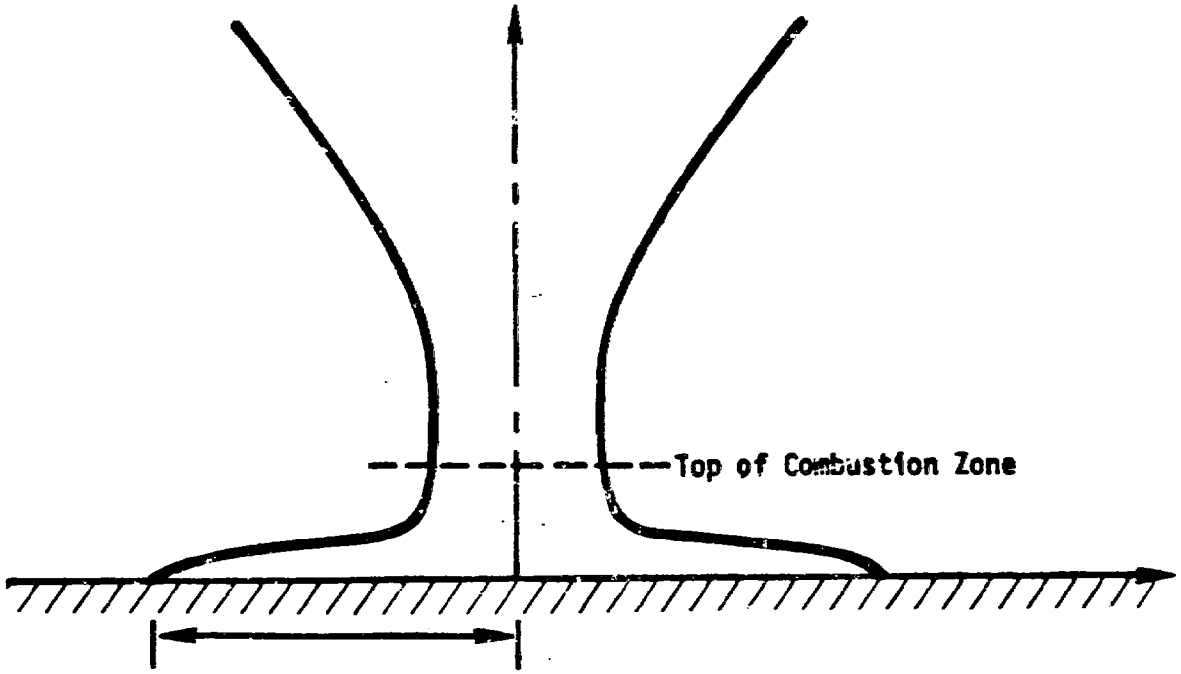

Figure 4. Schematic of the structure of a large-area fire in which there is no necking in of the plume above the completion-of-burning plane.

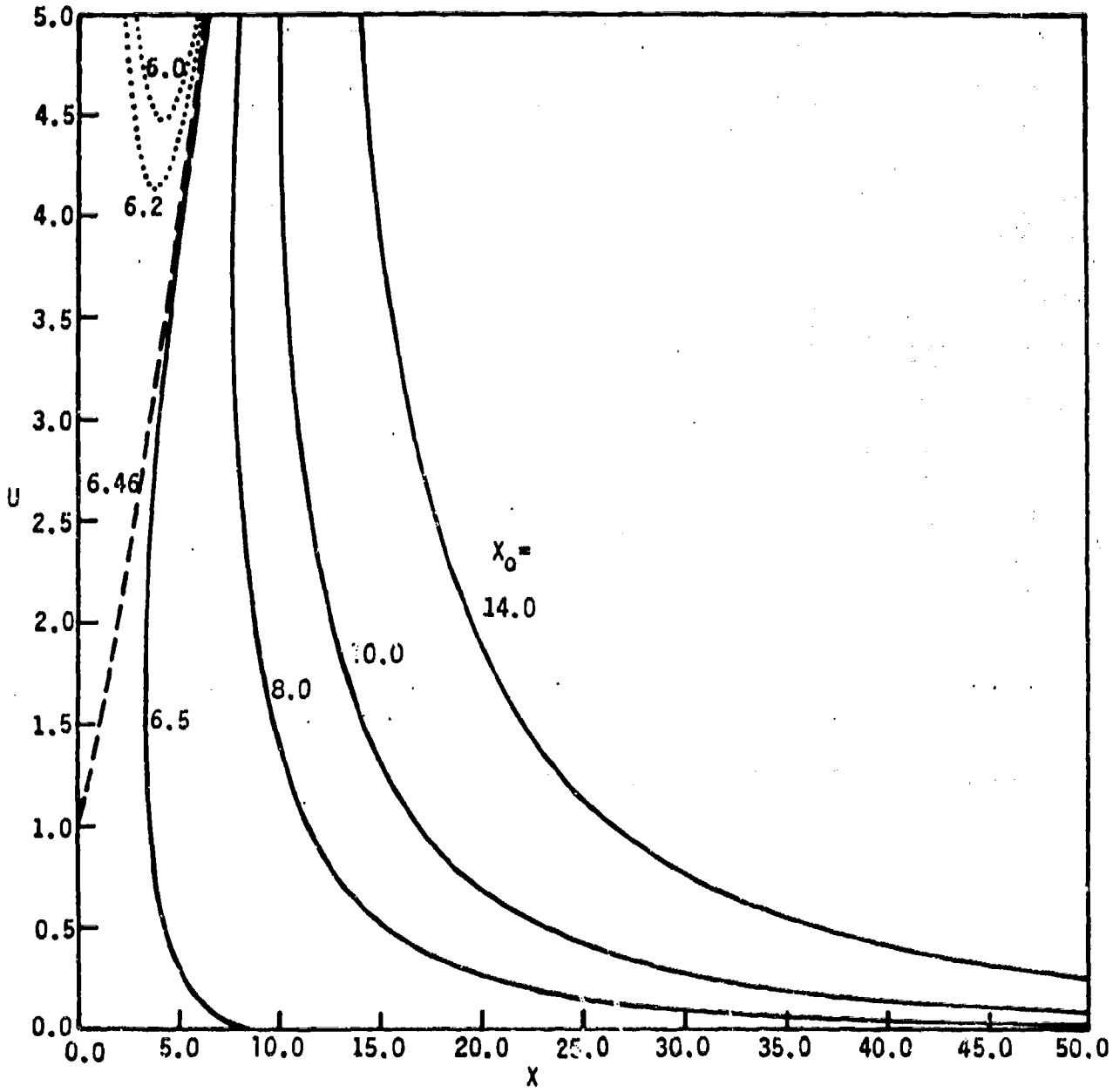

Figure 5. Phase-plane solution for the dimensionless updraft U as a function of dimensionless column radius X for the burning zone, where the singular solution (dashed line) distinguishes physically interesting solutions (solid lines) from unphysical solutions (dotted lines). The parameter X_0 characterizes the values of X at $U = U_0 = 5$.

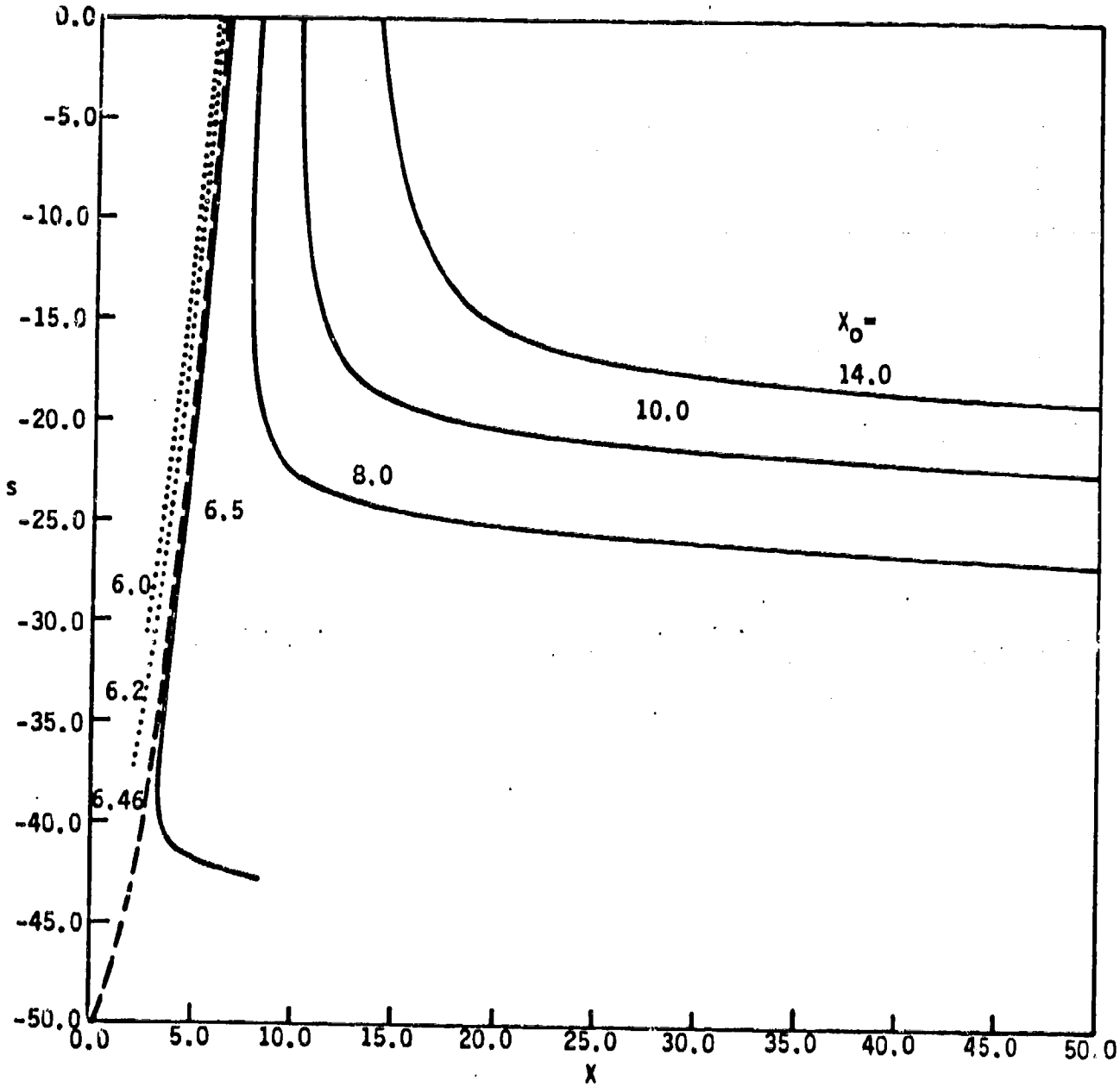

Figure 6. For the results of Figure 5, the dimensionless vertical distances below the completion-of-burning plane (s = 0) vs. dimensionless column radius X. where $X = X_o$ at $s = 0$.

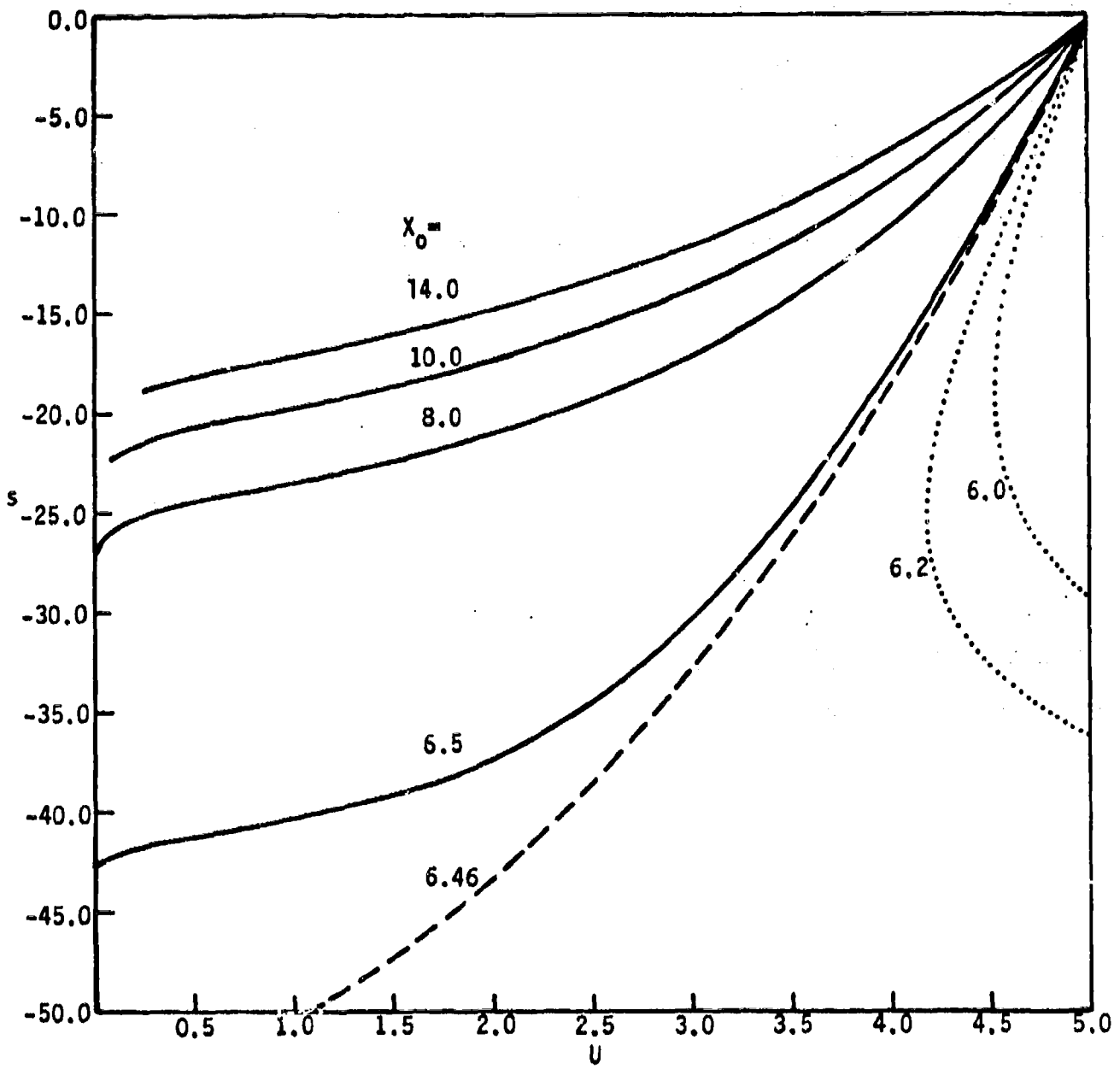

Figure 7. For the results of Figure 5, the dimensionless vertical distance s below the completion-of-burning plane (s = 0) vs. dimensionless column updraft U, where $U = U_o = 5$ at $s = 0$.

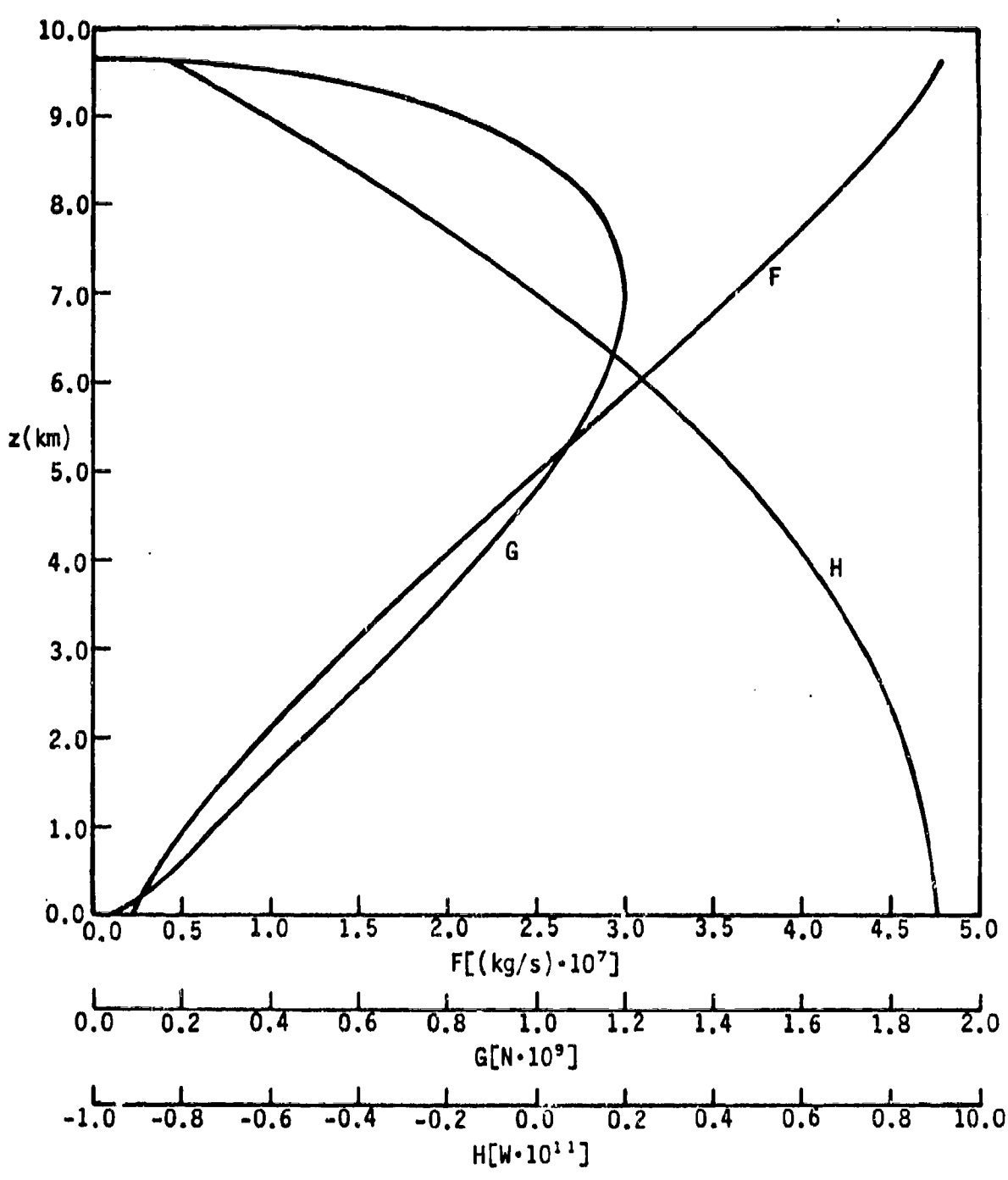

Figure 8. For the nominal (Hamburg) case, solution for the buoyant plume, from (5.1)-(5.8), as a function of altitude z above the completion-of-burning plane (z = 0). Here F is the mass flux, $\rho_a W b^2(1 - f)$; G is the momentum flux, $\rho_a W^2 b^2(1 - f)$; H is the buoyancy flux, $p_a f W b^2$.

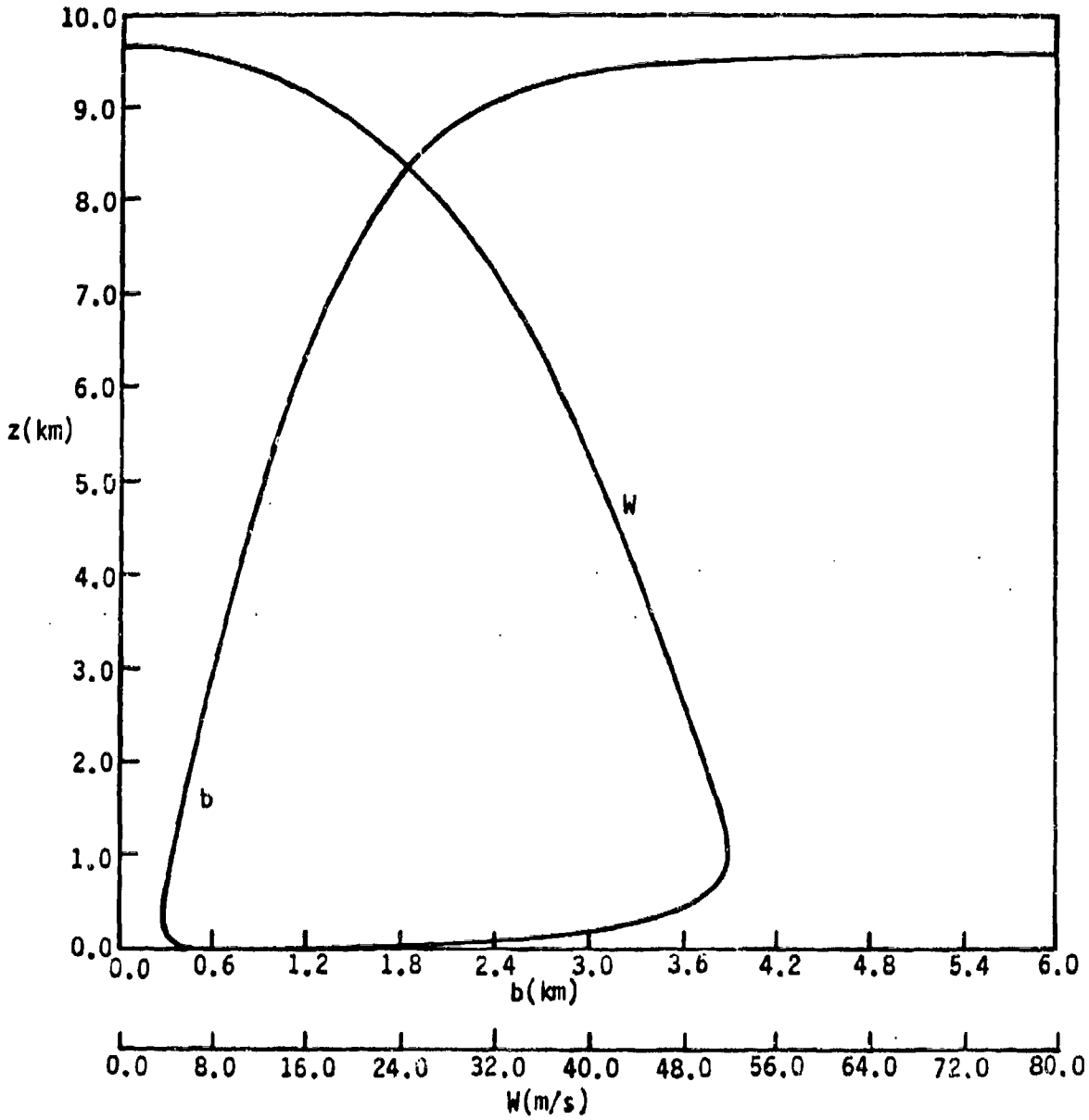

Figure 9. For the nominal case of Figure 8, the plume radius b and updraft W vs. altitude z <u>above</u> the completion-of-burning plane (z = 0).

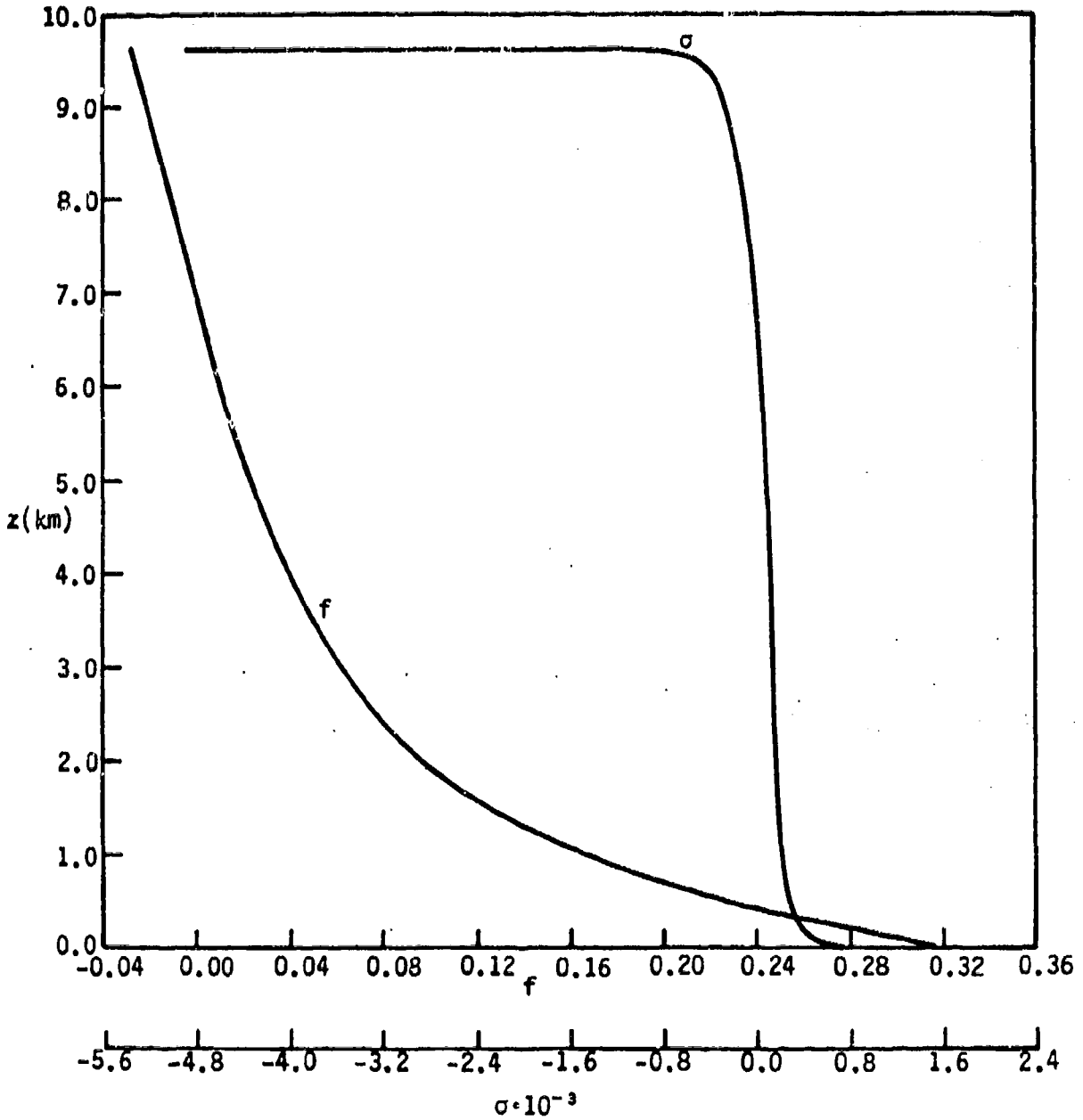

Figure 10. For the nominal case of Figure 8, the fractional density discrepancy of in-plume air from ambient, f, and the fractional pressure discrepancy of in-plume air from ambient, σ, vs. altitude z <u>above</u> the completion-of-burning plane (z = 0).

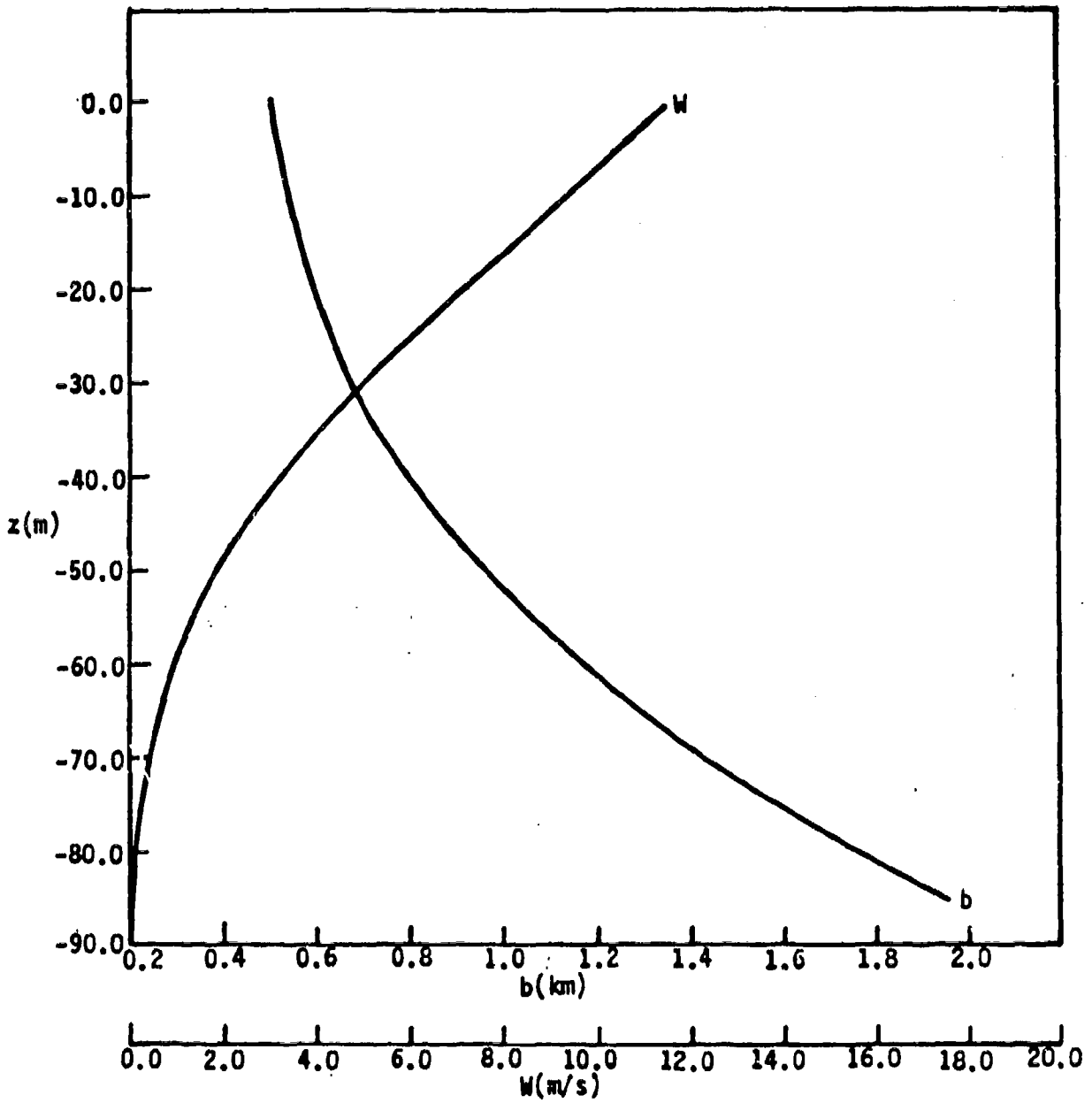

Figure 11. For the nominal case of Figure 8, the plume radius b and the updraft W vs. altitude z <u>below</u> the completion of burning plane (z = 0). The minimum value of z for which solution is given is the ground plane, where b = R, and the fire area $A = \pi R^2$.

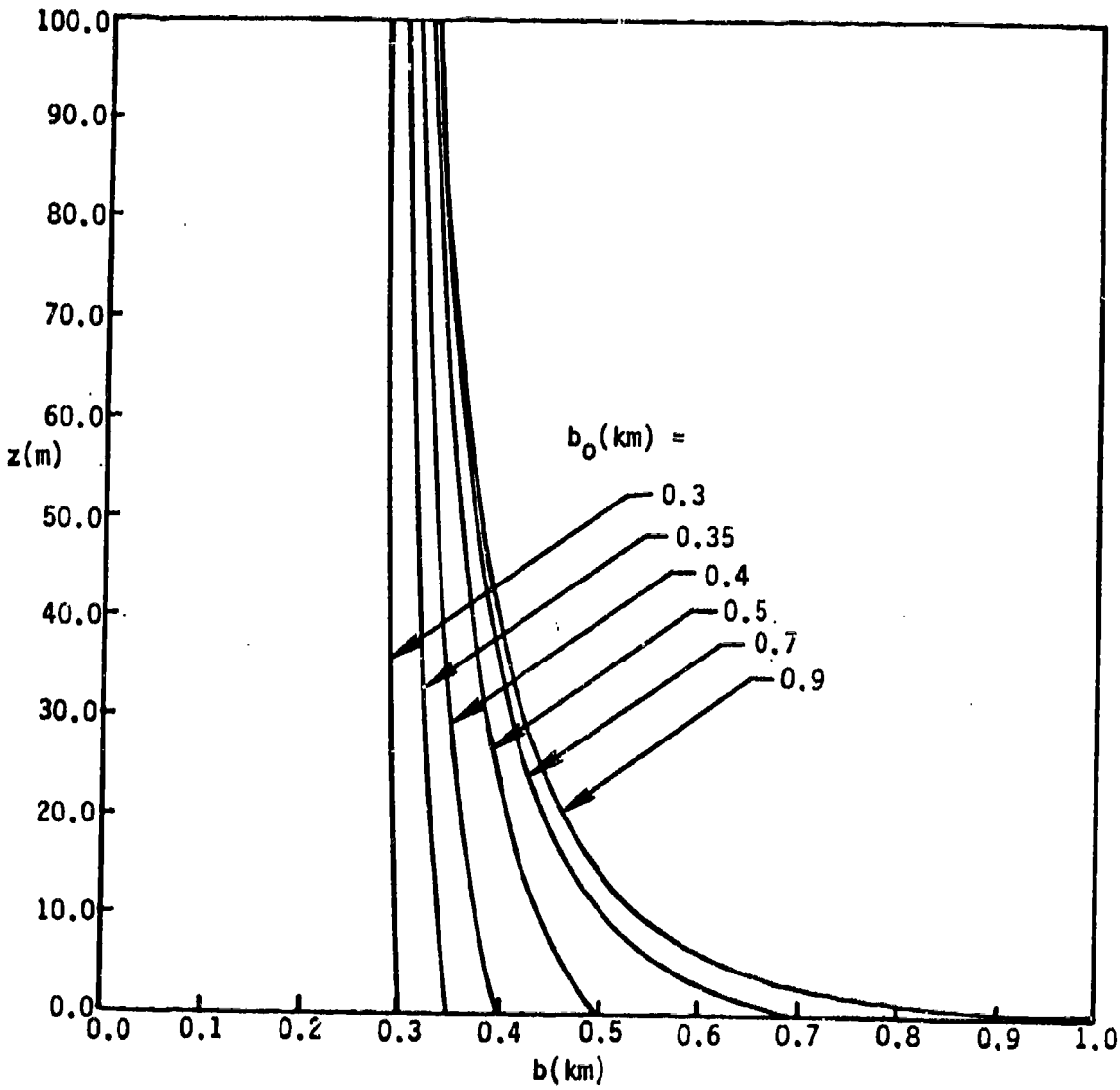

Figure 12. For the nominal case, except that $b_o[\equiv b(0)]$ is varied, the plume radius b vs. altitude z <u>above</u> the completion-of-burning plane (z = 0). Only the lowest 100 m of the weakly buoyant plume are depicted.

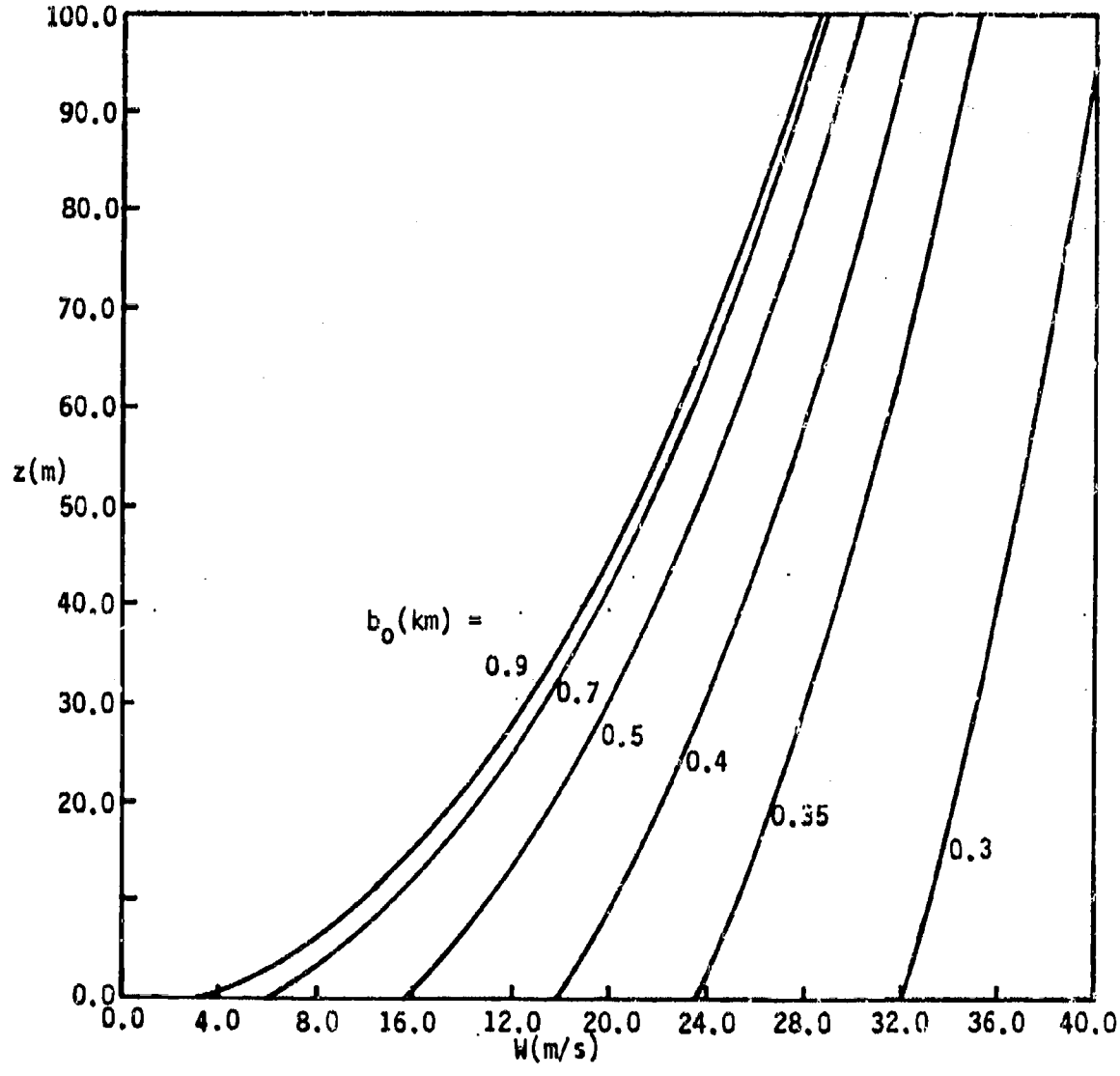

Figure 13. For the conditions of Figure 12 (i.e., the nominal case except that b_o is varied), the updraft W vs. altitude z above the completion-of-burning plane (z = 0). Only the lowest 100 m of the weakly buoyant plume are depicted.

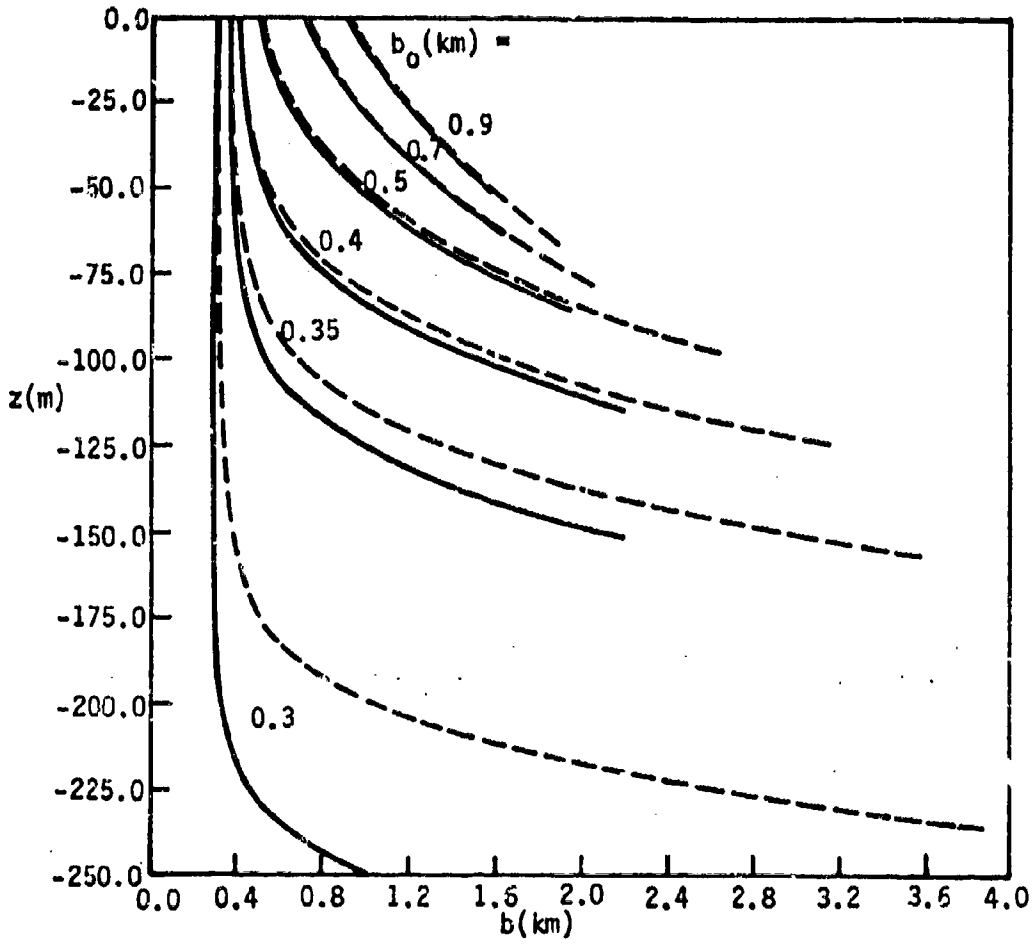

Figure 14. For the conditions of Figure 12 (i.e., the nominal case except that b_o is varied), the plume radius b vs. altitude z below the completion-of-burning plane (z = 0). The solid curves are for $\beta = 1$ (inviscid dynamics); the dashed curves are for $\beta = 0.5$ (losses ascribed to friction). The minimum value of z for which solution is given is the ground plane, where b = R, and the fire area $A = \pi R^2$.

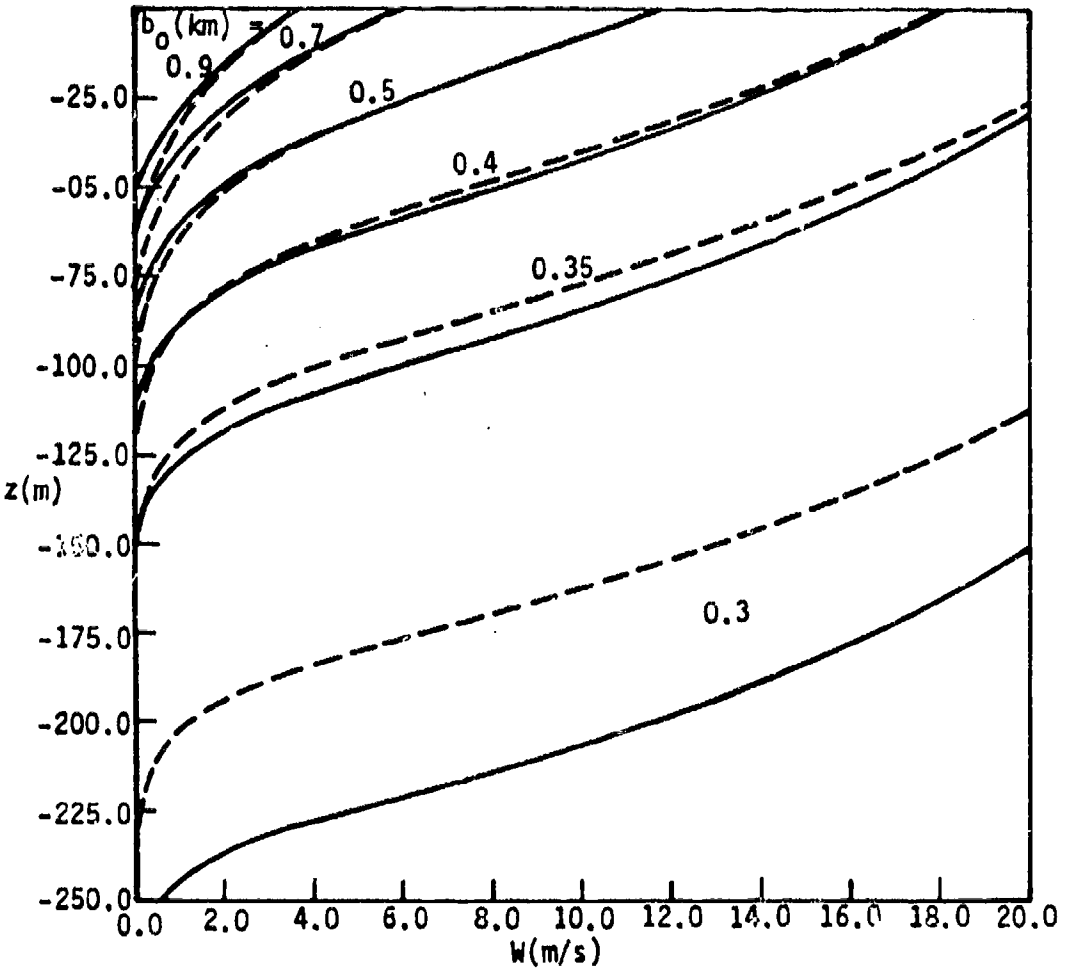

Figure 15. For the conditions of Figure 12 (i.e., the nominal case except that b_o is varied), the updraft W vs. altitude z <u>below</u> the completion-of-burning plane (z = 0). The solid curves are for β = 1 (inviscid dynamics); the dashed curves are for β = 0.5 (losses ascribed to friction). The minimum value of z for which solution is given is the ground plane, where b = R, and the fires area $A = \pi R^2$.

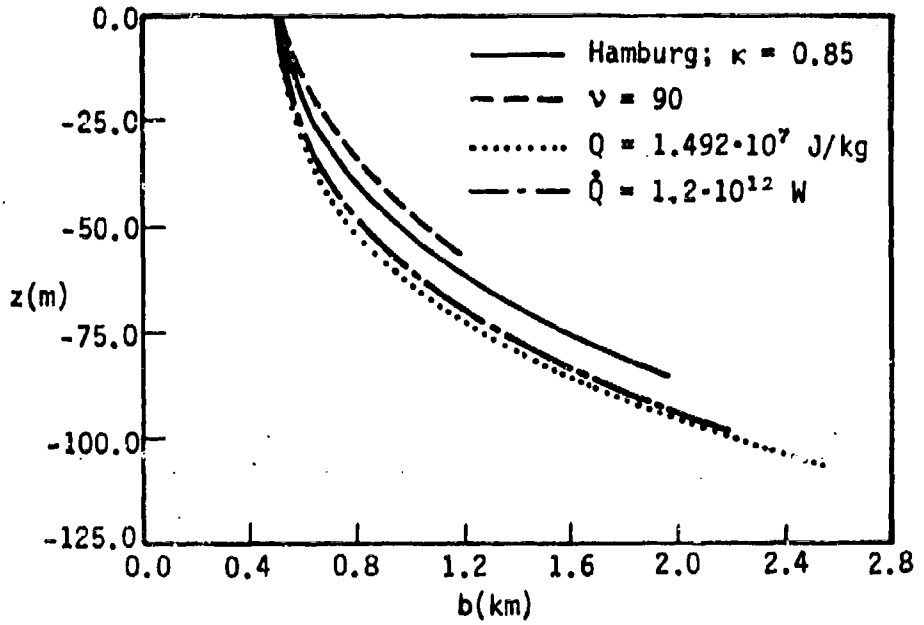

Figure 16. For the nominal case (including b_o = 500 m), except as explicitly noted, the plume radius b vs. altitude z below the completion-of-burning plane (z = 0). The minimum value of z for which solution is given is the ground plane, where b = R, and the fire area $A = \pi R^2$. The case $\kappa = 0.85$ is indistinguishable from the nominal (Hamburg) case, for which $\kappa = 0.95$.

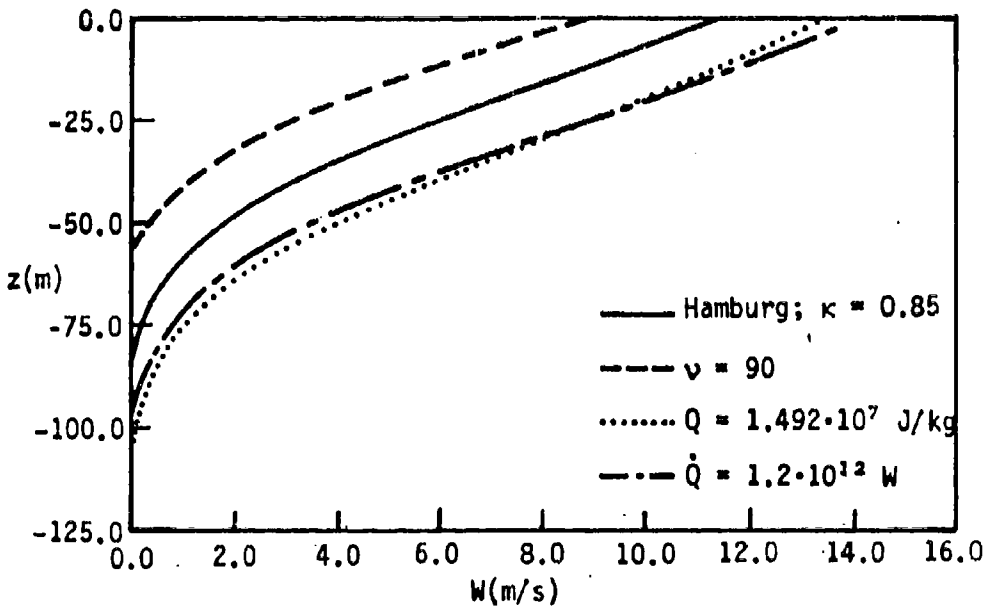

Figure 17. For the conditions of Figure 16 [the nominal case (including b_o = 500 m), except as explicitly noted], the updraft W vs. altitude z below the completion-of-burning plane (z = 0). The minimum value of z for which solution is given is the ground plane, where b = R, and the fire area $A = \pi R^2$. The case $\kappa = 0.85$ is indistinguishable from the nominal (Hamburg) case, for which $\kappa = 0.95$.

Appendix B.*

FIRESTORMS

G. F. Carrier

Pierce Hall
Harvard University
Cambridge, MA 02138
Hon. Member ASME

F. E. Fendell

P. S. Feldman

Engineering Sciences Laboratory
TRW Space and Technology Group
Redondo Beach, CA 90278

* Revised text of a technical paper appearing on pp. 55-64 of Fire Dynamics and Heat Transfer, edited by J.G. Quintiere, R.L. Alpert and R.A. Altenbirch. Volume 25 of the Heat Transfer Division of the American Society of Mechanical Engineers, New York, N.Y.

ABSTRACT

Quantitative criteria are sought for onset of firestorms, severe stationary (nonpropagating) holocausts arising via merger of fires from multiple simultaneous ignitions in a heavily fuel-laden urban environment. Within an hour, surface-level radial inflow from all directions sustains a large-diameter convective column that eventually reaches altitude of about 10 km (e.g., Hamburg, Dresden, Hiroshima). As the firestorm achieves peak intensity (a couple of hours after the ignitions), inflow speeds are inferred to attain 25-50 m/s; typically 12 km^2 are reduced to ashes, before winds relax to ambient levels in six-to-nine hours. Here the firestorm is interpreted to be a mesocyclone (rotating severe local storm). Even with exceedingly large heat release sustained over a concentrated area, in the presence of a very nearly autoconvectively unstable atmospheric stratification, onset of vigorous swirling on the scale of two hours requires more than concentration of circulation associated with the rotation of the earth; rather, a preexisting, if weak, circulation appears necessary for firestorm cyclogenesis.

NOMENCLATURE

$B(z,t)$ = radius of preexisting mesoscale vortex, m

$B_o(z)$ = $B(z,0)$, m

$\tilde{B}$ = reference acceleration for nonadiabatic atmosphere, m/s^2

$b(z,t)$ = e-folding radial distance for plume variables, m

b_i = "plume radius" at ground level, m

c_p = specific heat capacity at constant pressure for air, m^2/s^2-K

E = time-average strength of maintained heat source, W

$F(z,t)$ = centerline mass flux in plume, kg/s

$G(z,t)$ = centerline axial momentum flux in plume, N

g = gravitational acceleration, m/s^2

$H(z,t)$ = centerline energy flux in plume, W

$J(z,t)$ = "transversely averaged" momentum flux in plume, J

M = strength of maintained mass source, kg/s

$p(r,z,t)$ = pressure, Pa

$q(r,z,t)$ = swirl associated with plume, m/s

R = gas constant for air, $m^2/s^2 \cdot K$

r = cylindrical radial coordinate, m

$S(z,t)$ = angular momentum per mass derived from earth rotation, m^2/s

$T(r,z,t)$ = temperature, K

t = time, s

$u(r,z,t)$ = radial velocity component, m/s

$V(z)$ = swirl speed of preexisting mesoscale vortex, m/s

$v(r,z,t)$ = azimuthal velocity component, m/s

$W(x,t)$ = centerline axial velocity in plume, m/s

$w(r,z,t)$ = axial velocity component, m/s

z = axial distance above ground, m

z_i = distance from subterranean point source to ground, m

$\alpha(r,z,t)$ = entrainment functional defined in (16), taken as (39)

α_o = value of α in absence of rotation, 0.093

$\Gamma_o(z)$ = angular momentum per mass of preexisting mesoscale vortex, m^2/s

γ = $c_p/(c_p - R)$

ε = volumetric-flux equivalent of E [see (37)], m^3/s

θ = aximuthal cylindrical-polar coordinate

κ = polytropic exponent characterizing ambient-atmosphere stability [see (38)]

$\rho(r,z,t)$ = density, kg/m^3

$\sigma(z,t)$ = centerline plume pressure deficit, Pa

ϕ = strength of maintained momentum source, N; also, angular momentum per mass rv, m^2/s

ϕ_o = parameter appearing in entrainment functional (39), m^2/s

Ω = component of angular velocity of earth locally perpendicular to surface, s^{-1}

SUBSCRIPTS

a = ambient

i = initial, i.e., pertaining to $z = 0$

INTRODUCTION

In the aftermath of the atomic bombing of Hiroshima [1,2], and of the massive incendiary bombing of Hamburg [3-5] and Dresden [6], particularly virulent, long-lived, uncontrolled burning occurred that had few if any recorded precedents. About one-half hour after multiple simultaneous ignitions (in a heavily fuel-laden urban environment), effected either by radiative-precursor heating and blast-wave disruption [2] or by contact with burning magnesium and gelled gasoline dispersed from clustered cannisters [7], the fires merged to form a rather uniformly burning area of many square kilometers. Whereas the ambient winds were less than 4 m/s, the mass fire engendered radially inward winds at street level from all directions; about 2-3 hours after the initiating bombing, these

winds reached a peak intensity of about 20 m/s, with some estimates by professional firefighters of 50 m/s. The radially inward wind apparently precluded spread beyond the initially ignited area, though virtually everything combustible within this region was burned, before the winds subsided to moderate in speed and variable in direction about six hours after initiation. A single huge central convective column, into which the hot product gases flowed, rose to about 10 km. This rare nonpropagating fire, so distinct from more common ambient-wind-aided spreads, is termed a firestorm. The goal of the present investigation is to delineate, from thermohydrodynamic modeling, quantitative criteria for the onset of a firestorm; while some characterization of structure and properties is inevitably entailed, full detailed description of the event at peak intensity is not the prime objective.

In the interpretation given here, the term firestorm is apt. In a conventional meteorological context, storm suggests cyclonic wind about a center of low surface pressure, with precipitation from convectively induced advection [i.e., from buoyancy-caused ascent and saturation of warm moist air, with (1) radial influx under continuity, and (2) possible attendant spin-up under conservation of angular momentum associated with earth rotation or some locally enhanced level]. Hence a firestorm is a "heat cyclone" [8], a mesolow in which the exothermicity of combustion, as distinguished from the condensation of water vapor, induces free convection. Just as firestorms are exceptional fire events, so mesolows (thunderstorms with organized rotation, also referred to as tornado cyclones

and supercells) are uncommon relative to the total number of thunderstorms, and are characterized by horizontal scale of several kilometers and life-span of about six hours [9]. Further, just as the mesolow is characterized by towering cumulonimbi ascending through the depth of the troposphere to the tropopause, so the firestorm is characterized by a convective column ascending to exceptionally great height, e.g., 10 km at Hamburg.

The observation at low altitudes of appreciable radial flux from all directions toward the base of the centrally sited convective column corroborates, rather than contradicts, the primarily rotating nature of the bulk of the air motion. Investigation of the near-surface inflow layer near the center of a virgorously rotating air mass over a fixed flat surface shows that strong, purely swirling motion is altered to equally strong, purely radial influx near the ground, though immediately at the ground the no-slip constraint holds [10-12].

The firestorm is the exceptional event in that diffusive mechanisms normally relax spin-up, such that swirling is either modest or nil [13]. Allusions to the parallel between firestorms and tropospheric storms in the general sense of strong convection accompanied by strong surface winds are frequent. However, pertinence of the dynamic characteristics of a rapidly rotating air mass above a relatively fixed flat surface plane has been emphasized by Ebert [8], Emmons [14], and Long [15]; Ebert and Emmons suggest that the rotation of the air surrounding the plume suppresses entrainment such that the buoyant plume rises to exceptional altitude, while

Emmons and Long note that radial near-surface inflow is consistent with rapid higher-level swirling. Here, quantitative description seeking onset criteria is undertaken. It may be remarked that the well-known propensity for long-range, spotting-type (discontinuous) spread of free-burning fire via firebrands in the event of fire-whirls [16,17] suggests that the spatially confined character of recorded firestorms yet may have exceptions.

FORMULATION - OUTLINE

A fully established convective column exists over a maintained heat source of known strength (total enthalpy released per time) in an atmosphere of known stratification (temperature as a function of pressure, with relative humidity taken as negligible for circumstances of interest). That is, a conventional entraining, nonrotating plume exists above a fire approximated as a point source of heat, without associated release of momentum per time or mass per time. Ultimately, the point source is placed at a subterranean site, such that the plume width at ground level is ascribed observed values; arbitrarily taking the plume as entraining (in an adiabatic atmosphere with ground-level properties) and nonrotating, between subterranean site and ground, is accepted as yielding adequate description at ground level. Of course, the plume width at ground level is an approximation, as is the acceptance of finite mass and momentum input at ground level. Indeed, the strength of the heat source is also an estimate, since the fuel loading (average mass of combustible matter per area), exothermicity (heat released per mass of combustible matter, with adjustment, if required, for drying prior to burning), and fire duration are known, but the rate of heat release

in time is not known, and in fact the duration is more rigorously an output than an input. Nevertheless, the procedure avoids specifying even more (probably unavailable) detail as input.

A conventional integral-type plume theory yields the vertical structure of this convective column, in particular, the width, upward speed, and density discrepancy from ambient as functions of altitude above the source [18]. Typically, the plume spreads as the speed of ascent slows, ultimately to zero, owing to entrainment of heavier surrounding air into the convective column; even below the altitude of stagnation of ascent, the discrepancy in density between plume air and surrounding air vanishes and reverses, and above the height of zero discrepancy the validity of the entrainment concept is in doubt. In any case, this known solution serves as an initial condition to the questions of interest here: as a function of heat-source strength and dimension, ambient stratification, and ambient circulation, how long would spin-up require and how is the structure of the convective column altered. If spin-up would require more than a couple of hours, relaxation processes not included in the formulation are inferred to enter and to preclude cyclogenesis.

Seeking answers motivates three innovations. The aspect of time development must be added to the description of flow over a maintained source (as distinguished from time dependence associated with the starting plume or buoyant thermal). The plume is taken to respond in a quasisteady manner to the consequences of spin-up of the surrounding air, which introduces explicit temporal derivatives. Accordingly, conservation of angular momentum enters; conservation of radial momentum must be treated (since existence of appreciable

swirl implies existence of a significant radial pressure gradient), in contrast with a simple statement of radially invariant pressure, to which the conservation of radial momentum degenerates for a non-rotating column. Finally, the effective reduction of the entrainment parameter with spin-up of the surrounding air must be quantified [19,20]; with reduced entrainment, the spreading of the plume with altitude is decreased. There are two further considerations. First, if one concentrates on the strongly buoyant region near the fire, the lateral discrepancy in density (and temperature) between air in the plume and surrounding air warrants inclusion [21]. In the weakly buoyant region further above the fire, the density of air in the plume may be identified with the density of ambient air surrounding the plume (Boussinesq approximation); however, for a firestorm the convective column extends to such heights that the variation of ambient air with altitude warrants retention (modified Boussinesq approximation). Second, observations of intense Australian bushfires indicate several occasions, at peak burning, of clouds above the top of the convection column clearly being drawn down in the column [22]. However, no provision is to be made for evolution to a more intense stage of rotating flow incorporating two-cell structure (i.e., provision for a downdrift, at least near the axis at the top of the column, within an annular upflux).

FORMULATION - EQUATIONS

Consider an axisymmetric treatment in cylindrical polar coordinates (r,θ,z), with corresponding velocity components (u,v,w), of a plume above a maintained enthalpy source of strength E (given),

without associated mass-source strength M or momentum-source strength ϕ:

$$M \equiv 2\pi \int_0^{b\to 0} \rho w r dr = 0, \quad \phi \equiv 2\pi \int_0^{b\to 0} \rho w^2 r dr = 0 ,$$

$$E \equiv 2\pi \int_0^{b\to 0} \rho w c_p T_a \left(\frac{T-T_a}{T_a}\right) r dr > 0. \qquad (1)$$

The plume radius $b\to 0$ at the source; subscript a refers to ambient conditions, i.e., to conditions outside the plume where (in the absence of rotation) thermodynamic quantities are a known function of altitude z only.

The flow is so subsonic that (not too close to the source) the density, except for the gravitational term in the momentum equation, is well approximated by its ambient value, and variance of the temperature from ambient is linearly related to the variance from ambient of density (only). Here the ambient values vary with altitude because of the tropospheric scale of the phenomena. In the absence of adequate models, no provision for axially distributed chemical exothermicity is included.

The conservations equations for mass, radial momentum, axial momentum, and energy are taken to be described adequately by the following:

$$(\rho rw)_z + (\rho ru)_r = 0 ; \qquad (2)$$

$$(\rho ruw)_z + (\rho ru^2)_r + rp_r - \rho v^2 = 0 ; \qquad (3)$$

$$(\rho rw^2)_z + (\rho ruw)_r + rp_z + \rho rg = 0 ; \qquad (4)$$

$$(\rho wrc_pT)_z + (\rho urc_pT)_r + \rho rgw = 0 . \qquad (5)$$

Conservation of angular momentum involves time-derivative, advective, convective, and Coriolis terms, the last being important only when planetary vorticity is a significant source of angular momentum ($\phi \equiv rv$):

$$\rho r\phi_t + (\rho rw\phi)_z + (\rho ru\phi)_r + 2\Omega\rho r^2 u = 0 . \qquad (6)$$

The following Gaussian description is adopted for the dependent variables:

$$w(r,z,t) = W(z,t)\ \exp[-r^2/b^2(z,t)]\ , \tag{7}$$

$$p_a(z) - p(r,z,t) = \sigma(z,t)\ \exp[-r^2/b^2(z,t)]\ , \tag{8}$$

$$g\ \frac{\rho_a(z) - \rho(r,z,t)}{\rho_a(z)} = f(z,t)\ \exp[-r^2/b^2(x,t)]\ , \tag{9}$$

$$\phi(r,z,t) = \phi_{1a}(r,z,t) + \phi_{1b}(r,z,t) + \phi_2(r,z,t)\ , \tag{10}$$

where

$$\phi_{1a}(r,z,t) = S(z,t)\left\{1-\exp[-r^2/b^2(z,t)]\right\}\ , \tag{11}$$

$$\phi_{1b}(r,z,t) = \Gamma_o(z)\left\{1-\exp[-r^2/B^2(z,t)]\right\}\ , \tag{12}$$

$$\phi_2(r,z,t) = q(z,t)[r^2/b(z,t)]\exp[-r^2/b^2(z,t)]\ , \tag{13}$$

where ϕ_{1a} is a "response" to the Coriolis term and ϕ_{1b} is a "response" to the initial condition (in which a weak diffuse vortex preexists, the circulation Γ_o of which is invariant over time scales of interest, but the characterizing radius B of which, though initially large so B >> b, may decrease appreciably over the time span of interest). The contribution ϕ_2 describes plume-scale redistribution of angular momentum. The functions to be found, W, σ, f, b, B, S, and q, are all anticipated to be positive near the source; f goes to zero and changes sign at a finite distance above the source.

Also, the equation of state gives

$$p(r,z,t) = \rho(r,z,t)\ RT(r,z,t) \Longrightarrow p_a(z) = \rho_a(z)\ RT_a(z)\ . \tag{14}$$

Hydrostatics suffices for the ambient:

$$p_{a_z} = -\rho_a g\ . \tag{15}$$

The Taylor entrainment concept is introduced:

$$-\lim_{r\to\infty}(ru) = \alpha bW \ , \tag{16}$$

where, in the absence of swirl, $\alpha = \alpha_o$ ($\equiv 0.093$); in the presence of swirl, α is a functional of the swirl-associated variables.

Integration of (1) over r, from $r = 0$ (where $u = 0$) to $r\to\infty$ [where (16) holds], by use of (7) and upon setting $\rho(r,z,t) = \rho_a(z)$, gives

$$\frac{d}{dz}\left(\rho_a W b^2\right) = 2\alpha\rho_a W b \ . \tag{17}$$

Multiplying (15) by r and subtracting from (4) gives, upon integration over all r and use of (7)-(9) and setting $\rho \to \rho_a$, $w(r\to\infty,z,t) \to 0$, gives

$$\frac{d}{dz}\left[\left(\frac{\rho_a W^2}{2} - \sigma\right)b^2\right] = \rho_a f b^2 \ . \tag{18}$$

Equation (5) may be rewritten

$$\left\{\rho wr\left[c_p\left(T-T_a\right)\right]\right\}_z + \left\{\rho ur\left[c_p\left(T-T_a\right)\right]\right\}_r = \rho wrc_p T_{a_z} - \rho wrg \ ; \tag{19}$$

if $\rho\to\rho_a$ in all terms, by (14) and (15), and since $R = (c_p - c_v) = c_v(\gamma - 1)$,

$$\left\{\rho_a wr\left[c_p\left(T-T_a\right)\right]\right\}_z + \left\{\rho_a ur\left[c_p\left(T-T_a\right)\right]\right\}_r =$$

$$-\frac{\rho_a wr}{\gamma - 1}\frac{d}{dz}\left[\ell n\left(\frac{p_a}{\rho_a^{\gamma}}\right)\right] \ . \tag{20}$$

Integration over r and use of (7), (9), (14), and the Boussinesq relation [$(\partial T/\partial\rho)_p$ is evaluated in the ambient]

$$\frac{T(r,z,t)-T_a(z)}{T_a(z)} = \frac{1}{T_a(z)}\left(\frac{\partial T}{\partial\rho}\right)_p\left[\rho(r,z,t)-\rho_a(z)\right] \rightarrow \frac{T-T_a}{T_a} = \frac{\rho_a-\rho}{\rho_a} \quad ,(21)$$

gives

$$\frac{d}{dz}\left[p_a Wb^2\left(\frac{f}{g}\right)\right] = -\frac{2}{\gamma}\left(p_a Wb^2\right)\frac{d}{dz}\left[\ell n\left(\frac{p_a}{\rho_a^{\gamma}}\right)\right] . \qquad (22)$$

Integration of (3) over r yields zero from the perfect differential, and the axial derivative term yields a contribution of $O(b^3) = O[(\alpha z)^3]$, since, from the selfsimilar solution for a point source in an adiabatic nonrotating ambient, $b \doteq \alpha z$. But $\alpha = o(1)$, and perhaps even smaller under spin up. That is, the plume-scale radial inflow u, small relative to other velocity components in a nonrotating convective column, is reduced still further under spin-up (for heights above the surface-inflow layer), according to experiment [17]. Hence, (3) reverts to the cyclostrophic balance ($\rho \doteq \rho_a$)

$$\int_0^{\infty} p_r dr = \rho_a \int_0^{\infty} \frac{v^2}{r}\, dr \rightarrow \sigma = \rho_a \int_0^{\infty} \frac{(\phi_{1a}+\phi_{1b}+\phi_2)^2}{r^3}\, dr \quad . \qquad (23)$$

Execution of the integrals yields

$$\frac{\sigma b^2}{\rho_a} = \ell n 2\left[S^2 + \frac{b^2\Gamma_o^2}{B^2} + (qb)\,S\right] + \frac{(bq)^2}{4} +$$

$$\ell n\left[\left(\frac{B^2+b^2}{B^2}\right)\left(\frac{B^2+b^2}{b^2}\right)^{b^2/B^2}\right] S\Gamma_o + \left[\ell n\left(\frac{b^2+B^2}{B^2}\right)\right](qb)\,\Gamma_o \quad .(24)$$

In this context it may be helpful to note

$$I_1 = \int_0^\infty \frac{[1-\exp(-x^2)]^2}{x^2}\,dx = \ell n2 \ ,$$

$$I_2 = \int_0^\infty \frac{\exp(-x^2)}{x}\,[1-\exp(-x^2)]\,dx = \frac{I_1}{2} \ ; \tag{25}$$

$$I_3(T) = \int_0^\infty \frac{\exp(-Tx^2)}{x}\,[1-\exp(-x^2)]\,dx \longrightarrow$$

$$\frac{dI_3}{dT} = \frac{-(1/2)}{(1+T)T} \ , \ I_3(\infty) = 0 \ ; \tag{26}$$

$$I_4(A) = \int_0^\infty \frac{1-\exp(-x^2)}{x^3}\,[1-\exp(-Ax^2)]\,dx \longrightarrow$$

$$\frac{d^2I_4}{dA^2} = \frac{-(1/2)}{(1+A)A} \ , \ I_4(1) = \ell n2, \ I_4'(1) = I_2 \ . \tag{27}$$

Plume-associated dependent variables (b,W,f,q) are anticipated to change during firestorm onset more slowly in time than the scale of the preexisting vortex B. Accordingly, it is taken that $\phi_{2_t} << \phi_{1_t}$, where $\phi_1 \equiv (\phi_{1a} + \phi_{1b})$. Substitution of (10)-(13) in (6) is construed to yield three relations:

$$\rho r\phi_{1b_t} + \left(\rho ru\phi_{1b}\right)_r = 0 \ , \tag{28}$$

$$\left[\rho ru(\phi_{1a} + \phi_2)\right]_r + \left[\rho wr(\phi_2 + \phi_1)\right]_z = 0 \ , \tag{29}$$

$$\lim_{r\to\infty} \left\{\rho r\phi_{1_t} + \left[\rho ru(\phi_1 + \phi_2)\right]_r + \left[\rho rw(\phi_1 + \phi_2)\right]_z + 2\Omega r^2\rho u\right\} = 0 \ . \tag{30}$$

Integration of (28) over r yields

$$(B^2)_t = -\,2\alpha bW\ , \tag{31}$$

while (30) gives contributions from the first and last terms only:

$$S_t = 2\Omega\alpha bW\ . \tag{32}$$

Since $\Omega = 2^{\frac{1}{2}}\pi/24\ h^{-1}$ at midlatitudes and $\alpha < 0(0.1)$, the growth of swirl from the rotation of the earth is too slow to account for significant vorticity on the scale of two hours; although (32) is tentatively retained, the decrement of B in time from (31) is of more importance to spin-up if Γ_o has nonnegligible value. Finally, integration of (29) over r yields, if $\rho \doteq \rho_a$,

$$\frac{d}{dz}\left[\rho_a W b^2\left(\frac{qb}{4} + \frac{S}{2} + \frac{\Gamma_o b^2}{B^2+b^2}\right)\right] = 2\alpha\rho_a bWS \longrightarrow$$

$$\frac{d}{dz}\left[\rho_a b^2 W\left(\frac{qb}{4} + \frac{\Gamma_o b^2}{B^2+b^2}\right)\right] = 3\alpha\rho_a bWS + \frac{1}{2}\rho_a W b^2\frac{dS}{dz} \tag{33}$$

by transposition, with the aid of (17). Only the product (qb) occurs.

The equations may be brought into canonical form by introduction of the following functionals:

$$F = \rho_a b^2 W,\ G = \rho_a b^2 W^2,\ H = p_a W b^2 f/g,\ J = \rho_a b^2 W\left(\frac{qb}{4} + \frac{\Gamma_o b^2}{B^2+b^2}\right)\ , \tag{34a}$$

so, for instance,

$$\frac{dF}{dz} = 2\alpha(\rho_a G)^{\frac{1}{2}}\ ;\ \frac{dG}{dz} = 2g\left(\frac{\rho_a}{p_a}\right)\frac{HF}{G} + 2\frac{d(\sigma b^2)}{dz}\ ;$$

$$\frac{dH}{dz} = -\frac{2}{\gamma}\rho_a{}^{\gamma-1}\left[\frac{d}{dz}\left(\frac{p_a}{\rho_a{}^{\gamma}}\right)\right]F\ ;\ \frac{dB^2}{dt} = -\,2\alpha\left(\frac{G}{\rho_a}\right)^{\frac{1}{2}}\ . \tag{35}$$

$$W = \frac{G}{F}\ ,\ b = \frac{F}{(\rho_a G)^{\frac{1}{2}}}\ ,\ \frac{f}{g} = \frac{H}{(p_a/\rho_a)F}\ ,\ \frac{b^2}{B^2} = \beta^2\ ,\ qb = \frac{4J}{F} - \frac{4\Gamma_o\beta^2}{1+\beta^2}\ . \quad (34b)$$

Use of (7)-(9), (21), and (34) in (1) gives at the source

$$F = \frac{M}{\pi} = 0,\ G = \frac{2\phi}{\pi} = 0,\ H = \frac{2(\gamma-1)}{\pi\gamma}\,E\ . \quad (36)$$

A solution procedure is to adopt two half-steps in a simplistic form of time-splitting. The seven variables b, B, S, W, σ, q, f (or, equivalently, F, G, H, J, S, σ, B) are taken as known in z at a given time. In the first half step, B, S, and σ are updated via (31), (32), and (24); in (24), updated values of S, B, but not of b, q, are used. In the second half step, (17), (18), (22), and (33) are used to update F, G, H, J; in (18), the term $d(\sigma b^2)/dz$ is transposed and evaluated using the value of σb^2 from the first half step. While iteration on q, b in σ could be adopted, this procedure might be dispensed with. At time zero, $B^2 >> b^2$, so discarding all effects associated with swirl to obtain a classical initial plume is taken as an adequate approximation.

NONDIMENSIONALIZATION; AMBIENT STRATIFICATION; ENTRAINMENT FUNCTIONAL

If, in the translationally invariant set presented above, $z = 0$ denotes gound level, then nondimensionalization could be carried out in terms of the quantities $\rho_a(0)$, $T_a(0)$, $d\rho_a(0)/dz$, and E, where it is recalled that $p_a(0) = \rho_a(0)RT_a(0)$; it is convenient to define

$$\varepsilon \equiv \frac{E}{\rho_a(0)c_pT_a(0)}\ ,\ \frac{\text{volume}}{\text{time}}\ ;\ \tilde{B} \equiv \rho_a{}^{\gamma-1}(0)\ \frac{d}{dz}\left[\left(\frac{p_a}{\rho_a{}^{\gamma}}\right)\right]_{z=0}\ ,\ \frac{\text{length}}{\text{time}^2}\ . \quad (37)$$

The quantity $(p_a \rho_a^{-\gamma})_z$ is positive in a dry stable atmosphere (the case of prime interest here), zero in a dry neutrally stable atmosphere (a special case, the selfsimilar solution of which in a nonrotating atmosphere is classical), and negative in a dry unstable atmosphere (of no interest here). A length scale is furnished by $\varepsilon^{2/5}\tilde{B}^{-1/5}$; a time scale, $\varepsilon^{1/5}\tilde{B}^{-3/5}$; a speed scale, $\varepsilon^{1/5}\tilde{B}^{2/5}$. However, the neutral-stability, dry-adiabatic-atmosphere case $\tilde{B} = 0$ would require special treatment, so the advantages of nondimensionalization are taken to be outweighed by this limitation.

For purposes of a one-parameter characterization of stratification, a so-called polytropic atmosphere [23] is adopted ($1 \geqslant \kappa > 0$, where κ is given and piecewise constant); i.e., under (14) and (15), adoption of

$$p_a \sim \rho_a^{\kappa\gamma} \Rightarrow \frac{dT_a}{dz} = -\frac{g}{c_p}\left(\frac{\kappa\gamma - 1}{\kappa(\gamma - 1)}\right) ; \tag{38a}$$

$$\frac{dH}{dz} = 2(1-\kappa)\,\frac{p_a(0)}{[\rho_a(0)]^2}\left[\frac{\rho_a}{\rho_a(0)}\right]^{\kappa\gamma-2} F\,\frac{d\rho_a}{dz} . \tag{38b}$$

In fact, $1 \geqslant \kappa > \gamma^{-1}$, since temperature (aside from possible local inversion layers) decreases with altitude. Since firestorm-prone ambients are typically very dry, discussion of stability on a dry basis is apropos.

In the absence of experimental data beyond the general guidance that entrainment continually decreases as the air surrounding the plume is spun up above some threshold value, only a "schematic" functional is presented [ϕ_o an assigned constant; T an assigned function, with $T(0) = 1$]:

$$\alpha(b,z,t) = \alpha_o \; T\left\{\phi(b,z,t)\; U\left[\phi(b,z,t) - \phi_o\right]\right\}, \quad \frac{dT}{d\phi} \leq 0 \; . \tag{39}$$

BOUNDARY AND INITIAL CONDITIONS

At $z = 0$ for $t > 0$,

$$b = b_i, \text{ given} \; ; \; H = \frac{2(\gamma-1)}{\pi\gamma} E, \text{ given} \; . \tag{40}$$

One could let b_i vary in time, and could require that only the time average of H at $z = 0$ has the cited value; however, these quantities should be nearly constant over the interval for a fluid element to rise the vertical extent of the plume:

$$t_{rise}(t) = \int_0^{z_{top}} \left[W(z_1,t)\right]^{-1} dz_1 \; . \tag{41}$$

Here, $W(z_{top},t) \to 0$, and W is anticipated to be but weakly variant in time during firestorm onset. In the absence of specific data, b_i and $H(0,t)$ are held constant.

The initial condition at $t = 0$ is taken as:

$$S = 0, \text{ so } \frac{dS}{dz} = 0; \; B(z,0) = B_o(z) \text{ specified}, \tag{42}$$

where the choice for $B_o(z)$ is guided by the fact that $B_o(z)$ plays a role in the preexisting weak vortex that b plays in the current intense plume. Physically, one anticipates (on the basis of data for tropical cyclones and mesocyclones) that the pressure anomaly (i.e., pressure deficit on the centerline, from ambient value at the same altitude) decreases with increasing altitude (except possibly at low altitude). Therefore, one anticipates that Γ_o may decrease with altitude and may vanish at finite altitude. It is

convenient to introduce

$$V(z) = \frac{\Gamma_o(z)}{B_o(z)} \ . \tag{43}$$

SIMPLIFICATION

As anticipated below (32), spin-up associated with the rotation of the earth is negligible relative to spin-up associated with intensification of a preexisting vortex. (The preexisting circulation seems owing to fires from prior recent raids at Hamburg, and to orography at Hiroshima.) Hence, all terms involving S are ignored. Furthermore, rotation associated with the convective column itself is small during the firestorm-onset interval of prime interest here. Accordingly, all terms involving qb are ignored, and the equation for J is discarded completely. It may be confirmed a posteriori that principal evolution during spin-up is the decrease of the radius B of the preexisting mesoscale vortex. The problem devolves to (35), subject to (40) at $z = 0$ (see below) and to (42)-(43) at $t = 0$. Thus, if the axial pressure gradient is retained at all, (24) simplifies to

$$\sigma b^2 = \ell n 2 \ \rho_a \ \Gamma_o^2 b^2 / B^2 \ . \tag{44}$$

In fact, it seems reasonable to expect buoyancy to exceed the axial pressure gradient in magnitude during the spin-up interval of interest. Accordingly, during this time interval, b,W,f remain effectively identical to their initial (swirl-free) values given by (35) with the term $d(\sigma b^2)/dz$ discarded. For consistency, one expects $\phi < \phi_o$ in (39), so $\alpha = \alpha_o$.

If ρ_a is taken invariant over the range of altitude z of interest [so p_a is invariant in z from (38a)], if $\alpha = \alpha_o$ and $\kappa = 1$, and if $d(\sigma b^2)/dz = 0$, then from the first three relations of (35) and from (40) one recovers the known similarity solution [19]:

$$b = \frac{6}{5}\,\alpha_o(z+z_i),\quad W = \frac{5}{6\alpha_o}\left[\frac{18}{5\pi}\left(\frac{\alpha_o \epsilon g}{z+z_i}\right)\right]^{1/3},$$

$$\frac{f}{g} = \left[\frac{1}{3^5 g}\left(\frac{5}{\alpha_o}\right)^4\left(\frac{\epsilon}{\pi}\right)^2\frac{1}{(z+z_i)^5}\right]^{1/3}, \tag{45}$$

where

$$b_i = \frac{6}{5}\,\alpha_o\, z_i\,. \tag{46}$$

Although the procedure incurs spurious finite values for the mass flux F and the momentum flux G as $z = 0$ (investigated below), the above formulae furnish starting values at $z = 0$ for the plume solution at all times t during firestorm onset. The conventional procedure of placing an equivalent-strength point heat source at the subterranean site $z = -z_i$, with an adiabatic nonrotating atmosphere holding in $-z_i < z < 0$ (where $|z_i|$ is small enough relative to tropospheric scale height that ρ_a is effectively constant), has been taken as acceptable a procedure as any facile alternative for starting the plume solution at $z = 0$. Below, the relative insensitivity of results to choice of z_i is established by varying W(0) and f(0). The fact is that, with spin-up, a near-ground-level inflow is engendered, and absence of data giving temporal and spatial

resolution of the heat release at Hamburg precludes establishing the adequacy of adopting (46).

Further, because of the convenience of a closed-form expression, for the virtually adiabatic atmosphere holding in the pertinent lower troposphere at Hamburg, for given z_i and ε, (45) and (46) are utilized below, over the spin-up interval, in (31). However, the variation of ambient density and pressure with altitude for a not-quite-adiabatic lower troposphere is later examined as a check; in this check, (45) and (46) are used only to start the upward integration in z of (35) under (38), results being sought with the axial pressure gradient term both retained and discarded.

In short, if it is recalled that $\phi = rv$, one anticipates that B decreases from $B_o(z)$ to b as time t increases, such that v increases at radius b from virtually zero at $t = 0$ to almost $(2/3)[B_o(z)V(z)]/b(z)$, or $(2/3)\Gamma_o(z)/b(z)$, from (12), (31), and (43)--although, as $B \to b$, the domain of validity of the theory probably is being overextended. (The model fails as $B \to b$ because plume circulation qb should not be ignored, and input to the convective column from a rotating near-surface layer is not adequately incorporated.) The issue being investigated is whether the stratification as reflected in κ, (more importantly) the size of the intensely convective region as reflected in the parameter b_i, and (still more importantly) the rate of enthalpy release as reflected in the parameter ε are such that spin-up from weak preexisting-vortex swirl to about 15 m/s is achieved on the scale of two hours, as reported at Hamburg.

Thus, in the present interpretation, $\alpha = \alpha_o$ during the early stages of spin-up, such that B is reduced from B_o to b, presumably

in about two hours. Then, α is reduced significantly in appreciably swirling surroundings, so the plume ascends to exceptional altitude [see (39)]. While very preliminary evidence encourages the concept [19], far more data are required. The increase in plume altitude with decrease of α is suggested only very qualitatively below.

RESULTS

Nominal values for problem parameters, believed appropriate for the Hamburg firestorm, are presented in Table 1. The basis for the more critical of these parameter values is now discussed. An area of 12 km^2 with 157 kg/m^2 of combustible material was reduced (virtually completely) to ashes in about 6 h [24,25]; for adopted exothermicity of $1.86 \cdot 10^4$ J/g of combustibles, E = $O(10^{19}$ ergs/s), or, for plausible ambient reference (ground-level) atmospheric conditions, by (37), $\varepsilon = O(3 \cdot 10^{12}$ cm^3/s). This is an average value for ε: enhanced values at earlier time could be afforded by reduced values later. At the Hamburg airport at the time of the firestorm [24], between 0.3 and 3.0 km, $\kappa = 0.96$, and a higher value almost surely held in the Hammerbrook district itself; above 3 km or so, $\kappa = 0.75$. A value of κ somewhat greater than 0.95 near the ground, and somewhat greater than 0.75 at midtropospheric levels, typically is adopted, for the present, two-layer, piecewise-constant polytropic parameterization of atmospheric stability. From data taken at the Hamburg airport, the preexisting vortex is characterized at ground level [8, 24] by $V(0) = 4$ m/s and $B_o(0) = 8$ km, so $\Gamma_o(0) = O(3.2 \cdot 10^4$ m^2/s); the radius

of the strongly convective area at the ground $b_i = 0.5$ km. The other parameter assignments seem standard.

If one approximates the product of the plume-scale dependent variables bW, and entrainment factor α, as constant in time, then (31) yields [recall $B(z,0) = B_o(z)$]

$$B^2(z,t) = B_o^2(z) - 2\alpha bWt \ , \tag{47}$$

where, as previously noted, the equation is inappropriate for $B < O(b)$. If for explicitness one adopts $\kappa = 1$, such that the solution for an isopycnic nonrotating atmosphere, (45)-(46), is employed <u>for all z</u>, so

$$\alpha bW = \left(\frac{18}{5\pi}\,\alpha_o^4\right)^{1/3} \left[\varepsilon g (z+z_i)^2\right]^{1/3} \ , \tag{48}$$

then, from (10)-(12) and (45), since $rv = \phi \doteq \phi_{1b}$, at the plume edge $r = b$,

$$v(b,z,t) = \frac{B_o(z)\ V(z)}{b(z)} \left\{1-\exp\left[-\left(\frac{b(z)}{B(z,t)}\right)^2\right]\right\} \ . \tag{49}$$

One anticipates $B_o(z) \doteq \alpha_o z + B_o(0)$, where

$$v(b,z,t) = O[B_o(z)V(z)/b(z)] \ ,$$

for sufficient time t elapsed since ignition for B to decrease from B_o to b over the lower-tropospheric range of z for which $\Gamma_o > 0$. It is well worth noting from (47) and (48) that the magnitude of swirl is not greatly altered by small changes in B_o, but rather sensitive to changes in ε and b_i, and that spin-up, modest at early time, accelerates abruptly. Results are given in Fig. 1-7.

Neglecting the axial pressure gradient in the second of (35) gives b, W, f as functions of z independently of the spin-up, except as reflected in the value assigned α, from (35), (40), and (42). In particular, Figs. 8-10 give the vertical profiles of the plume-scale dependent variables for α_o, $(\alpha_o/10)$, $(\alpha_o/100)$, for several states of atmospheric stability reflected in κ. Two-order-of-magnitude decrement in α from α_o is required for doubling of the the plume altitude, so one infers that the sensitivity of α to $\phi(>\phi_o)$ is substantial. If a modest role holds for the axial pressure gradient, the decrement in time of the characterizing radius B of the preexisting vortex differs under (35) and (46) from the decrement in time calculated under (48). The distinction derives from the fact that $\kappa \ll 1$ in (35), whereas $\kappa = 1$ under (48); perhaps even more importantly, stratification of the ambient is included appropriately in (35), whereas density is held constant in the oversimplified (but explicit) relation (48). Results are given in Fig. 11.

A point raised earlier just below (46) concerns the spurious ground-level mass and momentum flux incurred by using (45) and (46) to initiate the plume calculation. As a check, ground-level updraft W(0) is decreased by a factor of four, and simultaneously the ground-level normalized density discrepancy f(0) is increased by a factor of four, such that the ground-level release of heat per time H(0) is invariant while the mass per time F(0) is reduced by a factor of four [see (34a)]. It turns out that for otherwise nominal assignment of values to problem parameters, such alteration of W(0) and f(0) results in a plume of height 5.1 km, as opposed to a height of 4.2 km without such alteration. Thus, imprecise ground-level mass

and momentum fluxes may not alter overall plume dynamics significantly. While, from (48), such alteration might seem to alter low-tropospheric spin-up, in fact a compensatory radial pressure gradient (not included here) may well enter to restore the influx to the values adopted. This nonhydrostatic-pressure-gradient contribution for strongly buoyant plumes is being investigated, and is to be described in a subsequent publication. Within the weakly buoyant formulation given here, calculations confirm that, uniformly in altitude over the time span for firestorm onset, the axial pressure gradient makes a fairly modest contribution to the balance of inertial and buoyant effects in the conservation of vertical momentum.

CONCLUSIONS

Current estimates for firestorm-onset criteria are as follows: "(1) at least 8 pounds of combustible per square foot of fire area, (2) at least half of the structures in the area on fire simultaneously, (3) a wind of less than 8 miles per hour at the time, and (4) a minimum burning area of about half a square mile" [2, pp. 299-300]. On the basis of the study described above, the following alternate criteria are proposed: (1) a localized heat release of order 10^{19} erg/s sustained for at least 2-3 hours; (2) a preexisting weak vortex characterized near ground level by swirl of 4 m/s at radius 8 km, such that preexisting angular momentum (per unit mass) near ground level is $3.2 \cdot 10^4$ m^2/s; (3) absence of a strong ambient crosswind, with less than 4 m/s perhaps being adequate constraint, but with total absence being even more conducive to firestorm onset; and (4) a very nearly dry-adiabatic lapse rate holding for the lowest few kilometers of the atmosphere. Lower-

tropospheric spin-up to about 20 m/s within 2-3 h seems plausible under such criteria. If the exothermicity of combustibles is taken to be that of dry woody matter consumed readily in forest fires, which is $1.86 \cdot 10^4$ J/g or so, then the requisite fuel loading appears to be about four times the 8 pounds per square foot cited earlier, if an area of 12 km^2 is entailed and the burning continues at high intensity for 6 h (as reported at Hamburg). The onset of swirling near the convective-column edge may be abrupt in that it can rise from nearly nil levels to 20 m/s or so within a half hour. The background angular momentum associated with the rotation of the earth is inadequate for spin-up to the cited swirl speed on the scale of 2 hours or so.

Further work on plumes whose base temperatures are $O(10^3$ K) and which are accompanied by significant swirl is impeded by the current absence of answers to the questions: (1) is the entrainment rate more properly related to <u>mass</u> entrained [i.e., $\rho_a \lim_{r\to\infty}(ru)$] per unit of axial <u>mass</u> flux [$bW \lim_{r\to 0} \rho$], or to <u>volume</u> entrained [$\lim_{r\to\infty}(ru)$] per unit of axial <u>volume</u> flux (bW); (2) by how much is the entrainment coefficient reduced by an increase in swirl. Answers can be furnished experimentally only. In fact, it is clear from already published laboratory experiments on firewhirls [19,20] that reduction in entrainment with swirl is highly significant.

ACKNOWLEDGMENT

The authors are grateful to technical monitors Mike Frankel and Tom Kennedy for the opportunity to pursue this investigation. This work was supported by the Defense Nuclear Agency under Contract DNA001-83-C-0104. The authors also wish to thank Ann McCollum and Asenatha McCauley for preparation of the manuscript and the figures.

REFERENCES

1. Bond, H., ed., Fire and the Air War, National Fire Protection Association, Boston, MA, 1946.

2. Glasstone, S., and Dolan, P. J., eds., The Effect of Nuclear Weapons, 3rd ed., U. S. Dept. of Defense and U. S. Dept. of Energy, Washington, DC, 1977.

3. Caidin, M., The Night Hamburg Died, Ballantine, New York, NY, 1960.

4. Musgrove, G., Operation Gomorrah--The Hamburg Firestorm Raids, Jane's, New York, NY, 1981.

5. Middlebrook, M., The Battle of Hamburg--Allied Bomber Forces against a German City in 1943, Charles Scribner's Sons, New York, NY, 1981.

6. Irving, D., The Destruction of Dresden, Ballantine, New York, NY, 1965.

7. Fisher, G. J. B., Incendiary Warfare, McGraw-Hill, New York, NY, 1946.

8. Ebert, C. H. V., "The Meteorological Factor in the Hamburg Fire Storm," Weatherwise, Vol. 16, 1963, pp. 70-75.

9. Brandes, E., "Mesocyclone Evolution and Tornadogenesis," Monthly Weather Review, Vol. 106, 1978, pp. 995-1011.

10. Carrier, G. F., "Swirling Flow Boundary Layers," Journal of Fluid Mechanics, Vol. 49, 1971, pp. 133-144.

11. Burggraf, O. R., Stewartson, K., and Belcher, R., "Boundary Layer Induced by a Potential Vortex," Physics of Fluids, Vol. 14 1971, pp. 1821-1833.

12. Carrier, G F., and Fendell, F. E., "Analysis of the Near-Ground Wind Field of a Tornado with Steady and Spatially Varying Eddy Viscosity," Wind Field and Trajectory Models for Tornado-Propelled Objects, Report NP-748, Electric Power Research Institute, Palo Alto, CA, 1978, pp. A-1 through A-45.

13. Dergarabedian, P., and Fendell, F., "Parameters Governing the Generation of Free Vortices," Physics of Fluids, Vol. 10, 1967, pp. 2293-2299.

14. Emmons, H. W., "Fundamental Problems of the Free Burning Fire," Tenth Symposium (International) on Combustion, Combustion Institute, Pittsburgh, PA, 1965, pp. 951-964.

15. Long, R. R., "Fire Storms," Fire Research Abstracts and Reviews, Vol. 9, 1966, pp. 53-68.

16. Graham, H. E., "Fire Whirlwinds," Bulletin of the American Meteorological Society, Vol. 36, 1965, pp. 99-103.

17. Lee, S. L. and Hellman, J. M., "Heat and Mass Transfer in Fire Research," Advances in Heat Transfer, Vol. 10, Academic, New-York, NY, 1974, pp. 219-284.

18. Morton, B. R., Taylor, G., and Turner, J. S., "Turbulent Gravitational Convection from Maintained and Instantaneous Sources," Proceedings of the Royal Society, Vol. A234, 1956, pp 1-23.

19. Emmons, H. W., and Ying, S.-J., "The Fire Whirl," Eleventh Symposium (International) on Combustion, Combustion Institute, Pittsburgh, PA, 1967, pp. 475-488.

20. Ying, S.-J., "The Fire Whirl," Technical Report, Engineering Sciences Laboratory, Division of Engineering and Applied Physics, Harvard University, Cambridge, MA, 1965.

21. Smith, R. K., "Radiation Effects on Large Fire Plumes," Eleventh Symposium (International) on Combustion, Combustion Institute, Pittsburgh, PA, 1967, pp. 507-515.

22. Taylor, R. J., Evans, S. T., King, N, K., Stephens, E. T., Packham, D. K., and Vines, R. G., "Convective Activity Above a Large-Scale Bushfire," Journal of Applied Meteorology, Vol. 12, 1973, pp. 1144-1150.

23. Prandtl, L., and Tietjens, O. G., Fundamentals of Hydro- and Aeromechanics, Dover, New York, NY, 1957.

24. Brunswig, H., Feuersturm uber Hamburg, Motorbuch, Stuttgart, Germany, 1981.

25. Schubert, R., "Examination of the Building Density and Fuel Loading in the Districts Eimsbüttel and Hammerbrook in the City of Hamburg as of July 1943," Translation, Project MU-6464, Stanford Research Institute, Menlo Park, CA, 1969.

Table 1. Nominal Values for Parameters

$B_o(0)$	=	$8.00 \cdot 10^5$ cm	α_o	=	$9.30 \cdot 10^{-2}$
$\tilde{B}$	=	$1.23 \cdot 10^1$ cm/s^2	$\Gamma_o(0)$	=	$3.20 \cdot 10^8$ cm^2/s
b_i	=	$5.00 \cdot 10^4$ cm	ε	=	$2.60 \cdot 10^{12}$ cm^3/s
c_p	=	$1.00 \cdot 10^7$ cm^2/s^2-K	κ	=	$\begin{cases} 9.90 \cdot 10^{-1}, & z < 2.74 \cdot 10^5 \text{ cm} \\ 8.30 \cdot 10^{-1}, & z > 2.74 \cdot 10^5 \text{ cm} \end{cases}$
E	=	$9.05 \cdot 10^{18}$ erg/s	γ	=	1.40
g	=	$9.80 \cdot 10^2$ cm/s^2	$\rho_a(0)$	=	$1.16 \cdot 10^{-3}$ g/cm^3
$p_a(0)$	=	$1.00 \cdot 10^6$ g/cm-s^2	$d\rho_a(0)/dz$	=	$1.17 \cdot 10^{-9}$ g/cm^4
R	=	$2.87 \cdot 10^6$ cm^2/s^2-K			
$T_a(0)$	=	$3.00 \cdot 10^2$ K			

Fig. 1 Profile of the characteristic radius B of the preexisting vortex vs. altitude above ground level z, at time t [ignition at t=0, with $B(z,0)=B_0(z)$, adopted as a plausible initial profile]. The decrement in B owing to convectively induced advection is computed for a constant-density atmosphere; the calculation is carried to the approximate altitude to which the ambient remained very nearly autoconvectively unstable at Hamburg. Here the volumetric flux of the heat source $\varepsilon=2.586\cdot10^{12}$ cm^3/s. As in all succeeding figures, parameter values are those of Table 1 except as explicitly noted.

Fig. 2 Swirl speed v, at time t = 0 at three altitudes z, vs. radial distance from the axis of symmetry, r, for the result of Fig. 1. (The peak swirl speed occurs at $r\doteq1.12$ B, for fixed altitude and time, for the Oseen-type vortex adopted.) Initial swirling is taken quite small. Here $\varepsilon=2.586\cdot10^{12}$ cm^3/s.

Fig. 3 Swirl speed v at time t=1.25 h, for the case of Figs. 1 and 2. Swirling remains modest.

Fig. 4 Swirl speed v at time t=2.5 h, for the case of Figs. 1, 2 and 3. Onset of intense swirling occurs within a span of one hour.

Fig. 5 Ground-level values of the swirl v and the preexisting-vortex radius B vs. time t, for the radius of peak swirl ($r\doteq1.12$ B). Order-of-magnitude decrement of ε extends spin-up to such long times that relaxational mechanisms presumably preclude firestorm onset.

Fig. 6 Ground-level values of the swirl v and the preexisting-vortex radius B vs. time t, for the radius of peak swirl ($r\doteq1.12$ B). Enlarging the radius of convection, b_1, shortens the spin-up time. Here $\varepsilon = 2.586\cdot10^{12}$ cm^3/s.

Fig. 7 Ground-level values of the swirl v and the preexisting vortex radius B vs. time t, for the radius of peak swirl ($r \doteq 1.12\ B$). The initial radius $B_0(z)$ is increased 2 km at all altitudes (denoted B_0 INC). This is presented both with V(z) decreased so Γ_0 is unchanged (denoted Γ_0 NOM), and with V(z) unaltered so Γ_0 is increased at all z (denoted V NOM). Modest increase of B_0 somewhat lengthens spin-up time. Here $\varepsilon = 2.586 \cdot 10^{12}$ cm^3/s.

Fig. 8 Plume radius b vs. altitude above ground level z. Ground-level values are obtained from (45)-(46); deviation of the axial pressure gradient from hydrostatic owing to rotation is neglected. Reduction by two orders of magnitude of the entrainment parameter nearly doubles plume height. Also displayed is the effect of altering the ambient stratification [decreasing κ from its value for neutrally buoyant condition ($\kappa = 1$) increases stability, with $\kappa = \gamma^{-1}$ holding for an isothermal layer]. When two values of κ are given for one curve, the first pertains to $z < 2.74$ km and the second, to $z > 2.74$ km. Although other sources give higher values, according to [24] the plume reached only 7 km.

Fig. 9 Vertical component of velocity on the axis of symmetry, W, vs. altitude above ground z, associated with the result of Fig. 8.

Fig. 10 Centerline density discrepancy from ambient, normalized by the ambient density and multiplied by the magnitude of the gravitational acceleration, f, vs. altitude above ground z, associated with the result of Figs. 8 and 9. Validity of the theory for altitudes for which $f < 0$ is problematic.

Fig. 11 Preexisting-vortex radius B vs. altitude above ground z at several times since ignition t, under nominal parameters (Table 1); also, the pre-existing angular momentum Γ_0 vs. z. Also, swirl speed v(1.12B,0,t) vs. t. Here, a variable-density, two-layer, polytropic atmosphere is adopted, whereas a constant-density (neutrally stable) atmosphere is adopted in Fig. 4.

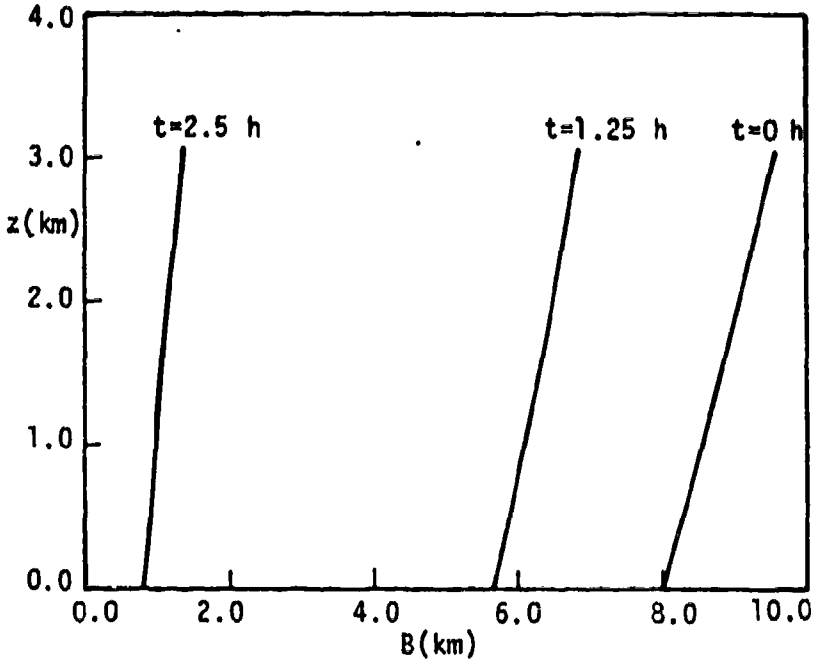

Figure 1.

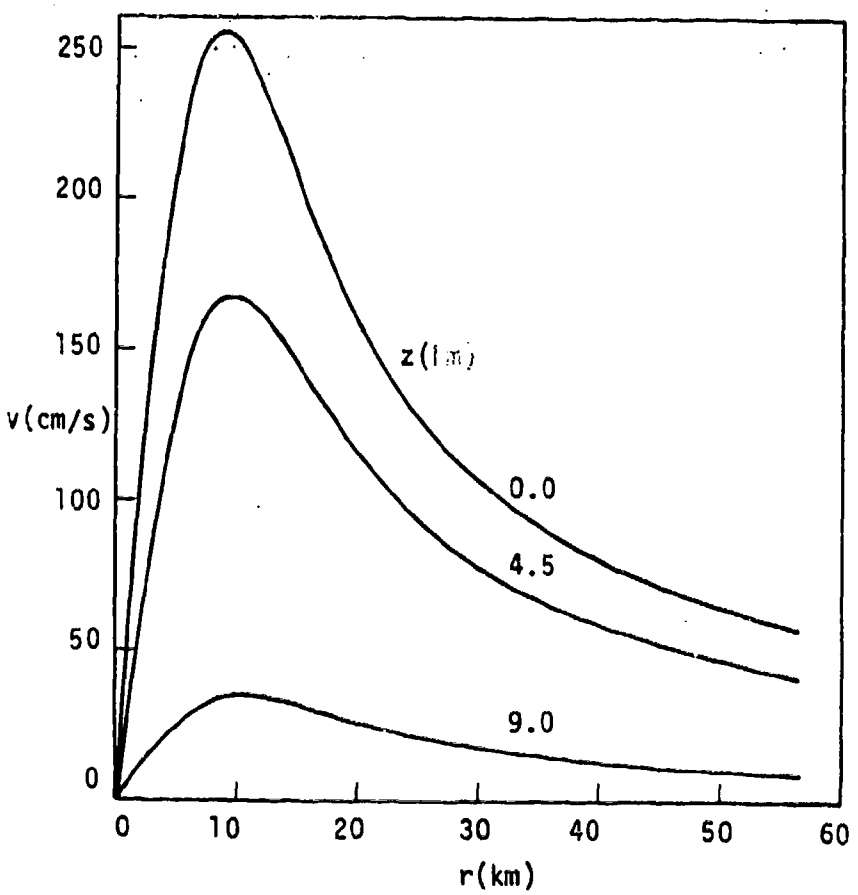

Figure 2.

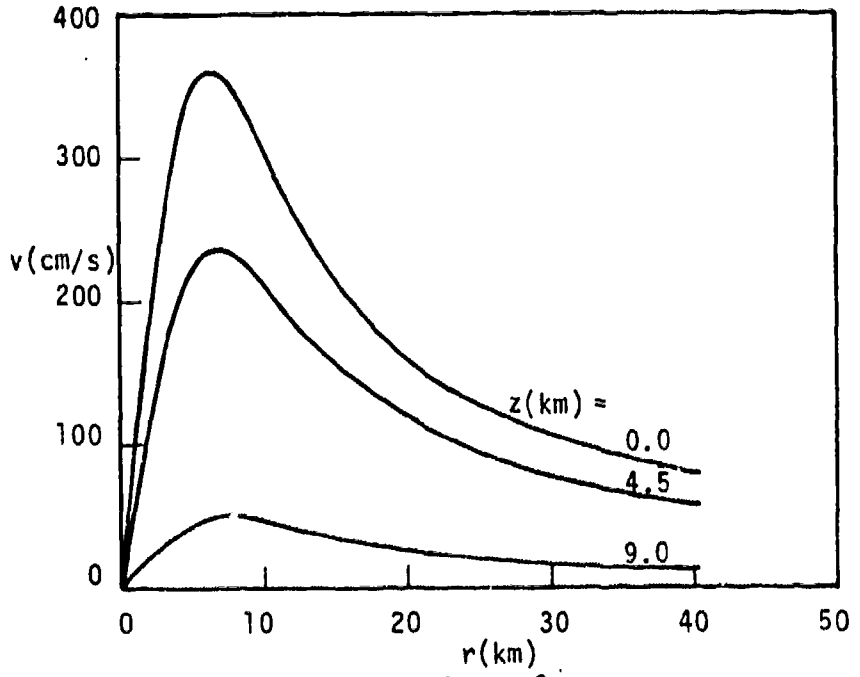

Figure 3.

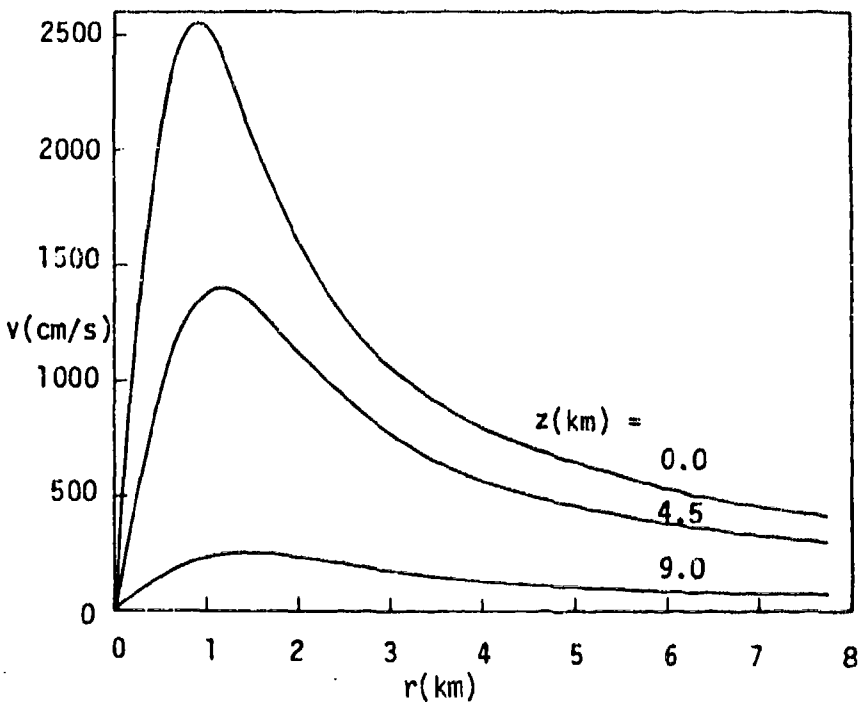

Figure 4.

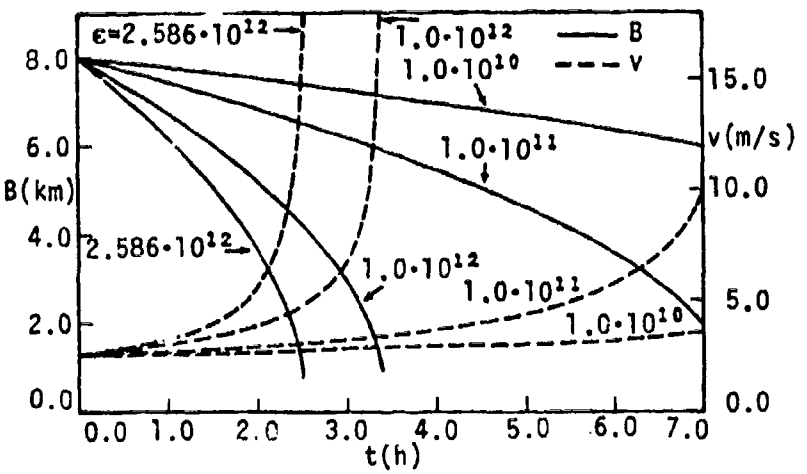

Figure 5.

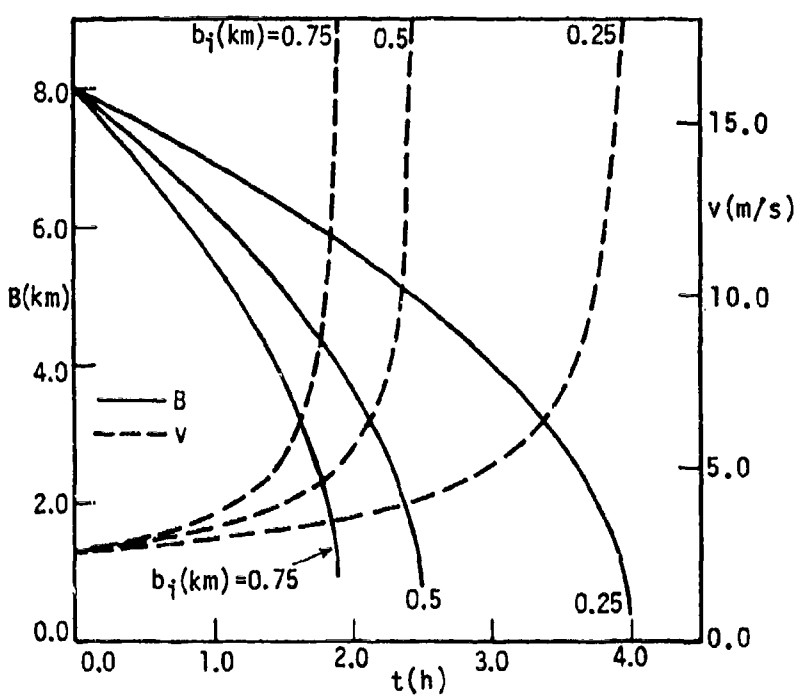

Figure 6.

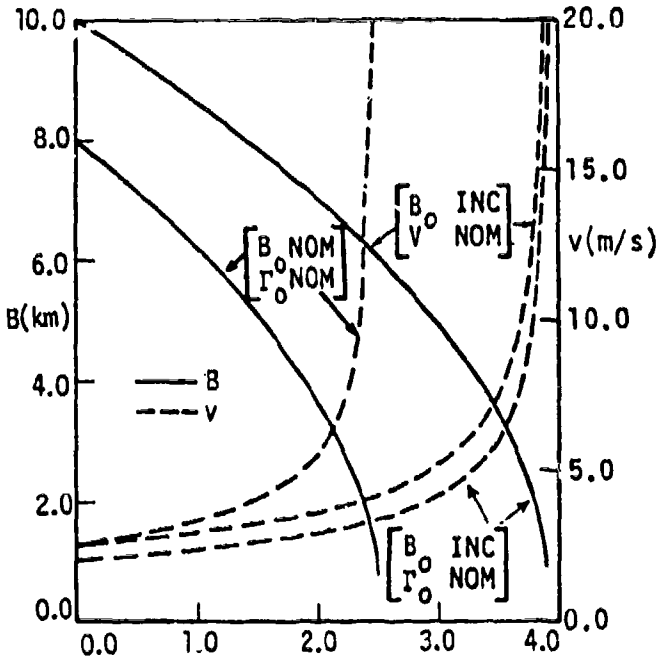

Figure 7.

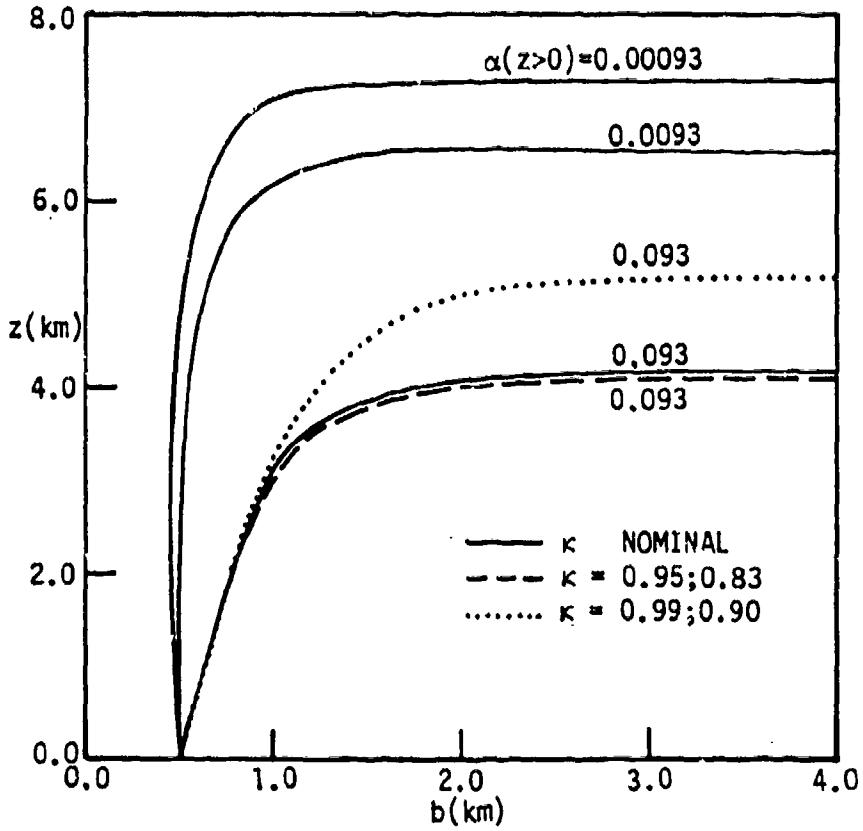

Figure 8.

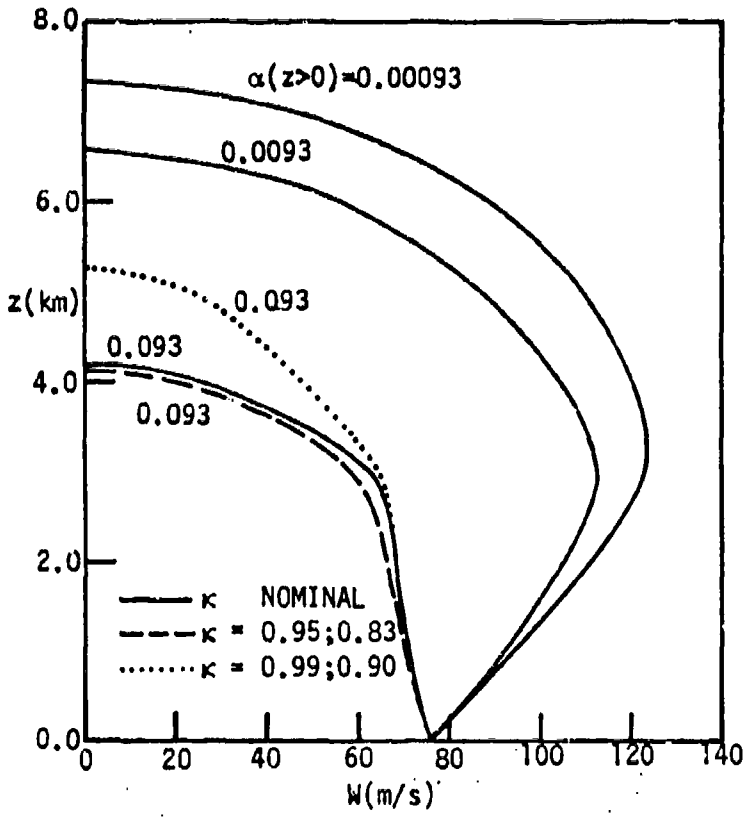

Figure 9.

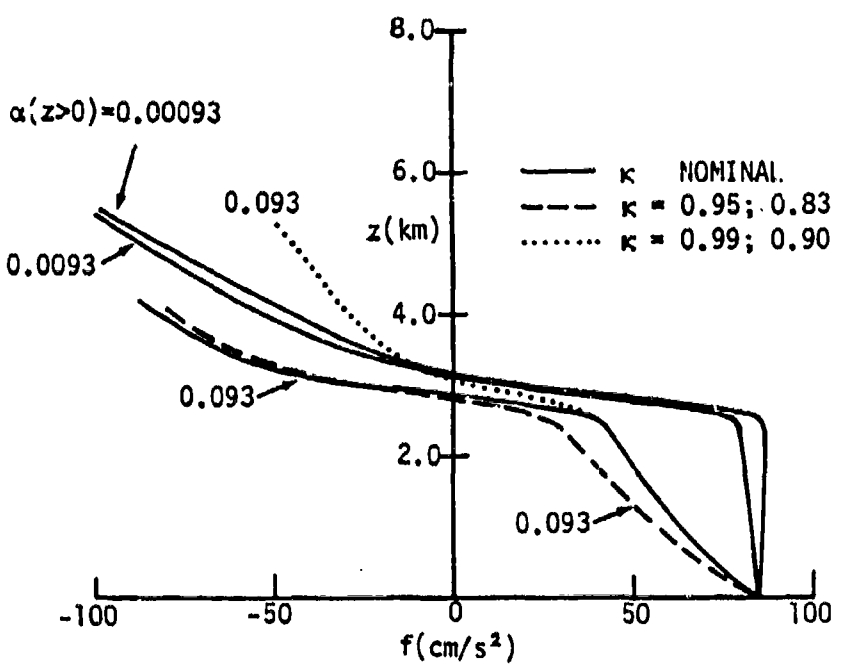

Figure 10.

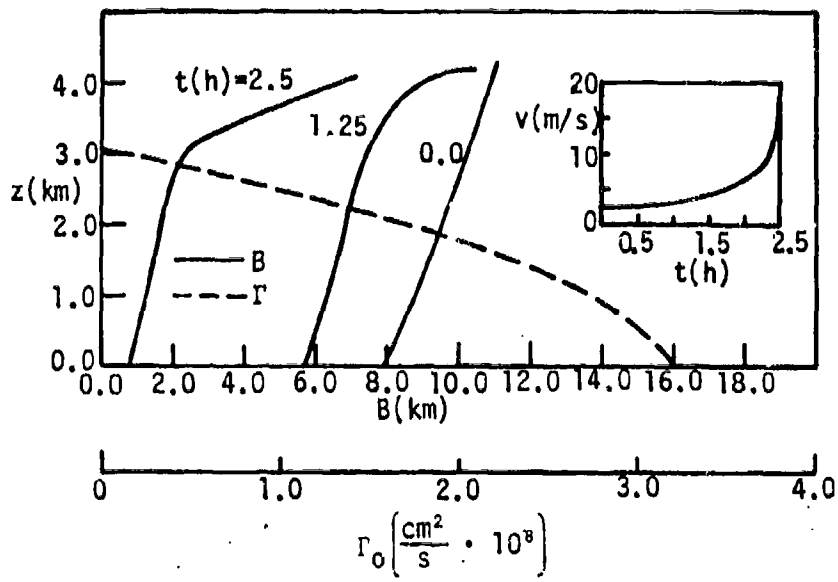
t(h)=2.5
1.25
0.0
4.0
3.0
2.0
1.0
0.0
z(km)
B
Γ
0.0 2.0 4.0 6.0 8.0 10.0 12.0 14.0 16.0 18.0
B(km)
20
v(m/s)
10
0
0.5 1.5 2.5
t(h)
0 1.0 2.0 3.0 4.0
$\Gamma_o \left[\frac{cm^2}{s} \cdot 10^8\right]$

Figure 11.

DISTRIBUTION LIST

DEPARTMENT OF DEFENSE

Defense Intelligence Agency
ATTN: DB-4C2, C. Wiehle
ATTN: WDB-4CR

Defense Nuclear Agency
ATTN: STSP
2 cys ATTN: SPTD
4 cys ATTN: STTI/CA

Field Command, Defense Nuclear Agency
ATTN: FCTT, W. Summa
ATTN: FCTXE

Joint Strat Tgt Planning Staff
ATTN: JLKS

OTHER GOVERNMENT AGENCIES

Dept of Commerc, Center for Fire Rsch
ATTN: R. Levine
ATTN: H. Buam
ATTN: G. Mullholland
ATTN: J. Quintierre

US Forest Service
ATTN: FFASR, C. Chandler

Federal Emergency Management Agency
ATTN: Asst Assoc Dir for Rsch, J. Kerr
ATTN: Ofc of Rsch/NP, D. Bensen
ATTN: H. Tovey

Office of Emergency Services
ATTN: W. Tonguet

FOREIGN GOVERNMENT AGENCY

Great Lakes Forest Rsch Ctr
ATTN: B. Stokes

DEPARTMENT OF ENERGY CONTRACTORS

University of California
Lawrence Livermore National Lab
ATTN: R. Hickman
ATTN: B. Bowman
ATTN: R. Perrett

Los Alamos National Laboratory
ATTN: J. Chapiak
ATTN: Dr D. Cagliostro

DEPARTMENT OF DEFENSE CONTRACTORS

California Research & Technology, Inc
ATTN: M. Rosenblatt

Center for Planning & Rsch, Inc
ATTN: R. Laurino
ATTN: J. Rempel

Charles Scawthorn
ATTN: C. Scawthorn

DEPARTMENT OF DEFENSE CONTRACTORS (Continued)

Factory Mutual Rsch Corp
ATT N: R. Friedman
ATTN: J. DeRis

Harvard University
ATTN: Prof G. Carrier

IIT Research Institute
ATTN: T. Waterman
ATTN: H. Napadensky
ATTN: A. Longenow

Institute for Defense Analyses
ATTN: L. Schmidt
ATTN: E. Bauer

Kaman Tempo
ATTN: DASIAC

Kaman Tempo
ATTN: DASIAC

Los Alamos Tech Assoc, Inc
ATTN: P. Hughes

Univ of Notre Dame du Lac
ATTN: A. Murty Kanury

Pacific-Sierra Research Corp
ATTN: H. Brode, Chairman SAGE
ATTN: R. Small

R&D Associates
ATTN: R. Turco
ATTN: F. Gilmore
ATTN: D. Holliday
ATTN: P. Haas

Rand Corp
ATTN: P. Davis

Rand Corp
ATTN: B. Bennett

Research Triangle Institute
ATTN: R. Frank

Science Applications, Inc
ATTN: D. Groce
ATTN: M. Drake
ATTN: M. McKay

Science Applications, Inc
ATTN: J. Cockayne

Scientific Services, Inc
ATTN: C. Wilton

SRI International
ATTN: J. Backovsky
ATTN: T. Goodale
ATTN: R. Alger

DEPARTMENT OF DEFENSE CONTRACTORS (Continued)

Stan Martin Associates
ATTN: S. Martin

SWETL, Inc
ATTN: T. Palmer

DEPARTMENT OF DEFENSE CONTRACTORS (Continued)

TRW Electronics & Defense Sector
2 cys ATTN: F. Fendell
2 cys ATTN: G. Carrier
2 cys ATTN: P. Feldman